2005:25

LICENTIATE THESIS

L

Exotic Phases of Matter in Compact Stars

Fredrik Sandin

Luleå University of Technology
Department of Applied Physics and Mechanical Engineering
Division of Physics

2005:25 | ISSN: 1402-1757 | ISRN: LTU-LIC -- 05/25 -- SE

Licentiate Thesis

Exotic Phases of Matter in Compact Stars

Jan Fredrik Sandin

Division of Physics
Luleå University of Technology
SE-971 87 Luleå
Sweden

E-mail: fredrik.sandin@ltu.se

May 8, 2005

ABSTRACT

Astrophysical observations constitute an increasingly important source of information, thanks to the high resolution of present and near-future terrestrial and orbiting observatories. Especially, the properties of matter at low temperatures and extremely high densities can only be studied by observations of compact stellar objects. Traditionally, astrophysicists distinguish between three different types of compact objects. These are white dwarfs, neutron stars, and black holes. Neutron stars are presumably unique astrophysical laboratories for a broad range of physical phenomena. Examples are exotic phases of matter at super-nuclear densities and hypothetical new states of matter, *e.g.*, superconducting quark matter.

This Licentiate thesis treats a subset of the exotic phases of matter that could exist in compact stellar objects. In particular, a model of three-flavour colour superconducting quark matter is derived and a signature for a new state of matter is suggested. The former is an effective so-called Nambu–Jona-Lasinio model of quark matter at high densities, which incorporates local colour and electric charge neutrality, as well as self consistently determined quark masses and superconducting condensates. The phase diagram of three-flavour colour superconducting quark matter is presented and the effect of superconducting condensates on the possible configurations of compact stars is discussed. In the second part of the thesis, it is shown that a hypothetical class of particles, so-called preons, which might be the building blocks of quarks and leptons, could allow for a new class of compact objects, preon stars. The properties of preon stars are estimated and potential methods to observe them are discussed.

Keywords: *Compact stars – Quark stars – Preon stars – Colour superconductivity.*

Appended Papers

Paper I

D. Blaschke, S. Fredriksson, H. Grigorian, A. M. Öztaş and F. Sandin, "The phase diagram of three-flavor quark matter under compact star constraints", arXiv:hep-ph/0503194. Submitted to *Phys. Rev.* **D**.

Paper II

J. Hansson and F. Sandin, "Preon stars: a new class of cosmic compact objects", arXiv:astro-ph/0410417. *Phys. Lett.* **B**, in press (2005).

Paper III

F. Sandin, "Compact stars in the standard model – and beyond", *Eur. Phys. J.* **C**, doi: 10.1140/epjcd/s2005-03-003-y. Also to appear in the proceedings of ISSP 2004.

Paper IV

J. Hansson and F. Sandin, "Looking in the right direction for fundamental constituents?". To be submitted for publication.

Preface

This Licentiate thesis constitutes a report on the preliminary results of my work for a Ph.D. degree in Physics. The research has been performed in collaboration with David Blaschke, Sverker Fredriksson, Hovik Grigorian, Johan Hansson and Ahmet Öztaş. For their guidance and support I am most grateful. I thank David Blaschke for his hospitality during my visit to Rostock. I would also like to express my gratitude to Mark Alford, Michael Buballa, Achim Geiser, Kostas Kokkotas, John Ralston, Sanjay Reddy, Avetis Sadoyan and Andrew Steiner for useful discussions, and for their helpful and inspiring attitude.

It is a pleasure to acknowledge the influence of my supervisor, Sverker Fredriksson, who is a great mentor. I thank my co-supervisor, Johan Hansson, for his support and his many ingenious ideas, which have inspired me to learn new aspects of physics. I am grateful to my office-mate, Erik Elfgren, for the numerous discussions on topics as diverse as vacuum energy and consciousness. I thank him and Tiia Grenman for their help with practical issues. I acknowledge support from the Swedish Graduate School of Space Technology.

Finally, I am grateful to Maria, Hanna, Lena and Jan for their support, and for being the wonderful people that they are.

Luleå in May 2005,

Fredrik Sandin

Acronyms

BNL	Brookhaven National Laboratory
CERN	European Organisation for Nuclear Research
EOS	Equation Of State
GRB	Gamma-Ray Burst
LHC	Large Hadron Collider
NJL	Nambu–Jona-Lasinio
NS	Neutron Star
QCD	Quantum Chromodynamics
QGP	Quark-Gluon Plasma
RHIC	Relativistic Heavy-Ion Collider
SM	Standard Model (of particle physics)
SQM	Strange Quark Matter

Units and Symbols

SI units are used in the Introduction. Unless explicitly stated otherwise, I use natural units, $\hbar = c = k_B = 1$, in subsequent chapters. Gravitational units, $G = c = 1$, are used in some of the appended papers. See Appendix A for further information. The Dirac gamma matrices, γ^μ, and the Gell-Mann generators, λ_i, are defined in Appendix B.

Table of Contents

Chapter 1

Introduction

Our universe, as we know it today, was created in the "big bang" about 13.7 billion (13.7×10^9) years ago. In the beginning, space was filled with a hot and dense energy bath, a fluid of radiation that presumably emerged from some type of "quantum fluctuation". The universe has ever since expanded and cooled down. We don't know much about the first 10^{-34} s after the big bang, more than that the universe seems to have undergone a period of extremely rapid expansion, so-called inflation. Inflation is mainly needed to explain the high level of isotropy in the cosmic microwave background, *i.e.*, the electromagnetic radiation that is observed in all directions in the sky.

The first matter particles, the quarks, started to emerge in the radiation fluid already after 10^{-32} s. Quarks are, as far as we know today, the fundamental constituents of a broad range of composite particles, so-called hadrons. The most well-known examples of hadrons are the neutrons and protons, which constitute atomic nuclei. It is believed that one extra quark per $\sim 10^9$ quark-antiquark pairs was created due to an asymmetry. That is why we mainly observe matter in the universe, rather than radiation (matter and antimatter annihilate) or antimatter. The creation of particles from "energy" can be qualitatively understood in terms of Einstein's famous equation $E = mc^2$, or as he originally wrote it, $m = E/c^2$. This equation suggests that energy, E, and mass, m, are somehow related, or perhaps even the same thing, since the speed of light, c, is set to unity with an appropriate choice of units. The origin of mass is still a great mystery at the conceptual level. The rules of Nature for creating massive particles out of energy is, on the other hand, amazingly well understood within the energy range that has been studied in particle physics experiments.

Hadrons started to form after about one microsecond, when the universe had been sufficiently cold and diluted. About 0.1 milliseconds after the big bang, leptons started to emerge in the matter-radiation fluid. The most well-known example of leptons is the electrons, which constitute the negative charge in atoms. After about one minute, helium nuclei, and a small fraction of deuterium and lithium nuclei,

started to form by fusion reactions. A few minutes later, the primordial matter content of the universe had been created. It roughly consisted of 75% hydrogen nuclei, 25% helium nuclei, and small amounts of deuterium and lithium nuclei. Neutral atoms did not form until several hundred thousand years later, when the universe had cooled down to a temperature of about 3000 K. When that happened, the universe became effectively transparent to photons; light could then propagate freely in the universe. The light from that time is the cosmic microwave background radiation that we observe in the sky today. Due to the expansion of the universe, *i.e.*, of the space-time fabric, the light waves have been "stretched" (redshifted) on their journey and arrive here at Earth as microwaves, even though they started out in the early universe as visible, mainly orange, light.

As the universe expanded, small density fluctuations in the primordial radiation fluid were enhanced by gravity and eventually gave rise to large clouds of hydrogen and helium, which continued to contract due to gravity and friction. The first stars and galaxies were created in such gas clouds. Even today we observe large clouds of interstellar gas, consisting mostly of molecular hydrogen and helium, and small amounts of dust and heavier elements, which have been created by thermonuclear fusion reactions in stars. Some beautiful examples of interstellar clouds where new stars are being formed are the Horsehead Nebula (Barnard 33) in Orion, the Trifid Nebula (M20) in Sagittarius and the Eagle Nebula in Serpens, see the false-colour image[1] on the next page. The gas clouds range in size from a fraction of a light year[2] to several hundred light years and in mass from about 10 to 10^7 solar masses. Stars more massive than a few solar masses often form in small groups in the densest regions of the clouds. About 60-70% of all stars have a companion star, *i.e.*, half of all stars on the sky are "binaries".

1.1 Compact Objects

Stars have different size, the smallest not even deserving the name, since the pressure and temperature inside them are insufficient to start fusion. Other stars are huge and deplete their energy rapidly. As the thermonuclear fusion reactions diminish in the core of stars, the thermal pressure decreases. Eventually, a critical point is reached. When the force of gravity is no longer balanced by the thermal pressure the star starts to collapse. What happens after that depends on the mass of the progenitor star. If the star is a few times more massive than the Sun, the collapse is eventually halted due to the "degeneracy pressure" of electrons and a so-called white dwarf forms. If the star is more massive, around ten solar masses, the

[1] In a false-colour image, the colours do not necessarily represent the colour of the light that entered the camera, since filters are used to, *e.g.*, separate the light from different chemical elements.

[2] The speed of light in vacuum is $\sim 300\,000$ km/s. One light year is the distance the light travels in one year, which is $\sim 9\,460\,800\,000\,000$ km. For comparison, the diameter of our galaxy is about 100 000 light years and the distance to the Andromeda galaxy is more than two million light years.

Eagle Nebula
M16

Hubble Heritage

NASA, ESA and The Hubble Heritage Team (STScI/AURA) • Hubble Space Telescope ACS • STScI-PRC05-12b

collapse continues until the atomic nuclei start to "overlap" and the core stabilises as a dense neutron star. For progenitor stars of still higher mass, the collapse is assumed to lead to the formation of a black hole.

The threshold mass, when a star collapses to a black hole instead of a neutron star is, however, only approximately known, since the details of the collapse are poorly understood. White dwarfs, neutron stars and black holes are extremely dense objects, so-called compact objects, which are left behind in the debris when normal stars "die". That is, when most of the nuclear fuel has been consumed and they collapse under the pull of gravity. With the exception of small black holes, which evaporate quickly due to "Hawking radiation", and accreting neutron stars and white dwarfs, all three types of compact objects are essentially static over the lifetime of the universe and therefore represent the final stage of stellar evolution. Some properties of these objects are presented in Table 1-1. The false-colour image

Table 1-1: Distinguishing traits of the three different types of compact stellar objects traditionally considered in astrophysics. Here, $\mathrm{M}_\odot \simeq 1.99 \times 10^{30}$ kg is the mass of the Sun.

Object	Mass	Radius	Mean Density
White dwarf	$\lesssim 1.4\ \mathrm{M}_\odot$	$\sim 10^4$ km	$\lesssim 10^7$ g/cm^3
Neutron star	$\sim 1 - 3\ \mathrm{M}_\odot$	~ 10 km	$\lesssim 10^{15}$ g/cm^3
Black hole	Arbitrary	$2GM/c^2$	$\sim M/R^3$

on the next page shows the Cat's Eye nebula in Draco, which is situated about 3000 light years from the Earth in the direction of the north ecliptic pole. The halo of matter has been ejected from the bright central object, which previously was a star similar to our Sun. Actually, this particular nebula is so complex that it has been suggested that the central object has a companion star. Eventually, the bright object in the centre will collapse into a white dwarf. For a more detailed description of compact objects, I recommend [1; 2].

1.2 Neutron Stars

The gravitational energy that is released when a massive star collapses causes a giant explosion, a so-called supernova, which expel a large fraction of the star into the interstellar medium. This is how the heavy elements in the universe were created. Neutron stars are created in the aftermath of some of the core collapse supernovæ explosions, as was first suggested by Walter Baade and Fritz Zwicky already in 1934 [3]. Following the collapse, the core of the star is compressed to a hot proto-neutron star, which cools rapidly due to neutrino emission, leaving a hot neutron

Cat's Eye Nebula • NGC 6543

Hubble Heritage

NASA, ESA, HEIC and The Hubble Heritage Team (STScI/AURA)
Hubble Space Telescope ACS • STScI-PRC04-27

star. During the collapse, roughly 99% of the gravitational energy is emitted in the form of neutrinos. Only 0.01% of the energy is carried away by photons, still, supernovæ are sufficiently bright to outshine their host galaxies. The remaining gravitational energy ($\sim$ 1%) is converted into the kinetic energy of the expelled crust.

Neutron stars are extremely dense objects. The environment in the central regions resembles the early universe, except that the temperature is lower. Due to the low temperature and high density, neutron stars are presumably unique astrophysical laboratories for a broad range of physical phenomena. Examples are exotic phases of matter at super-nuclear densities (hyperons, baryon resonances and boson condensates) and the potential existence of new states of matter, *e.g.*, colour superconducting quark matter, see Chapters 2 and 3, and [4; 5]. Hence, the name "neutron star" is presumably a misnomer. In the following, however, I simply refer to these objects as "neutron stars". Some competing theories for the structure of neutron stars are illustrated in Figure 1.1.

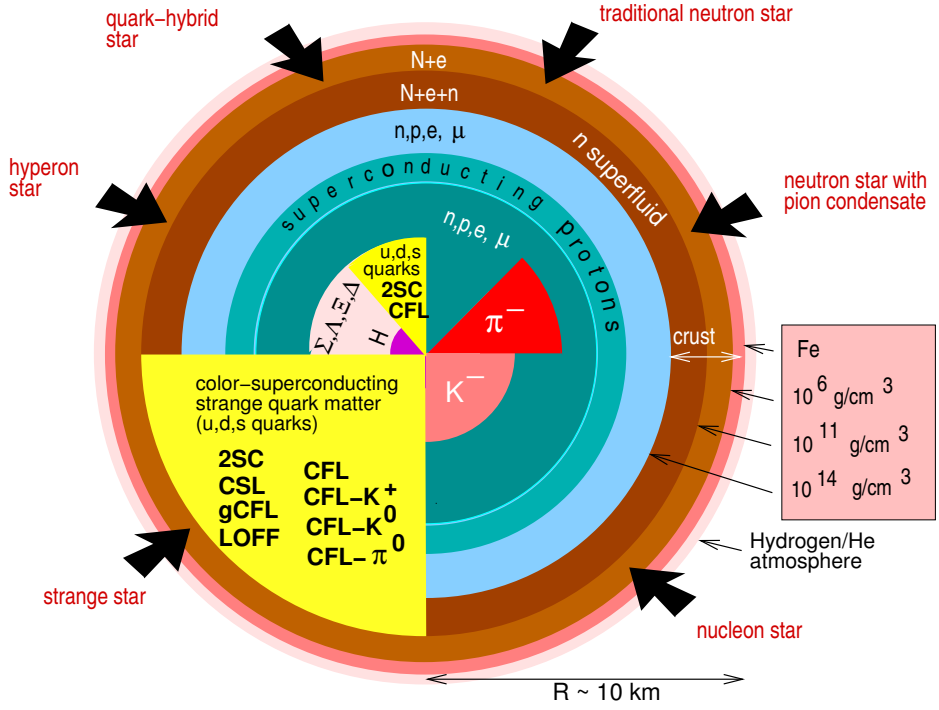

Figure 1.1: Novel phases of subatomic matter in the interior of a neutron star, as suggested by different theories. Reprinted figure with permission from F. Weber, *Prog. Part. Nucl. Phys.* **54**, 193 (2005). Copyright 2004 by Elsevier Ltd.

Over the last decade, observations of neutron stars have provided data that is complementary and often inaccessible to terrestrial laboratories. The density in neutron stars is of the order of 10^{15} g/cm^3. To get an impression of how large this density is, imagine that a tablespoon of material from the interior regions of a neutron star would have a mass of about one billion (10^9) tonnes. It is impossible to create even a tiny macroscopic sample of matter with such high density in terrestrial laboratories. Due to the high resolution of present and near-future terrestrial and orbiting observatories, *e.g.*, the Chandra X-ray satellite, the International Gamma-Ray Astrophysics Laboratory (INTEGRAL), Super-Kamiokande and the Sudbury Neutrino Observatory, neutron stars constitute an increasingly important source of information. We are entering the era of "astronuclear physics". This is an exciting field of research, where compact stars and the (current) fundamental theories of matter and space-time, *i.e.*, the standard model of particle physics and general relativity, are intimately connected and play a central role.

1.3 Preon Stars

In the standard model of particle physics (SM), quarks and leptons are considered as fundamental entities. It is clear, however, that the SM is not able to explain the matter content of the universe, especially the vast amounts of so-called dark matter needed to explain, *e.g.*, the rotation of galaxies and structure formation. There seems to be no hope of explaining the abundance of dark matter without introducing new fundamental particles. The SM is therefore considered to be approximate and incomplete. The SM also suffers from a number of conceptual shortcomings. For example, it does not explain the particle family structure, *i.e.*, why there are six types of quarks and six types of leptons organized into three families. Also, most quarks and leptons are unstable and decay into lighter flavours. There have been numerous situations in the past when properties like these have turned out to be a result of compositeness, *i.e.*, that the particles are composed of a number of other particles. The most recent example is the large number of hadrons that puzzled physicists a half-century ago, before the quarks were discovered.

Preons constitute a conjectured, more fundamental level of elementary particles, beneath the quarks and leptons of the SM. If preons exist, we have shown that a new class of stable compact objects could exist [6; 7], see also [8]. In Figure 1.2, the radius and density of preon stars can be compared to the radius and mean density of various other objects in the universe. A potential method to observe preon stars and a comparison with data are presented in [9]. The interested reader is referred to the appended papers for more information. The presentation given there is rather self-consistent. For more information about preon models and the shortcomings of the SM, see, *e.g.*, [10; 11; 12] and references therein.

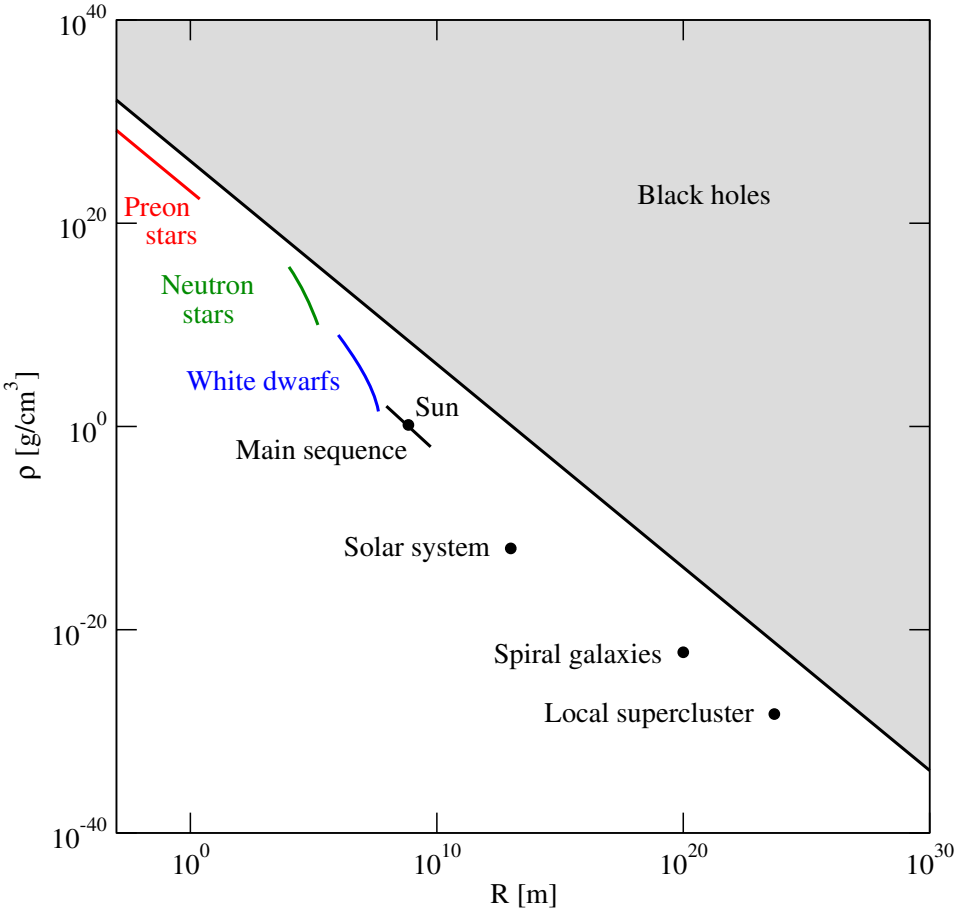

Figure 1.2: The radius and mean density of various objects in the universe. The preon star sequence represents solutions for different values of the free parameter of the model, the preon "energy scale" (the inverse length-scale in a hypothetical form factor of preon wave functions), see Figure 1 and Figure 2 in [6].

1.4 This Thesis

This Licentiate thesis treats a subset of the exotic phases of matter that could exist in compact stellar objects. In particular, a model of colour superconducting quark matter is presented and a signature for a new state of matter is suggested. The thesis is divided into two main parts, the introductory chapters and the appended research papers. In Chapter 2 and Chapter 3, some basic concepts of quark matter and colour superconductivity are introduced. The model of three-flavour colour superconducting quark matter is presented in Paper I. The influence of superconducting condensates on the evolution and possible configurations of compact stars are also discussed in that paper. Some details of this model are discussed in Chapter 3. In Paper II and Paper III, the novel idea of preon stars is introduced and the properties of these objects are estimated. Some astrophysical consequences are also discussed. In Paper IV, a potential method to observe preon stars is discussed and a comparison with gamma-ray burst data is presented.

Chapter 2

Quark Matter

The properties of matter at low temperatures are relatively well known below the density when neutrons start to drip out of atomic nuclei, which occurs around $\sim 4 \times 10^{11}$ g/cm^3. In the vicinity of the nuclear saturation density, $\sim 3 \times 10^{14}$ g/cm^3, this is to a less extent the case. At even higher densities, the properties of matter are highly uncertain. The exploration of the phase structure of high density matter is one of the most exciting and active fields of Quantum Chromodynamics (QCD) and strong interaction physics. The properties of matter at high densities are of fundamental importance for our understanding of the early universe and why it evolved into what we experience today. At high densities, *e.g.*, in the interior regions of neutron stars, the properties of matter are intimately connected to the properties of the fundamental constituents and the rules of the microscopic world. This field of research therefore benefits from a joint effort of the particle physics community and the astrophysics community. Due to the high level of activity in the field, a complete review is beyond the scope of this thesis. In this and the following chapter, I only introduce some of the most relevant concepts. The interested reader is referred to the literature for further information, see, *e.g.*, [5; 13; 14; 15; 16; 17] and references therein.

2.1 Quarks and Gluons

Hadrons, *e.g.*, protons and neutrons, are composite particles that are composed of quarks. Two important subclasses of hadrons are the mesons and the baryons, which are composed of two and three quarks, respectively. Quarks are strongly interacting particles, which means that they interact by mediating gluons, the force carriers of the strong nuclear force. Quarks also interact by the electromagnetic force, the weak nuclear force and the gravitational force, but these three forces are typically several orders of magnitude weaker than the force mediated by the strong interaction, at least on microscopic scales. Analogously to the electric charge, which

is associated with the electromagnetic force, there are charges associated with the strong interaction, co-called colour charges. Like colour, which can be decomposed into three distinct components, *e.g.*, red, green and blue, the charge of quarks can be described with three independent components. It is therefore common practise to denote the charge of quarks with red (r), green (g) and blue (b).

Colour was originally introduced in order to reconcile early quark models of baryons with the Pauli exclusion principle. An additional quantum number was needed in order to explain how quarks could coexist inside the proton, in otherwise identical states. Eventually it turned out, however, that the "colours" are the charges associated with the strong nuclear force. Unlike the charge-neutral photons, which mediate the electromagnetic force, gluons carry colour charge. Roughly speaking, a gluon has both colour and anticolour ($\bar{r}$, $\bar{g}$, $\bar{b}$) charge. Naively, there would hence be nine different possibilities ($r\bar{r}$, $r\bar{g}$, $r\bar{b}$, $g\bar{r}$, $g\bar{g}$, $g\bar{b}$, $b\bar{r}$, $b\bar{g}$ and $b\bar{b}$) for the charge of a gluon. The colour-neutral superposition, $r\bar{r}$–$g\bar{g}$–$b\bar{b}$, does not correspond to a gluon, however, so there are only 8 gluons. Each gluon is orthogonal to the colour-neutral state. Since gluons carry both colour and anticolour charges, a quark that interacts strongly changes colour (antiquarks have anticolour charge). Since gluons are charged, they can also interact with each other. Free quarks and gluons have never been detected. It is believed that they are always confined in composite colour-neutral aggregates, such as mesons and baryons. So far, six different flavours of quarks have been identified in particle physics experiments. The flavours are: down (d), up (u), strange (s), charm (c), bottom (b) and top (t). The current masses[1] and the electric charge of the six different types of quarks are presented in Table 2-1.

Table 2-1: Electric charge and approximate current masses of quarks [18].

Quark flavour	u	d	s	c	b	t
Current mass [MeV]	1.5-4	4-8	80-130	1150-1350	~ 4500	~ 175000
Electric charge	$+\frac{2}{3}$	$-\frac{1}{3}$	$-\frac{1}{3}$	$+\frac{2}{3}$	$-\frac{1}{3}$	$+\frac{2}{3}$

At low energies, the interaction between quarks and gluons is "strong", *i.e.*, the coupling constant is large, and it is hence not possible to describe the interactions in standard perturbation theory. At high densities or temperatures, on the other hand, the strong nuclear force effectively gets weaker, since the coupling constant decreases when the relative energy of the interacting quarks (or gluons) increases.

[1] The current mass (or "bare" mass) of a quark, is the mass that is measured in high-energy particle collisions. This mass is lower than the "constituent" mass of the quarks. As an example, the mass of a neutron is $\sim$ 939.6 MeV, while the total bare mass of the constituent quarks is $m_u + 2\,m_d \lesssim 20$ MeV. The additional mass of the neutron is mainly due to strong interactions.

This phenomenon is called asymptotic freedom and was theoretically discovered already in 1973 [19; 20]. Since quarks are asymptotically free, perturbation theory and effective models of the strong interaction can be applied at high densities.

2.2 Quark-Gluon Plasma

It was suggested already in the 1960s that matter might be in the form of deconfined quarks in the core of neutron stars [21; 22], see also [23; 24]. In the 1970s, rather soon after it became clear that hadrons consist of quarks and gluons, and the asymptotic behaviour of the strong interaction had been understood [19; 20], it was suggested that quarks should be in the deconfined state at high temperatures and densities [25]. The arguments were roughly that the infrared problems, which are related to long-range interactions, are absent in a dense medium due to screening, and that the interaction is weak enough for a perturbative approach. It was suggested in [25] that the quark model implies that super-dense states of matter, *e.g.*, in neutron stars and the early universe, should be composed of deconfined quarks, rather than hadrons. See also [26].

A heuristic argument for the existence of deconfined quark matter follows directly from the asymptotic behaviour of the strong interaction. Since the strong force becomes arbitrarily weak as the quarks are squeezed closer together, matter should behave as an ideal Fermi gas of quarks at asymptotically high densities and/or temperatures. A phase transition from the confined hadronic phase to a deconfined phase, a so-called quark-gluon plasma (QGP), is therefore expected at sufficiently high temperatures, T, or quark number chemical potentials, μ. This is illustrated in the phase diagram in Figure 2.1, which resembles the diagrams by, *e.g.*, [27; 28]. The possibility that Cooper pairs of quarks could form in dense QGP was suggested already in the mid 1970s [25], however, the idea did not get much attention until quite recently. The phase diagram in Figure 2.1 remained the standard picture for about two decades.

One of the ultimate goals of heavy-ion collision experiments is to create and identify the QGP. The first indications of a QGP were reported in press releases at CERN (SPS) and BNL (RHIC) a few years ago, though the interpretation of the data is still under debate. In a press release at BNL this spring (in April) it was claimed that some of the observations at BNL fit with the theoretical predictions for a QGP, but that there are discrepancies between the experimental data and the theoretical predictions based on simple models of QGP formation. There is little doubt that the QGP will be created with the more powerful LHC, which is currently being built at CERN. QGP did for sure exist in the early universe, a few microseconds after the big bang when the density and temperature was high, see Chapter 1. QGP could also exist in the interior of neutron stars. An important task is therefore to identify observational signatures for a QGP in compact stars. A fundamental prerequisite

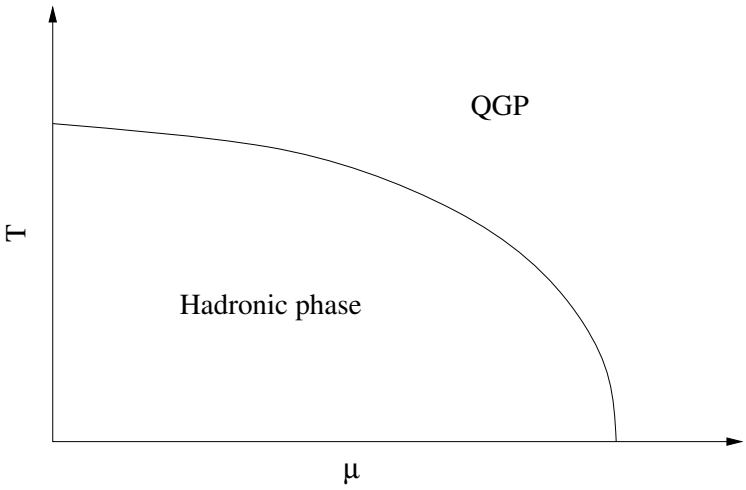

Figure 2.1: Schematic phase diagram from the pre-colour superconductivity era. Due to asymptotic freedom, a phase transition from the confined hadronic phase to a deconfined quark-gluon plasma (QGP) phase is expected at high values of the quark number chemical potential, μ, and temperature, T.

for this mission is to obtain a better understanding of the microscopic properties of QGP, at temperatures and chemical potentials relevant for compact stars.

2.3 The Strange Quark Matter Hypothesis

The idea that strange quark matter (SQM) may constitute the ground state of strongly interacting dense matter, rather than ^{56}Fe, was proposed already in 1971 [26] and later on in [29]. The latter paper attracted a great deal of attention and stimulated a large number of further investigations, *e.g.*, it ultimately inspired the current extensive search for SQM, so-called "strangelets", in heavy-ion collisions and astrophysical signals of deconfined quark matter in compact stars. The essence of the hypothesis is that the energy per baryon, *i.e.*, three quarks, in three-flavour quark matter may be smaller than the $\sim$ 930 MeV per baryon in nuclear matter. This would render the SQM phase more stable than nuclear matter and atomic nuclei. If correct, the SQM hypothesis would have implications of fundamental importance for our understanding of the early universe and its evolution to the present day [2].

[2]When RHIC was commissioned, one of the potential "disaster scenarios" was that the heavy-ion collisions would create a small droplet of SQM that would devour the Earth [30]. The argument against that is the empirical fact that the moon still exists, even though it is constantly exposed to cosmic rays with extremely high energies. On the other hand, in a heavy-ion collision, the centre of mass is fixed in space, which is not the case in cosmic ray events. This is, perhaps, a more

In contrast to nuclei, where quarks are confined to individual colour neutral nucleons, SQM presumably is an extended or even macroscopic piece of matter, which is composed of deconfined u, d and s quarks. An essential point is that a large fraction of s quarks ($n_s \sim n_u \sim n_d$) might be necessary for a stable droplet of SQM to form, since hypernuclei, *e.g.*, nuclei that contain hyperons, have higher masses than ordinary nuclei of the same mass number. This might be the explanation for the empirical fact that quarks are confined into hadrons in ordinary matter, as subsequent weak decay processes cannot create sufficient amounts of long-lived s quarks for stable SQM to form. It is also possible that SQM is stable only for a sufficiently large number of quarks, as surface effects could make confined states energetically favourable for smaller systems. In any case, three-flavour quark matter inevitably has lower energy than two-flavour quark matter at high densities, due to the additional Fermi sea of the s quarks. Neglecting the influence of leptons, for simplicity, electric neutrality requires that two-flavour quark matter is composed of twice as many d quarks as u quarks, see Table 2-1. For a relativistic degenerate Fermi system, the number densities, n_i, are related to the chemical potentials, μ_i, by

$$n_i \propto g_i \mu_i^3, \tag{2.1}$$

where g_i is the degeneracy factor. For quarks, two spin states and three colour states for each flavour yields $g_i = 6$. Hence, if $n_d = 2n_u$, the chemical potentials are related by

$$\mu_d = 2^{1/3} \mu_u. \tag{2.2}$$

If the chemical potential of the d quarks is greater than the mass of the s quark, the system can lower its energy by transforming some of the d quarks into s quarks by weak interactions,

$$s + u \leftrightarrow d + u. \tag{2.3}$$

This process continues until all three flavours are in equilibrium with respect to the weak interactions. At asymptotically high densities, the number densities and Fermi energies of all three flavours should hence be equal [3]. This result is valid also when the influence of leptons is taken into account.

down-to-earth example of the implications of the SQM hypothesis.

[3] Actually, at sufficiently high densities, all six flavours of quarks should be present in quark matter due to weak interactions. Compact stars, however, become unstable before the chemical potential reaches the c quark mass. Quarks more massive than the s quark are therefore absent in compact stars. c, b and t quarks are only relevant for the hot and dense plasma in the early universe, and in particle physics experiments. See, *e.g.*, [31] and [5] for a discussion about the non-appearance of charm quarks in compact stars.

2.4 Quantum Chromodynamics

The properties of the strong interaction are, in principle, described by Quantum Chromodynamics (QCD). The QCD Lagrangian is[4]

$$\mathcal{L} = \bar{q}_i^{\alpha} \left(i\gamma_\mu D^\mu_{\alpha\beta} - m_i \right) q_i^{\beta} - \frac{1}{4} F^a_{\mu\nu} F_a^{\mu\nu}, \tag{2.4}$$

where m_i are the current masses of the quark fields, q_i^α, which have six flavour (u, d, s, c, b, t) and three colour (r, g, b) degrees of freedom, see Section 2.1. Here, $\{i, j, k\}$ are flavour indices, $\{\alpha, \beta, \gamma\}$ are colour indices and $\{a, b, c, d, e\}$ are other (dummy) indices. The colour gauge-invariant derivative, D^μ, is

$$D^\mu_{\alpha\beta} = \delta_{\alpha\beta}\partial^{\,\mu} - ig\frac{[\lambda_a]_{\alpha\beta}}{2} G_a^{\,\mu}, \tag{2.5}$$

where G_a^μ are the eight gluon fields, $a = 1, ..., 8$, and λ_a are the Gell-Mann generators, see Appendix B. The gluon field strength tensor, $F_a^{\mu\nu}$, is defined as

$$F_a^{\mu\nu} = \partial^{\,\mu} G_a^{\,\nu} - \partial^{\nu} G_a^{\,\mu} - g f_{abc} G_b^{\,\mu} G_c^{\,\nu}, \tag{2.6}$$

where g is the strong interaction coupling constant and f_{abc} are the $\mathrm{SU}(3)_c$ group structure constants, see Appendix B.3. The QCD Lagrangian is invariant under SU(3) transformations in colour space. The strong interactions conserve baryon number, electric charge and quark flavour. Only the weak interactions allow for flavour change. The colour current density, j_a^μ, and the colour charge generators, Q_a, are

$$j_a^\mu = \partial_\nu F_a^{\mu\nu}, \tag{2.7}$$

$$Q_a = \int \mathrm{d}^3x \, j_a^\mu. \tag{2.8}$$

Since isolated quarks and gluons have never been observed, only aggregates of quarks and gluons with zero net colour charge (or colour singlets) should have finite energy. A consequence of this is discussed in Section 3.3.

Due to the presence of the last term in (2.6), QCD is a non-Abelian gauge theory, *i.e.*, the gluon fields do not commute. The non-Abelian character of QCD has a number of implications that makes it difficult to obtain quantitative predictions from the theory, *e.g.*, the gluons have colour charge and interacts with other gluons, as well as themselves (self-coupling). This can readily bee seen by expanding the last

[4]The current quark masses, m_i, that enters the QCD Lagrangian is forbidden by the chiral symmetry of the electroweak part of the SM. The quark masses are generated by spontaneous symmetry breaking. In addition, there are effective ghost and gauge-fixing terms which enter both the QCD and electroweak Lagrangians. Here, only QCD is considered and the current masses therefore enters the Lagrangian explicitly.

term in (2.4). There is one term that is linear in the coupling constant, g, (a three-point interaction) and one term that is quadratic in g (a four-point interaction). Due to the complexity of the theory, one has to rely on Monte Carlo calculations on the lattice [32; 33] and effective models. Until recently, the Monte Carlo approach has been restricted to zero chemical potential and was therefore not suitable for studying the properties of dense matter. It has also been necessary to extrapolate the results for large values of the u and d current quark masses. Recently, progress has been made both in the case of finite chemical potentials and realistic current quark masses, see, *e.g.*, [34; 35] and references therein. It is still necessary, however, to rely on non-perturbative effective models of QCD to investigate the properties of bulk matter at intermediate densities. The most widely used model for this purpose is the MIT bag model [36], which originally was developed as an effective model of (confined) hadrons [37; 38]. Nambu–Jona-Lasinio (NJL) models are frequently used when the effect of dynamical quark masses is important, rather than confinement, see Chapter 3.

Chapter 3

Colour Superconductivity

Since QCD is asymptotically free [19; 20] a Fermi surface of nearly free quarks should form at high densities. Thus, for sufficiently low temperatures, the remaining attractive interaction should lead to the formation of Cooper pairs [39] near the Fermi surface. The qualitative argument for this is simple: For an infinite system of non-interacting fermions at $T = 0$, all states are occupied up to the Fermi momentum p_F, and all other states are empty, *i.e.*, the occupied states form a Fermi sphere. The free energy cost, $|E(\vec{p}_F) - \mu|$, for creating a quark at the Fermi surface is zero. The presence of a weak attraction between the quarks will lower the free energy and render the Fermi sphere unstable. According to Bardeen-Cooper-Schrieffer (BCS) theory [40; 41], a condensate of Cooper pairs will therefore form, which creates a gap in the excitation spectrum that prevents excitations with vanishing free energy, see Figure 3.4. The existence of a pairing gap in the excitation spectrum of cold interacting Fermi systems has recently been verified in experiments, see, *e.g.*, [42]. Since Cooper pairs are bosons, they condense into the lowest energy state at zero temperature, forming a Bose condensate. In the presence of one or more such condensates, the ground state of QGP is a colour superconductor. This is analogous with ordinary superconductors, except that quarks, unlike electrons, have different flavours and carry both colour and electric charge.

The possibility that quarks could form Cooper pairs in dense QGP was suggested already in the mid 1970s [25]. Despite further investigations [43; 44; 45], the idea did not get much attention. More than one decade later, results of non-perturbative low-energy models of QCD showed that the diquark pairing gaps are of the order of 100 MeV [46; 47; 48]. This is much larger than predicted by earlier models and the existence of superconducting condensates could therefore have important (observable) consequences. The investigation of the QCD phase diagram at high densities has since gained momentum and a remarkably rich phase structure has been identified [16; 49; 15; 50; 14; 51; 52; 53; 54; 55; 4]. The main reason for studying the low-temperature and high density domain of the QCD phase diagram is the possible existence of such phases in compact stars. Observable effects of

superconducting condensates are expected, *e.g.*, in the cooling behaviour and the magnetic field evolution. For more information, see Paper I and references therein. In the following, I introduce the model of colour superconducting quark matter that is presented in Paper I. It is assumed that the reader has some knowledge in finite temperature field theory, for an introduction, see [56]. Some basic thermodynamic relations can be found in Appendix C.

3.1 Nambu–Jona-Lasinio Model

The Nambu–Jona-Lasinio (NJL) model was originally developed by Yoishiro Nambu and Giovanni Jona-Lasinio in 1961 [57; 58] as a means to explain the mass gap in the spectrum of interacting nucleons (quarks was not yet invented at that time). The idea was that the gap could be explained analogously to the energy gap of a superconductor in BCS theory, which had been invented a few years earlier [40; 41]. In order to explain the large nucleon mass in terms of (nearly) massless fermions, Nambu and Jona-Lasinio introduced a Lagrangian for a nucleon field, ψ, with a point-like four-fermion interaction,

$$\mathcal{L} = \bar{\psi}(i\partial\!\!\!/ - m)\psi + g\left[(\bar{\psi}\psi)^2 + (\bar{\psi}i\gamma_5\tau\psi)^2\right]. \tag{3.1}$$

Here, m is the bare mass of the nucleon, g is a coupling constant and τ is a Pauli matrix acting in isospin space. The self-energy induced by the four-point interaction generates an effective mass of the nucleon, which can be greater than the bare mass, even when $m = 0$. The NJL model has later on been reinterpreted as as schematic model of (deconfined) quarks, which incorporates the effect of density and temperature dependent effective ("constituent") quark masses in a self-consistent manner. For further information about NJL models, see [51].

3.1.1 Lagrangian

The starting point here is an NJL-type Lagrangian for three-flavour quark matter, with a quark-quark interaction term, $\mathcal{L}_{qq}$, and a four-point quark-antiquark interaction in the colour singlet scalar/pseudoscalar channel

$$\mathcal{L}_{\mathit{eff}} = \bar{q}(i\partial\!\!\!/ - \hat{m} + \hat{\mu}\gamma^0)q + G_S\sum_{a=0}^{8}\left[(\bar{q}\tau_a q)^2 + (\bar{q}i\gamma_5\tau_a q)^2\right] + \mathcal{L}_{qq}. \tag{3.2}$$

Here, $\hat{m} = \mathrm{diag}(m_u, m_d, m_s)$ is the current quark mass matrix in flavour space and $\hat{\mu}$ is the chemical potential matrix in colour and flavour space (see Section 3.3). For $a = 1...8$, τ_a are the generators of SU(3), *i.e.*, the Gell-Mann matrices, while $\tau_0 = \sqrt{2/3} \times 1$. Observe the similarities with the original Lagrangian by Nambu and Jona-Lasinio (3.1). The quark fields, q, in flavour and colour space are

$$q^T = (\psi_{ur}, \psi_{ug}, \psi_{ub}, \psi_{dr}, \psi_{dg}, \psi_{db}, \psi_{sr}, \psi_{sg}, \psi_{sb}), \tag{3.3}$$

where each entry is a Dirac spinor and $\bar{q} = q^\dagger\gamma^0$. The dimensionful coupling constant, G_S, must be determined by experiments. A six-point 't Hooft interaction, which mixes all three flavours, is introduced by some authors in order to explain the mass splitting of the η and η' mesons. It is not known, however, if this difference should appear at the mean-field level, see the discussion in Paper I. The six-point interaction is therefore neglected here. The quark-quark interaction term, $\mathcal{L}_{qq}$, in (3.2) is introduced in order to allow for condensation of Cooper pairs ("diquarks"). In general, a diquark condensate is defined as an expectation value

$$\langle q^T \mathcal{O} q \rangle, \tag{3.4}$$

where $\mathcal{O}$ is an operator acting in the Dirac, flavour and colour spaces. Since quarks are fermions and obey the Pauli principle, $\{\psi_a, \psi_b\} = 0$, the operator $\mathcal{O}$ must be antisymmetric

$$q^T \mathcal{O} q = \mathcal{O}_{ab} q_a g_b = -\mathcal{O}_{ab} q_b g_a = -q^T \mathcal{O}^T q. \tag{3.5}$$

There are many possible operators that satisfy this condition [51]. The most important diquark condensates are on the form

$$s_{ab} = \langle q^T C \gamma_5 \tau_a \lambda_b q \rangle, \tag{3.6}$$

where C is the charge conjugation operator (see Appendix B) and τ_a (λ_b) are the antisymmetric Gell-Mann generators, λ_2, λ_5 and λ_7, in flavour (colour) space. This corresponds to diquark condensation in the scalar colour-antitriplet channel, which is the most attractive channel in one-gluon exchange and instanton-mediated interactions. The corresponding diquark contribution to the Lagrangian is

$$\mathcal{L}_{qq} = G_D \sum_{a=2,5,7} \sum_{b=2,5,7} (\bar{q} i \gamma_5 \tau_a \lambda_b C \bar{q}^T)(q^T C i \gamma_5 \tau_a \lambda_b \, q), \tag{3.7}$$

where G_D is the coupling constant.

In general, (3.6) is a 3x3 matrix with orthogonal rows and columns in colour and flavour space. This matrix can therefore be brought to triangular form by SU(3) rotations, so (3.6) has six non-zero elements. A Ginzburg-Landau analysis, see Section 5.1.1 in [51], shows that there are two ground states

$$s_{22} \neq 0 \;\text{ and }\; s_{ab} = 0 \;\text{ if }\; (a,b) \neq (2,2), \tag{3.8}$$

$$s_{22} = s_{55} = s_{77} \neq 0 \;\text{ and }\; s_{ab} = 0 \;\text{ if }\; a \neq b. \tag{3.9}$$

This is the two-flavour colour superconducting (2SC) phase and the colour-flavour locked (CFL) phase, respectively. It has been shown that for three flavours, the ground state of QCD at asymptotic densities is the CFL phase [59; 60]. For three degenerate flavours, the same is true for NJL-type models. Therefore, only the diagonal elements, s_{22}, s_{55} and s_{77} of (3.6) are considered here.

3.1.2 Mean-field Lagrangian

In order to obtain the mean-field thermodynamic potential, the Lagrangian is linearised in the diquark and quark-antiquark ("chiral") condensates. The hereby obtained mean-field Lagrangian (in Hartree approximation) is

$$\begin{aligned}\mathcal{L}^{MF} &= \bar{q}_{i\alpha}\left[i\partial\!\!\!/\delta_{ij}\delta_{\alpha\beta} - (\hat{m}_{ij} - 4G_S\langle\bar{q}_{i\alpha}q_{j\beta}\rangle\delta_{ij})\delta_{\alpha\beta} + \hat{\mu}_{ij,\alpha\beta}\gamma^0\right]q_{j\beta} \\ &-2G_S\sum_i\langle\bar{q}_i q_i\rangle^2 - \sum_{k,\gamma}\frac{|\Delta_{k\gamma}|^2}{4G_D} + \frac{1}{2}\left[\bar{q}_{i\alpha}\widehat{\Delta}_{ij,\alpha\beta}\,q^C_{j\beta} + \bar{q}^C_{i\alpha}\widehat{\Delta}^\dagger_{ij,\alpha\beta}\,q_{j\beta}\right], \end{aligned} \tag{3.10}$$

where the diquark gaps, $\Delta_{k\gamma}$, are

$$\Delta_{k\gamma} = 2G_D\langle\bar{q}_{i\alpha}i\gamma_5\epsilon_{\alpha\beta\gamma}\epsilon_{ijk}q^C_{j\beta}\rangle, \tag{3.11}$$

and

$$\widehat{\Delta}_{ij,\alpha\beta} = i\gamma_5\epsilon_{\alpha\beta\gamma}\epsilon_{ijk}\Delta_{k\gamma}. \tag{3.12}$$

Here, $\{\alpha,\ \beta,\ \gamma\}$ are colour indices ($r = 1$, $g = 2$ and $b = 3$) and $\{i,\ j,\ k\}$ are flavour indices ($u = 1$, $d = 2$ and $s = 3$). The Gell-Mann matrices in (3.6) has been replaced with Levi-Civita symbols in order to explicitly show the colour and flavour structure of the Lagrangian. This is possible since the diquark condensates are antisymmetric in colour and flavour. A consequence of this asymmetry is that the colour and flavour degrees of freedom of the diquark gaps are "locked"

$$\Delta_{ur} = \Delta_{ds}, \quad \Delta_{dg} = \Delta_{us}, \quad \Delta_{sb} = \Delta_{ud}. \tag{3.13}$$

According to (3.10), the chiral condensates, $\langle\bar{q}_{i\alpha}q_{j\beta}\rangle$, contribute to the masses of the quarks. The constituent mass matrix in flavour space is

$$M = \mathrm{diag}(m_u + \phi_u,\, m_d + \phi_d,\, m_s + \phi_s), \tag{3.14}$$

where

$$\phi_i = -4G_S\langle\bar{q}_i q_i\rangle \tag{3.15}$$

are the chiral gaps. By introducing eight-component Nambu-Gorkov spinors

$$\Psi = \begin{bmatrix} q \\ q^C \end{bmatrix} \quad \text{and} \quad \bar{\Psi} = \begin{bmatrix} \bar{q} & \bar{q}^C \end{bmatrix}, \tag{3.16}$$

the mean-field Lagrangian (3.10) can be written

$$\begin{aligned}\mathcal{L}^{MF} &= -\frac{\phi_u^2 + \phi_d^2 + \phi_s^2}{8G_S} - \frac{\Delta_{ud}^2 + \Delta_{us}^2 + \Delta_{ds}^2}{4G_D} \\ &+ \frac{1}{2}\bar{\Psi}\begin{bmatrix} i\partial\!\!\!/ - M + \hat{\mu}\gamma^0 & \widehat{\Delta} \\ \widehat{\Delta}^\dagger & i\partial\!\!\!/ - M - \hat{\mu}\gamma^0 \end{bmatrix}\Psi. \end{aligned} \tag{3.17}$$

Here, the diquark gaps have been denoted with flavour indices according to (3.13).

3.2 Thermodynamic Potential

The grand canonical thermodynamic potential can be obtained from the mean-field Lagrangian (3.17) within the imaginary-time formalism [56]. The partition function, Z, is as a functional integral of the fields

$$Z = N\int [d\bar{\Psi}][d\Psi]e^{S} = N\int [d\bar{\Psi}][d\Psi]\exp\left(\int_0^\beta d\tau\int d^3x\,\mathcal{L}^{MF}\right), \quad (3.18)$$

where $\beta = 1/T$ and N is a normalisation factor. The thermodynamic potential is

$$\Omega = -T\,\frac{\ln Z}{V}. \quad (3.19)$$

After expanding the spinors in Fourier series and performing the functional integrals over Grassman variables, see [56], the thermodynamic potential (3.19) is

$$\begin{aligned}\Omega(T,\mu) &= \frac{\phi_u^2+\phi_d^2+\phi_s^2}{8G_S}+\frac{\Delta_{ud}^2+\Delta_{us}^2+\Delta_{ds}^2}{4G_D}\\ &- T\sum_n\int\frac{d^3p}{(2\pi)^3}\frac{1}{2}\mathrm{Tr}\ln\left(\frac{1}{T}S^{-1}(i\omega_n,\vec{p})\right)-\Omega_0+\Omega_e, \quad (3.20)\end{aligned}$$

where $\omega_n = (2n+1)\pi T$ are the Matsubara frequencies for fermions and μ is the quark number chemical potential, see Section 3.3. $S^{-1}(p)$ is the inverse propagator of the quark fields at four momentum $p = (i\omega_n, \vec{p})$,

$$S^{-1}(i\omega_n,\vec{p}) = \begin{bmatrix} \not{p}-M+\hat{\mu}\gamma^0 & \widehat{\Delta} \\ \widehat{\Delta}^\dagger & \not{p}-M-\hat{\mu}\gamma^0 \end{bmatrix}, \quad (3.21)$$

where $\not{p} = \gamma^\mu p_\mu$. The thermodynamic potential at zero temperature and quark number chemical potential, $\Omega_0 = \Omega(T=0,\,\mu=0)$, has been subtracted in order to get zero pressure in vacuum. Explicitly,

$$\Omega_0 = \frac{\phi_{0u}^2+\phi_{0d}^2+\phi_{0s}^2}{8G_S}-2N_c\sum_i\int\frac{d^3p}{(2\pi)^3}\sqrt{M_i^2+p^2}, \quad (3.22)$$

where ϕ_{0i} are the vacuum values of the chiral gaps. The thermodynamic potential of ultrarelativistic electrons,

$$\Omega_e = -\frac{1}{12\pi^2}\mu_e^4-\frac{1}{6}\mu_e^2T^2-\frac{7}{180}\pi^2T^4, \quad (3.23)$$

has also been added to (3.20). Electrons must be taken into account in order to ensure that matter is electric charge neutral, see Section 3.3.

The trace in (3.20) can be evaluated with the identity $\mathrm{Tr}\ln(D) = \ln\det(D)$ (see Appendix E), and the Matsubara sum can, in principle, be calculated with the

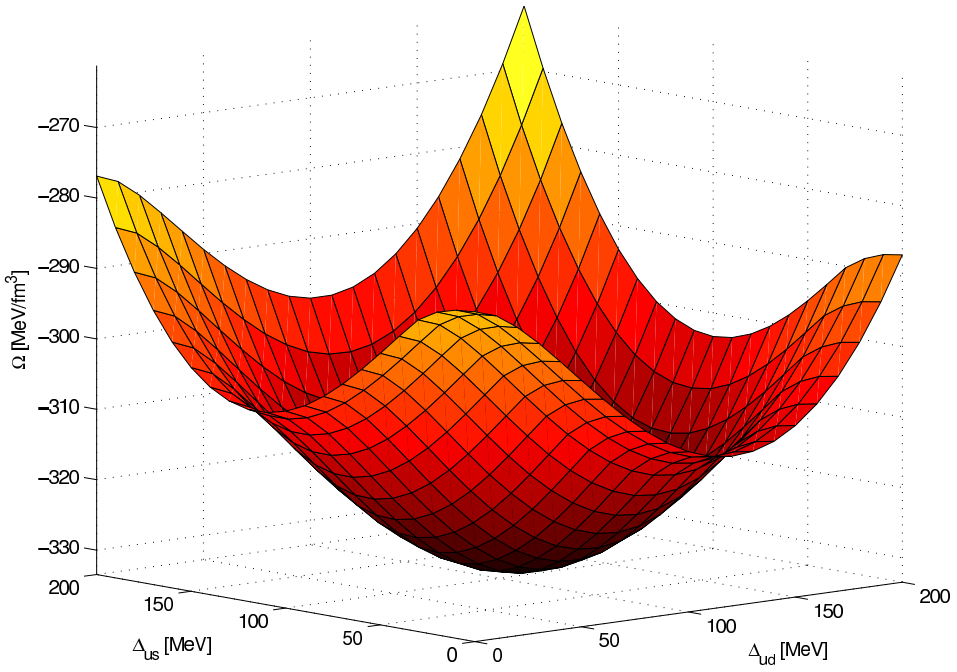

Figure 3.1: The grand canonical thermodynamic potential (3.20) at $\mu = 500$ MeV and $T = 0$, as a function of the diquark gaps Δ_{ud} and Δ_{us}. The global minima is at $\Delta_{ud} \simeq 114.8$ MeV and $\Delta_{us} \simeq 108.7$ MeV. All other quantities are fixed at their physical values, *i.e.*, at the global minima of Ω. Local electric and colour charge neutrality are imposed, see Section 3.3. Compare with Figure 1 and Figure 7 in Paper I.

method outlined in Appendix D.1. An alternative method, which explicitly yields the dispersion relations of the "quasiparticles" in the superconducting condensates, is described in Chapter 3.4. The values of the chiral and diquark gaps are determined by minimization of the thermodynamic potential (3.20), *i.e.*, the free energy. At the global minima of Ω, the pressure is $P = -\Omega$, see Appendix C. The energy minimization conditions can be formulated as a set of "gap equations",

$$\frac{\partial\Omega}{\partial\phi_u} = \frac{\partial\Omega}{\partial\phi_d} = \frac{\partial\Omega}{\partial\phi_s} = 0, \tag{3.24}$$

$$\frac{\partial\Omega}{\partial\Delta_{ud}} = \frac{\partial\Omega}{\partial\Delta_{us}} = \frac{\partial\Omega}{\partial\Delta_{ds}} = 0, \tag{3.25}$$

for the chiral and diquark gaps, respectively. It is not sufficient to find a stationary point of the thermodynamic potential, however, since the physical solution is the global minima of Ω. This can readily be understood by considering the relation between free energy and pressure, $P = -\Omega$. A local fluctuation with higher free

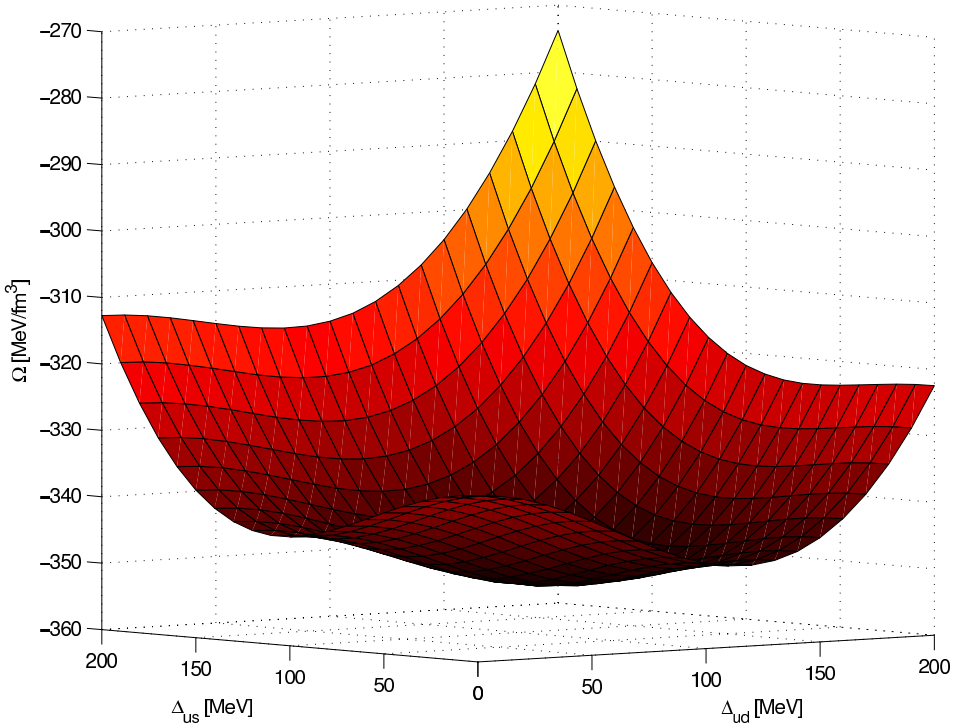

Figure 3.2: The grand canonical thermodynamic potential (3.20) at $\mu = 500$ MeV and $T = 40$ MeV, as a function of the diquark gaps Δ_{ud} and Δ_{us}. The global minima is at $\Delta_{ud} \simeq 107.2$ MeV and $\Delta_{us} \simeq 91.9$ MeV. All other quantities are fixed at their physical values. There are three competing extrema, one minima and two saddle points. If the system is heated to $T \simeq 53.1$ MeV at constant quark number chemical potential, μ, a phase transition occurres. For 53.1 MeV $\leq T \leq$ 72.8 MeV, the global minima is at $\Delta_{us} = 0$ and $\Delta_{ud} > 0$. Compare the relative size of the three extrema in this figure and in Figure 3.1. As the system undergoes heating, the phase where all three flavours participate in the superconducting condensate becomes less favourable, see Figure 5 in Paper I.

energy than the surrounding medium has lower pressure and is therefore unstable. In Figure 3.1 and Figure 3.2 the thermodynamic potential is plotted as a function of two diquark gaps. All other variational parameters are fixed at their physical values. The parameters of the model, *e.g.*, the coupling constants, are the same as in Paper I.

3.3 Charge Neutrality

Bulk matter (in compact stars) should be electric and colour charge neutral. Strictly speaking, matter should be in a colour singlet state. The free energy cost for projecting a colour neutral system into the colour singlet state is, however, negligible in the thermodynamic limit [61]. Therefore, only (local) colour neutrality is considered here. There are in total four conserved charges, the electric charge and three colour charges. The electric charge, Q, is (see Table 2-1)

$$n_Q = \frac{2}{3}n_u - \frac{1}{3}n_d - \frac{1}{3}n_s - n_e, \tag{3.26}$$

where n_e is the number density of electrons. The contribution from muons could also be included, but it is neglected here. For the colour charges it is practical to introduce the following linear combinations of charge densities [51]

$$n_3 = n_r - n_g, \tag{3.27}$$

$$n_8 = \frac{1}{\sqrt{3}}\left(n_r + n_g - 2n_b\right), \tag{3.28}$$

$$n = n_r + n_g + n_b, \tag{3.29}$$

where n is the total quark number density. The baryon number density is proportional to the quark number density, n, so baryon number is also a conserved quantity. The conserved charges in (3.26-3.29) have four associated chemical potentials, μ_Q, μ_3, μ_8 and μ. The number densities are related to the chemical potentials by (see Appendix C)

$$n_a = -\frac{\partial\Omega}{\partial\mu_a}. \tag{3.30}$$

The chemical potential of the electrons, μ_e, which appears in (3.23), is related to the electric charge chemical potential by $\mu_e = -\mu_Q$. The chemical potential matrix in colour and flavour space is

$$\hat{\mu} = \mu + \left(\frac{\tau_3}{2} + \frac{\tau_8}{2\sqrt{3}}\right)\mu_Q + \lambda_3\mu_3 + \lambda_8\mu_8, \tag{3.31}$$

where λ_a (τ_a) are Gell-Mann generators in colour (flavour) space. The quark number chemical potential, μ, is related to the baryon number chemical potential by $\mu = \mu_B/3$. Matter is electric and colour charge neutral if

$$n_Q = n_3 = n_8 = 0. \tag{3.32}$$

Thus, according to (3.30), the charge neutrality conditions are

$$\frac{\partial\Omega}{\partial\mu_Q} = \frac{\partial\Omega}{\partial\mu_3} = \frac{\partial\Omega}{\partial\mu_8} = 0. \tag{3.33}$$

In Figure 3.3 the thermodynamic potential is plotted as a function of μ_Q and μ_8. All other variational parameters are fixed at their physical values.

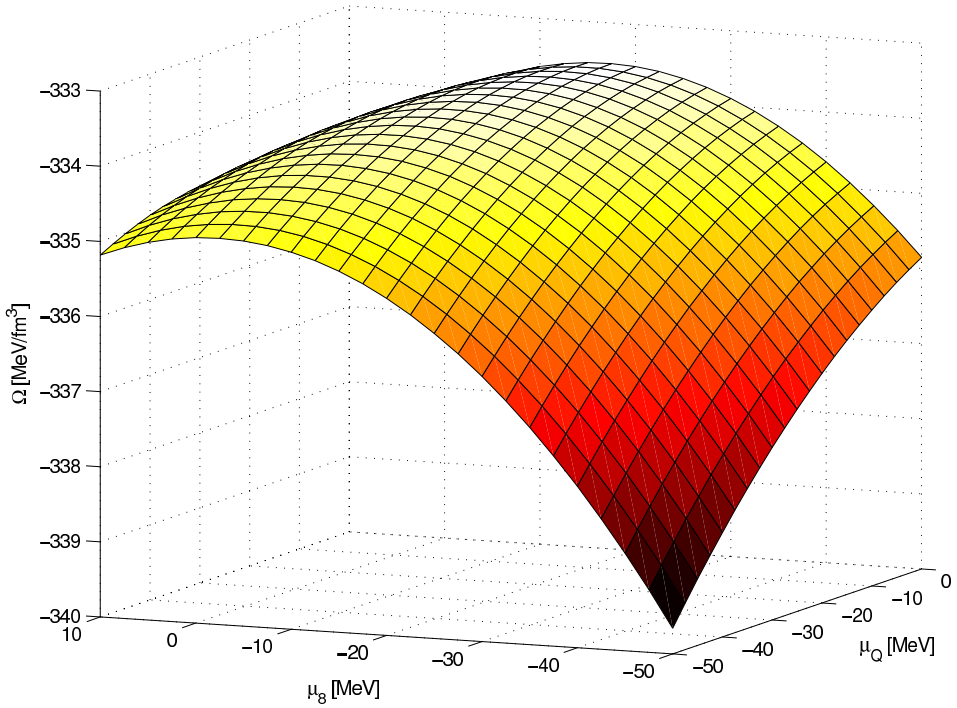

Figure 3.3: The grand canonical thermodynamic potential (3.20) at $\mu = 500$ MeV and $T = 0$, as a function of the chemical potentials μ_Q and μ_8. The charge neutrality conditions (3.33) are satisfied for $\mu_Q \simeq 0$ and $\mu_8 = -16.9$ MeV. All other quantities are fixed at their physical values. The free energy increases when charge neutrality is imposed. Compare with Figure 3 in Paper I.

3.4 Dispersion Relations

The Matsubara sum in the thermodynamic potential (3.20) can be evaluated on closed form, see Chapter II in Paper I and Appendix D. See also [62; 55]. The result is

$$\begin{aligned}\Omega(T,\mu) &= \frac{\phi_u^2+\phi_d^2+\phi_s^2}{8G_S}+\frac{\Delta_{ud}^2+\Delta_{us}^2+\Delta_{ds}^2}{4G_D} \\ &- \frac{1}{2}\int\frac{d^3p}{(2\pi)^3}\sum_a\left(\frac{E_a}{2}+T\ln\left(1+e^{-E_a/T}\right)\right)+\Omega_e-\Omega_0, \qquad (3.34)\end{aligned}$$

where E_a are the eigenvalues of the Hermitian matrix

$$\begin{bmatrix} -\gamma^0\vec{\gamma}\cdot\vec{p}-\gamma^0 M+\hat{\mu} & \gamma^0\widehat{\Delta}C \\ \gamma^0 C\widehat{\Delta}^\dagger & -\gamma^0\vec{\gamma}^T\cdot\vec{p}+\gamma^0 M-\hat{\mu}\end{bmatrix}. \qquad (3.35)$$

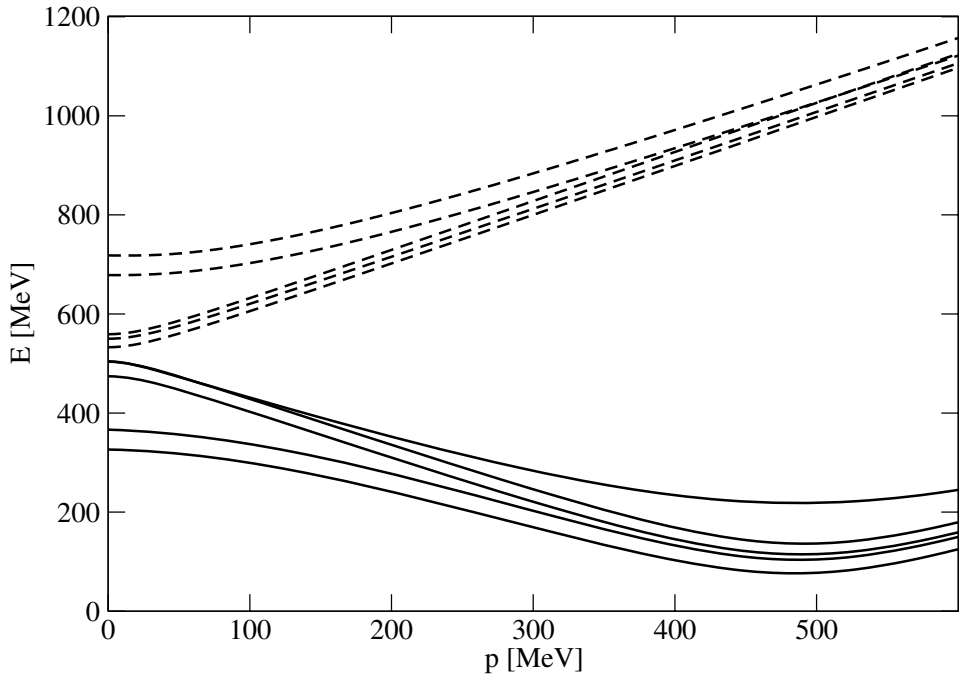

Figure 3.4: Quasiparticle (diquark) excitation energies at $\mu = 500$ MeV and $T = 0$ vs. the momentum, p. Solid lines represent the dispersion relations of quark pairs, while dashed lines represent the dispersion relations of antiquark pairs. All excitations are "gapped", *i.e.*, there is a forbidden energy band above the Fermi surface ($E = 0$).

Due to the colour, flavour and Nambu-Gorkov degrees of freedom, (3.35) is a 72x72 matrix. The explicit structure, as well as a simplified version of this matrix is given in the Appendix of Paper I. The eigenvalues, E_a, of this matrix are the dispersion relations of the quasiparticles, *i.e.*, the momentum dependent diquark excitation energies, see Figure 3.4. The model of three-flavour colour superconducting quark matter presented in Paper I is essentially (3.22-3.25) and (3.33-3.35).

Chapter 4

Concluding Remarks

The phase diagram of three-flavour colour superconducting quark matter is presented in Paper I. The influence of the superconducting condensates on the structure and cooling evolution of compact stars is also investigated. It is found that the colour-flavour locked (CFL) phase exists only at high values of the quark number chemical potential. At intermediate values, quark matter is in the (mixed) two-flavour colour superconducting (2SC) phase. It is shown that gapless excitations do not occur at temperatures relevant for compact star evolution. An improved analysis is needed in order to investigate the robustness of these results, in particular by including non-local form factors and the effects of the hadronic medium on the colour superconducting condensates. For the solutions to the stellar structure equations, the influence of a hadronic shell remains to be investigated. The numerical tools that have been developed will be a valuable resource in the forthcoming work.

In Paper II it is suggested that preons, which might be the building blocks of quarks and leptons, could allow for a new class of stable compact stars, so-called preon stars. The idea is further developed in Paper III, where the possibility that preon stars formed in the early universe is investigated and a potential method to observe them is discussed. In Paper IV the observational signature of preon stars is compared to data. It is shown that preon stars can explain the peculiar absorption-line features that have been observed in the spectra of some gamma-ray bursts. The preon star hypothesis has been recognized in the media, see, *e.g.*, [8], and it has been awarded by the International School of Subnuclear Physics.

Bibliography

[1] N. K. Glendenning, *Compact Stars: Nuclear Physics, Particle Physics, and General Relativity*. New York, USA: Springer (2000) 467 p.

[2] S. L. Shapiro and S. A. Teukolsky, *Black holes, white dwarfs, and neutron stars: The physics of compact objects*. New York, USA: Wiley (1983) 645 p.

[3] W. Baade and F. Zwicky, *Phys. Rev.* **45**, 138 (1934).

[4] D. Blaschke, S. Fredriksson, H. Grigorian, A. M. Öztaş, and F. Sandin, `arXiv:hep-ph/0503194`. Submitted to *Phys. Rev.* **D**.

[5] F. Weber, *Prog. Part. Nucl. Phys.* **54**, 193 (2005); `arXiv:astro-ph/0407155`.

[6] J. Hansson and F. Sandin, `arXiv:astro-ph/0410417`. *Phys. Lett.* **B**, in press (2005).

[7] F. Sandin, *Eur. Phys. J.* **C** (2004), `doi:10.1140/epjcd/s2005-03-003-y`. Also to appear in the proceedings of ISSP 2004.

[8] H. Muir, *New Scientist* **184**, 19 (2004).

[9] J. Hansson and F. Sandin. Appended, to be submitted for publication.

[10] I. A. D'Souza and C. S. Kalman, *Preons: Models of leptons, quarks and gauge bosons as composite objects*. Singapore, Singapore: World Scientific (1992) 108 p.

[11] J.-J. Dugne, S. Fredriksson, and J. Hansson, *Europhys. Lett.* **57**, 188 (2002); `arXiv:hep-ph/0208135`.

[12] S. Fredriksson, `arXiv:hep-ph/0309213`. Proc. of the Fourth Tegernsee Int. Conf. on Particle Physics Beyond the Standard Model, ed. by H.-V. Klapdor-Kleingrothaus. Heidelberg, Germany: Springer-Verlag (2004), 1117 p.

[13] M. Gyulassy and L. McLerran, *Nucl. Phys.* **A750**, 30 (2005); arXiv:nucl-th/0405013.

[14] D. H. Rischke, *Prog. Part. Nucl. Phys.* **52**, 197 (2004); arXiv:nucl-th/0305030.

[15] M. G. Alford, *Ann. Rev. Nucl. Part. Sci.* **51**, 131 (2001); arXiv:hep-ph/0102047.

[16] K. Rajagopal and F. Wilczek, arXiv:hep-ph/0011333.

[17] H. Heiselberg and M. Hjorth-Jensen, *Phys. Rept.* **328**, 237 (2000); arXiv:nucl-th/9902033.

[18] **Particle Data Group** Collaboration, S. Eidelman *et al.*, *Phys. Lett.* **B592**, 1 (2004); http://pdg.lbl.gov.

[19] D. J. Gross and F. Wilczek, *Phys. Rev. Lett.* **30**, 1343 (1973).

[20] H. D. Politzer, *Phys. Rev. Lett.* **30**, 1346 (1973).

[21] D. Ivanenko and D. F. Kurdgelaidze, *Astrofiz.* **1**, 479 (1965).

[22] D. Ivanenko and D. F. Kurdgelaidze, *Lett. Nuovo Cim.* **2**, 13 (1969).

[23] N. Itoh, *Progr. Theoret. Phys.* **44**, 291 (1970).

[24] F. Iachello, W. D. Langer, and A. Lande, *Nucl. Phys.* **A219**, 612 (1974).

[25] J. C. Collins and M. J. Perry, *Phys. Rev. Lett.* **34**, 1353 (1975).

[26] A. R. Bodmer, *Phys. Rev.* **D4**, 1601 (1971).

[27] J. Cleymans, R. V. Gavai, and E. Suhonen, *Phys. Rept.* **130**, 217 (1986).

[28] H. Meyer-Ortmanns, *Rev. Mod. Phys.* **68**, 473 (1996); arXiv:hep-lat/9608098.

[29] E. Witten, *Phys. Rev.* **D30**, 272 (1984).

[30] W. Busza, R. L. Jaffe, J. Sandweiss, and F. Wilczek, *Rev. Mod. Phys.* **72**, 1125 (2000); arXiv:hep-ph/9910333.

[31] C. Kettner, F. Weber, M. K. Weigel, and N. K. Glendenning, *Phys. Rev.* **D51**, 1440 (1995).

[32] E. Laermann and O. Philipsen, *Ann. Rev. Nucl. Part. Sci.* **53**, 163 (2003); arXiv:hep-ph/0303042.

[33] S. Muroya, A. Nakamura, C. Nonaka, and T. Takaishi, *Prog. Theor. Phys.* **110**, 615 (2003); arXiv:hep-lat/0306031.

[34] **HPQCD** Collaboration, C. T. H. Davies *et al.*, *Phys. Rev. Lett.* **92**, 022001 (2004); arXiv:hep-lat/0304004.

[35] Z. Fodor and S. D. Katz, *JHEP* **04**, 050 (2004); arXiv:hep-lat/0402006.

[36] E. Farhi and R. L. Jaffe, *Phys. Rev.* **D30**, 2379 (1984).

[37] A. Chodos, R. L. Jaffe, K. Johnson, C. B. Thorn, and V. F. Weisskopf, *Phys. Rev.* **D9**, 3471 (1974).

[38] A. Chodos, R. L. Jaffe, K. Johnson, and C. B. Thorn, *Phys. Rev.* **D10**, 2599 (1974).

[39] L. N. Cooper, *Phys. Rev.* **104**, 1189 (1956).

[40] J. Bardeen, L. N. Cooper, and J. R. Schrieffer, *Phys. Rev.* **106**, 162 (1957).

[41] J. Bardeen, L. N. Cooper, and J. R. Schrieffer, *Phys. Rev.* **108**, 1175 (1957).

[42] C. Chin, M. B. A. Altmeyer, S. Riedl, S. Jochim, J. H. Denschlag, and R. Grimm, *Science* **305**, 1128 (2004); arXiv:cond-mat/0405632.

[43] B. C. Barrois, *Nucl. Phys.* **B129**, 390 (1977).

[44] S. C. Frautschi. Presented at Workshop on Hadronic Matter at Extreme Energy Density, Erice, Italy, Oct 13-21, 1978.

[45] D. Bailin and A. Love, *Phys. Rept.* **107**, 325 (1984).

[46] M. G. Alford, K. Rajagopal, and F. Wilczek, *Phys. Lett.* **B422**, 247 (1998); arXiv:hep-ph/9711395.

[47] R. Rapp, T. Schafer, E. V. Shuryak, and M. Velkovsky, *Phys. Rev. Lett.* **81**, 53 (1998); arXiv:hep-ph/9711396.

[48] D. Blaschke and C. D. Roberts, *Nucl. Phys.* **A642**, 197 (1998); arXiv:nucl-th/9807008.

[49] D. K. Hong, *Acta Phys. Polon.* **B32**, 1253 (2001); arXiv:hep-ph/0101025.

[50] T. Schafer, arXiv:hep-ph/0304281.

[51] M. Buballa, *Phys. Rept.* **407**, 205 (2005); arXiv:hep-ph/0402234.

[52] H.-C. Ren, arXiv:hep-ph/0404074.

[53] M. Huang, arXiv:hep-ph/0409167.

[54] A. Schmitt, *Phys. Rev.* **D71**, 054016 (2005); arXiv:nucl-th/0412033.

[55] S. B. Ruster, V. Werth, M. Buballa, I. A. Shovkovy, and D. H. Rischke, arXiv:hep-ph/0503184.

[56] J. I. Kapusta, *Finite-Temperature Field Theory.* New York, USA: Cambridge University Press (1993) 232 p.

[57] Y. Nambu and G. Jona-Lasinio, *Phys. Rev.* **122**, 345 (1961).

[58] Y. Nambu and G. Jona-Lasinio, *Phys. Rev.* **124**, 246 (1961).

[59] T. Schafer, *Nucl. Phys.* **B575**, 269 (2000); arXiv:hep-ph/9909574.

[60] N. J. Evans, J. Hormuzdiar, S. D. H. Hsu, and M. Schwetz, *Nucl. Phys.* **B581**, 391 (2000); arXiv:hep-ph/9910313.

[61] P. Amore, M. C. Birse, J. A. McGovern, and N. R. Walet, *Phys. Rev.* **D65**, 074005 (2002); arXiv:hep-ph/0110267.

[62] A. W. Steiner, S. Reddy, and M. Prakash, *Phys. Rev.* **D66**, 094007 (2002); arXiv:hep-ph/0205201.

[63] M. Buballa and M. Oertel, *Nucl. Phys.* **A703**, 770 (2002); arXiv:hep-ph/0109095.

Appendix A

Units

A.1 Natural Units

Since the speed of light in vacuum, c, and the reduced Planck constant, $\hbar$, are frequently encountered constants in high-energy physics, it is convenient to choose units such that these two constants are set to unity. In these so-called natural units, length, time and mass are related by [18]

$$c = 1 = 2.99792458 \times 10^{8} \text{ m s}^{-1}, \tag{A.1}$$
$$\hbar = 1 = 1.05457168 \times 10^{-34} \text{ kg m}^{2} \text{ s}^{-1}. \tag{A.2}$$

Mass is related to energy by $m = E/c^2$, so mass and energy have the same unit. If the unit of energy is MeV (1 eV= $1.60217653 \times 10^{-19}$ J) and the unit of length is fm (10^{-15} m),

$$\hbar c = 197.33 \text{ MeV fm}, \tag{A.3}$$
$$\hbar = 6.5821 \times 10^{-22} \text{ MeV s}. \tag{A.4}$$

The following conversion factors are useful

$$1 \text{ MeV}^3 = 1.3015 \times 10^{-7} \text{ fm}^{-3}, \tag{A.5}$$
$$1 \text{ MeV}^4 = 2.3201 \times 10^{5} \text{ g cm}^{-3}, \tag{A.6}$$
$$1 \text{ MeV fm}^{-3} = 1.7827 \times 10^{12} \text{ g cm}^{-3}. \tag{A.7}$$

In finite temperature field theory, it is convenient to choose the unit of temperature such that Boltzmann's constant is set to unity,

$$k_B = 1 = 8.617343 \times 10^{-5} \text{ eV K}^{-1}. \tag{A.8}$$

Temperatures can then be expressed in MeV,

$$1 \text{ MeV} = 1.1605 \times 10^{10} \text{ K}. \tag{A.9}$$

A.2 Gravitational Units

For compact star calculations, it is convenient to choose units such that $c = G = 1$. In these so-called gravitational units, length, time and mass are related by [18]

$$c = 1 = 2.99792458 \times 10^8 \text{ m s}^{-1}, \tag{A.10}$$
$$G = 1 = 6.6742 \times 10^{-11} \text{ m}^3 \text{ kg}^{-1} \text{ s}^{-2}. \tag{A.11}$$

It is common practise to express all quantities in km (10^3 m). The following conversion factors are useful

$$1 \text{ s} = 2.9979 \times 10^5 \text{ km}, \tag{A.12}$$
$$1 \text{ kg} = 7.4260 \times 10^{-31} \text{ km}, \tag{A.13}$$
$$1 \text{ g cm}^{-3} = 7.4237 \times 10^{-19} \text{ km}^{-2}, \tag{A.14}$$
$$1 \text{ MeV fm}^{-3} = 1.3234 \times 10^{-6} \text{ km}^{-2}. \tag{A.15}$$

The total gravitational mass of a star is typically given in units of the solar mass,

$$1 \text{ M}_\odot = 1.4766 \text{ km}. \tag{A.16}$$

Appendix B

Matrices and Generators

B.1 Pauli Matrices

The Pauli matrices, σ_a, are infinitesimal generators of SU(2), which typically are used to describe the spin of non-relativistic fermions. In the standard basis

$$\sigma_1 = \begin{bmatrix} 0 & 1 \\ 1 & 0 \end{bmatrix}, \quad \sigma_2 = \begin{bmatrix} 0 & -i \\ i & 0 \end{bmatrix}, \quad \sigma_3 = \begin{bmatrix} 1 & 0 \\ 0 & -1 \end{bmatrix}. \tag{B.1}$$

These matrices satisfy the commutation and anticommutation relations

$$[\sigma_a, \sigma_b] = 2i\,\epsilon_{abc}\,\sigma_c, \tag{B.2}$$

$$\{\sigma_a, \sigma_b\} = 2\delta_{ab}, \tag{B.3}$$

and are traceless and Hermitian.

B.2 Dirac Matrices

The Dirac matrices, $\gamma^\mu = (\gamma^0, \gamma^1, \gamma^2, \gamma^3)$, are defined by the anticommutation relations $\{\gamma^\mu, \gamma^\nu\} = 2\eta^{\mu\nu}$, where $\eta^{\mu\nu}$ is the Minkowski metric. In the Weyl (or chiral) basis, the Dirac matrices are

$$\gamma^0 = \begin{bmatrix} 0 & 1 \\ 1 & 0 \end{bmatrix}, \quad \gamma^a = \begin{bmatrix} 0 & \sigma_a \\ -\sigma_a & 0 \end{bmatrix}, \tag{B.4}$$

where 1 is the 2x2 identity matrix and σ_a are the Pauli matrices. In this representation, the chirality matrix is

$$\gamma^5 \equiv \gamma_5 \equiv i\gamma^0\gamma^1\gamma^2\gamma^3 = \begin{bmatrix} -1 & 0 & 0 & 0 \\ 0 & -1 & 0 & 0 \\ 0 & 0 & 1 & 0 \\ 0 & 0 & 0 & 1 \end{bmatrix}, \tag{B.5}$$

and the charge conjugation matrix is

$$C = i\gamma^2\gamma^0 = \begin{bmatrix} 0 & -1 & 0 & 0 \\ 1 & 0 & 0 & 0 \\ 0 & 0 & 0 & 1 \\ 0 & 0 & -1 & 0 \end{bmatrix}. \tag{B.6}$$

B.3 Gell-Mann Matrices

The Gell-Mann matrices, λ_a, are infinitesimal generators of SU(3),

$$\begin{aligned} \lambda_1 &= \begin{bmatrix} 0 & 1 & 0 \\ 1 & 0 & 0 \\ 0 & 0 & 0 \end{bmatrix}, \quad \lambda_2 = \begin{bmatrix} 0 & -i & 0 \\ i & 0 & 0 \\ 0 & 0 & 0 \end{bmatrix}, \\ \lambda_3 &= \begin{bmatrix} 1 & 0 & 0 \\ 0 & -1 & 0 \\ 0 & 0 & 0 \end{bmatrix}, \quad \lambda_4 = \begin{bmatrix} 0 & 0 & 1 \\ 0 & 0 & 0 \\ 1 & 0 & 0 \end{bmatrix}, \\ \lambda_5 &= \begin{bmatrix} 0 & 0 & -i \\ 0 & 0 & 0 \\ i & 0 & 0 \end{bmatrix}, \quad \lambda_6 = \begin{bmatrix} 0 & 0 & 0 \\ 0 & 0 & 1 \\ 0 & 1 & 0 \end{bmatrix}, \\ \lambda_7 &= \begin{bmatrix} 0 & 0 & 0 \\ 0 & 0 & -i \\ 0 & i & 0 \end{bmatrix}, \quad \lambda_8 = \tfrac{1}{\sqrt{3}} \begin{bmatrix} 1 & 0 & 0 \\ 0 & 1 & 0 \\ 0 & 0 & -2 \end{bmatrix}. \end{aligned} \tag{B.7}$$

These matrices satisfy the commutation relations,

$$[\lambda_a, \lambda_b] = i f_{abc} \lambda_c, \tag{B.8}$$

where f_{abc} are the antisymmetric group structure constants. The Gell-Mann matrices are used, *e.g.*, to describe colour charge, in a similar way as the Pauli matrices are used to describe spin and isospin. Like the Pauli matrices, the Gell-Mann matrices are traceless and Hermitian.

Appendix C

Thermodynamic Relations

In the following, a list of frequently encountered thermodynamic relations in finite temperature field theory is presented. If variational parameters are introduced, *e.g.*, condensate fields, the functions given below are at the extremum with respect to variations of these parameters. For a system described by a Hamiltonian, H, and a set of conserved number operators, $\hat{N}_i$, the grand canonical partition function is

$$Z(\mu, T, V) = \mathrm{Tr}\, e^{-\beta(H-\mu_i \hat{N}_i)}. \tag{C.1}$$

Here, μ_i are the chemical potentials conjugate to the conserved charges and $\beta = 1/T$. The number operators must be Hermitian and must commute with H, as well as with each other. In most modern applications, it is convenient to express the partition function as a functional integral of the fields

$$Z(\mu, T, V) = N \int [\phi]\, e^{S}, \tag{C.2}$$

where N is a normalisation factor and S is the action,

$$S = \int_0^\beta d\tau \int d^3x\, \mathcal{L}. \tag{C.3}$$

For further information, see [56]. The grand canonical thermodynamic potential is

$$\Omega(\mu, T) = -\frac{T \ln Z}{V}. \tag{C.4}$$

The pressure, P, is related to the thermodynamic potential by

$$P(\mu, T) = -\Omega(\mu, T), \tag{C.5}$$

at the global minimum of Ω with respect to all variational parameters.

The entropy density, s, and number densities, n_i, are

$$s(\mu, T) = \frac{\partial P(\mu, T)}{\partial T}, \tag{C.6}$$

$$n_i(\mu, T) = \frac{\partial P(\mu, T)}{\partial \mu_i}. \tag{C.7}$$

The thermodynamic potential should be normalised such that the pressure in vacuum, $P = -\Omega(0, 0)$, is zero. The energy density, ϵ, then is

$$\epsilon = Ts + \sum_i \mu_i \, n_i - P. \tag{C.8}$$

Appendix D

Matsubara Sums

The following Matsubara sum is frequently encountered in finite temperature field theory, see, *e.g.*, [4; 55],

$$T\sum_n \ln\left(\frac{\omega_n^2+\omega^2}{T^2}\right), \tag{D.1}$$

where $\omega_n = (2n+1)\pi T$ are the Matsubara frequencies for fermions. The standard result is

$$T\sum_n \ln\left(\frac{\omega_n^2+\omega^2}{T^2}\right) = \omega + 2T\ln(1+e^{-\omega/T}). \tag{D.2}$$

A brief derivation of this relation is given in [56]. There are, however, a few points that are important to understand. The full derivation is therefore given here for clarity. First rewrite the logarithm as an integral and change the order of summation and integration,

$$\begin{aligned}
&\sum_{n=-\infty}^{\infty} \ln\left(\frac{\omega_n^2+\omega^2}{T^2}\right) = \\
&\sum_{n=-\infty}^{\infty} \int_1^{\omega^2/T^2} \frac{d(\theta^2)}{\theta^2+(2n+1)^2\pi^2} + \ln(1+(2n+1)^2\pi^2) = \\
&\int_1^{\omega^2/T^2} \sum_{n=-\infty}^{\infty} \frac{1}{\theta^2+(2n+1)^2\pi^2} d(\theta^2) + \sum_{n=-\infty}^{\infty} \ln(1+(2n+1)^2\pi^2).
\end{aligned} \tag{D.3}$$

The standard residue summation formula

$$\sum_{n=-\infty}^{\infty} \frac{1}{(n-x)(n-y)} = \frac{\pi(\cot(\pi x)-\cot(\pi y))}{y-x}, \tag{D.4}$$

can be used to evaluate the first sum in (D.3),

$$\sum_{n=-\infty}^{\infty} \frac{1}{\theta^2+(2n+1)^2\pi^2} = \frac{1}{4\pi^2} \sum_{n=-\infty}^{\infty} \frac{1}{(n-\frac{\pi-i\theta}{2\pi})(n-\frac{\pi+i\theta}{2\pi})} =$$
$$\frac{1}{4\pi^2} \frac{\pi\left(\cot\left(\frac{\pi-i\theta}{2}\right)-\cot\left(\frac{\pi+i\theta}{2}\right)\right)}{4i\theta/\pi} = \frac{1}{2\theta}\tanh\left(\frac{\theta}{2}\right) = \frac{1}{\theta}\left[\frac{1}{2}-\frac{1}{e^\theta+1}\right]. \quad \text{(D.5)}$$

Equations (D.3) and (D.5) yield

$$\sum_{n=-\infty}^{\infty} \ln\left(\frac{\omega_n^2+\omega^2}{T^2}\right) =$$
$$\int_1^{\omega^2/T^2} \frac{1}{\theta}\left[\frac{1}{2}-\frac{1}{e^\theta+1}\right] d(\theta^2) + \sum_{n=-\infty}^{\infty} \ln(1+(2n+1)^2\pi^2) =$$
$$-\frac{|\omega|}{T} + 2\ln(1+e^{|\omega|/T}) + 1 - 2\ln(1+e^1) + \sum_{n=-\infty}^{\infty} \ln(1+(2n+1)^2\pi^2) =$$
$$-\frac{|\omega|}{T} + 2\ln(e^{|\omega|/T}(1+e^{-|\omega|/T})) +$$
$$1 - 2\ln(1+e^1) + \sum_{n=-\infty}^{\infty} \ln(1+(2n+1)^2\pi^2) =$$
$$\frac{|\omega|}{T} + 2\ln(1+e^{-|\omega|/T}) +$$
$$\left[1 - 2\ln(1+e^1) + \sum_{n=-\infty}^{\infty} \ln(1+(2n+1)^2\pi^2)\right]. \quad \text{(D.6)}$$

Terms independent of T and $\omega = \omega(\mu)$ do not contribute to the physical quantities (see Chapter C) and can hence be dropped. Since the expression on the left-hand side of (D.6) is even in ω, the expression simplifies to

$$\sum_{n=-\infty}^{\infty} \ln\left(\frac{\omega_n^2+\omega^2}{T^2}\right) = \frac{\omega}{T} + 2\ln\left(1+e^{-\omega/T}\right), \quad \text{(D.7)}$$

which essentially is (D.2). One can explicitly verify that the expression on the right-hand side of (D.7) is even in ω,

$$f(T,\omega) - f(T,-\omega) = \frac{2\omega}{T} + 2\ln\left(1+e^{-\omega/T}\right) - 2\ln\left(1+e^{\omega/T}\right) =$$
$$\frac{2\omega}{T} + 2\ln\left(\frac{1+e^{-\omega/T}}{1+e^{\omega/T}}\right) = \frac{2\omega}{T} + 2\ln\left(\frac{1+e^{-\omega/T}}{1+e^{\omega/T}} \times \frac{1-e^{-\omega/T}}{1-e^{-\omega/T}}\right) =$$

$$\frac{2\omega}{T} + 2\ln\left(\frac{1-e^{-2\omega/T}}{e^{\omega/T}-e^{-\omega/T}}\right) = \frac{2\omega}{T} + 2\ln\left(\frac{1-e^{-2\omega/T}}{e^{\omega/T}(1-e^{-2\omega/T})}\right) =$$
$$\frac{2\omega}{T} + 2\ln\left(e^{-\omega/T}\right) = \frac{2\omega}{T} - \frac{2\omega}{T} = 0. \tag{D.8}$$

D.1 Numerical Evaluation

In general, Matsubara sums can be more complicated than (D.1). If an analytical solution cannot be obtained, it is possible to evaluate the Matsubara sum numerically if the divergent terms can be accounted for. It is not possible to evaluate, *e.g.*, (D.1) directly on a computer, due to the divergent sum on the right-hand side of (D.6). The solution to this problem is to subtract a Matsubara sum that can be evaluated analytically, such that the difference of the two sums is convergent. The original Matsubara sum can then be recovered by adding the analytical solution of the subtracted sum, neglecting all unphysical terms. It is crucial to subtract a Matsubara sum that is "similar" to the sum that should be computed, in order to get (rapid) convergence. A nice heuristic example where this method has been used can be found in [63].

Appendix E

Determinants

In finite temperature field theory, determinants are frequently used to express the trace of various operators, *e.g.*, the statistical density matrix in (C.1). This is due to the identity

$$\mathrm{Tr}\ \ln S = \ln \det S, \tag{E.1}$$

where S is the operator. The following relations are useful to simplify and evaluate determinants

$$\det S \equiv \left|\ S\ \right| \equiv \left|\begin{array}{cc} A & B \\ C & D \end{array}\right| = \left|\ A\ \right| \left|\ D - CA^{-1}B\ \right|. \tag{E.2}$$

The NxN block matrices A, B, C and D should be ordered wisely using the identities

$$\left|\begin{array}{cc} A & B \\ C & D \end{array}\right| = \left|\begin{array}{cc} D & C \\ B & A \end{array}\right| = (-1)^N \left|\begin{array}{cc} B & A \\ D & C \end{array}\right| = (-1)^N \left|\begin{array}{cc} C & D \\ A & B \end{array}\right|. \tag{E.3}$$

These relations can be used recursively to evaluate and simplify determinants. The dimension of the operator is reduced by a factor two for each recursion. The trade-off being that the inverse of one submatrix must be evaluated for each recursion (in numerical applications) or that the matrix elements become more involved (in analytical applications). The proof of (E.2) is straightforward, consider a matrix on the form

$$S = \left[\begin{array}{cc} A & B \\ C & D \end{array}\right], \tag{E.4}$$

where A, B, C and D are NxN submatrices. If A has an inverse, it follows that

$$\left[\begin{array}{cc} I & 0 \\ -CA^{-1} & I \end{array}\right] \left[\begin{array}{cc} A & B \\ C & D \end{array}\right] = \left[\begin{array}{cc} I & B \\ 0 & -CA^{-1}B + D \end{array}\right] \left[\begin{array}{cc} A & 0 \\ 0 & I \end{array}\right], \tag{E.5}$$

where I is the NxN identity matrix.

Cofactor expansion yields

$$\begin{vmatrix} A & 0 \\ 0 & I \end{vmatrix} = \mid A \mid, \tag{E.6}$$

$$\begin{vmatrix} I & 0 \\ -CA^{-1} & I \end{vmatrix} = 1, \tag{E.7}$$

$$\begin{vmatrix} I & B \\ 0 & -CA^{-1}B + D \end{vmatrix} = \mid D - CA^{-1}B \mid. \tag{E.8}$$

Since $\det(AB) = \det(A)\det(B)$ it follows that

$$\begin{vmatrix} A & B \\ C & D \end{vmatrix} = \mid A \mid \mid D - CA^{-1}B \mid, \tag{E.9}$$

which completes the proof.

Summary of

Appended Papers

I. The phase diagram of three-flavour colour superconducting quark matter is investigated within a Nambu–Jona-Lasinio model. Local colour and electric charge neutrality are imposed. The influence of the various superconducting condensates on the structure and cooling evolution of compact stars are investigated. It is found that: i) the colour-flavour locked phase exists only at high values of the quark number chemical potential. ii) gapless excitations do not occur at temperatures relevant for compact star evolution. iii) the mass defect due to cooling can be of the order of 0.1 $M_\odot$.

II. It is suggested that preons allow for a new class of stable compact stars, so-called preon stars. The density, mass and radius of preon stars are estimated and the general relativistic stability conditions are evaluated. Some astrophysical consequences of preon stars are discussed.

III. The suggestion in **Paper II** is put into perspective. The possibility that preon stars formed in the early universe is discussed and a method to detect them is suggested.

IV. The observational signature of preon stars, as outlined in **Paper III**, is compared with gamma-ray burst (GRB) data. It is shown that preon stars can explain the peculiar absorption-line features that have been found in some low-energy GRB spectra.

Paper I

The phase diagram of three-flavor quark matter under compact star constraints

D. Blaschke,[1,*] S. Fredriksson,[2,†] H. Grigorian,[3,‡] A.M. Öztaş,[4,§] and F. Sandin[2,¶]

[1] *Gesellschaft für Schwerionenforschung mbH (GSI), D-64291 Darmstadt, Germany, and Bogoliubov Laboratory for Theoretical Physics, JINR Dubna, 141980 Dubna, Russia*
[2] *Department of Physics, Luleå University of Technology, SE-97187 Luleå, Sweden*
[3] *Institut für Physik, Universität Rostock, D-18051 Rostock, Germany, and Department of Physics, Yerevan State University, 375025 Yerevan, Armenia*
[4] *Department of Physics, Hacettepe University, TR-06532 Ankara, Turkey*

The phase diagram of three-flavor quark matter under compact star constraints is investigated within a Nambu–Jona-Lasinio model. Local color and electric charge neutrality is imposed for β-equilibrated superconducting quark matter. The constituent quark masses and the diquark condensates are determined selfconsistently in the plane of temperature and quark chemical potential. Both strong and intermediate diquark coupling strengths are considered. We show that in both cases, gapless superconducting phases do not occur at temperatures relevant for compact star evolution, *i.e.*, below $T \sim 50$ MeV. The stability and structure of isothermal quark star configurations are evaluated. For intermediate coupling, quark stars are composed of a mixed phase of normal (NQ) and two-flavor superconducting (2SC) quark matter up to a maximum mass of 1.21 $M_\odot$. At higher central densities, a phase transition to the three-flavor color flavor locked (CFL) phase occurs and the configurations become unstable. For the strong diquark coupling we find stable stars in the 2SC phase, with masses up to 1.326 $M_\odot$. A second family of more compact configurations (twins) with a CFL quark matter core and a 2SC shell is also found to be stable. The twins have masses in the range 1.301...1.326 $M_\odot$. We consider also hot isothermal configurations at temperature $T = 40$ MeV. When the hot maximum mass configuration cools down, due to emission of photons and neutrinos, a mass defect of 0.1 $M_\odot$ occurs and two final state configurations are possible.

PACS numbers: 12.38.Mh, 24.85.+p, 26.60.+c, 97.60.-s

I. INTRODUCTION

Theoretical investigations of the QCD phase diagram at high densities have recently gained momentum due to results of non-perturbative low-energy QCD models [1, 2, 3] of color superconductivity in quark matter [4, 5]. These models predict that the diquark pairing condensates are of the order of 100 MeV and a remarkably rich phase structure has been identified [6, 7, 8, 9]. The main motivation for studying the low-temperature domain of the QCD phase diagram is its possible relevance for the physics of compact stars [10, 11, 12]. Observable effects of color superconducting phases in compact stars are expected, *e.g.*, in the cooling behavior [13, 14, 15, 16, 17], magnetic field evolution [18, 19, 20, 21], and in burst-type phenomena [22, 23, 24, 25, 26].

The most prominent color superconducting phases with large diquark pairing gaps are the two-flavor scalar diquark condensate (2SC) and the color-flavor locking (CFL) condensate. The latter requires approximate SU(3) flavor symmetry and occurs therefore only at rather large quark chemical potentials, $\mu_q > 430 - 500$ MeV, of the order of the dynamically generated strange quark mass M_s, whereas the 2SC phase can appear already at the chiral restoration transition for $\mu_q > 330 - 350$ MeV [27, 28, 29]. Note that the quark chemical potential in the center of a typical compact star is expected to not exceed a value of ~ 500 MeV, so that the volume fraction of a strange quark matter phase will be insufficient to entail observable consequences. However, when the strange quark mass is considered not dynamically, but as a free parameter independent of the thermodynamical conditions, it has been shown that for not too large M_s the CFL phase dominates over the 2SC phase [30, 31]. Studies of the QCD phase diagram with fixed strange quark mass have recently been extended to the discussion of gapless CFL (gCFL) phases [32, 33, 34]. The gapless phases occur when the asymmetry between Fermi levels of different flavors is large enough to allow for zero energy excitations while a finite pairing gap exists. They have been found first for the 2SC phase (g2SC) within a dynamical chiral quark model [35, 36].

Any scenario for compact star evolution that is based on the occurence of quark matter relies on the assumptions about the properties of this phase. It is therefore of prior importance to obtain a phase diagram of three-flavor quark matter under compact star constraints with selfconsistently determined dynamical quark masses. In the present paper we will employ the Nambu–Jona-Lasinio (NJL) model to delineate the different quark matter phases in the plane of temperature and chemical potential. We also address the question whether CFL quark matter and gapless phases are likely to play a role in compact star interiors.

*Electronic address: Blaschke@theory.gsi.de
†Electronic address: Sverker.Fredriksson@ltu.se
‡Electronic address: Hovik.Grigorian@uni-rostock.de
§Electronic address: oztas@hacettepe.edu.tr
¶Electronic address: Fredrik.Sandin@ltu.se

II. MODEL

In this paper, we consider an NJL model with quark-antiquark interactions in the color singlet scalar/pseudoscalar channel, and quark-quark interactions in the scalar color antitriplet channel. We neglect the less attractive interaction channels, *e.g.*, the isospin-singlet channel, which could allow for weak spin-1 condensates. Such condensates allow for gapless excitations at low temperatures and could be important for the cooling behaviour of compact stars. However, the coupling strengths in these channels are poorly known and we therefore neglect them here. The Lagrangian density is given by

$$\begin{aligned}\mathcal{L} &= \bar{q}_{i\alpha}(i\partial\!\!\!/\delta_{ij}\delta_{\alpha\beta} - M^0_{ij}\delta_{\alpha\beta} + \mu_{ij,\alpha\beta}\gamma^0)q_{j\beta} \\ &+ G_S\sum_{a=0}^{8}\left[(\bar{q}\tau^a_f q)^2 + (\bar{q}i\gamma_5\tau^a_f q)^2\right] \\ &+ G_D\sum_{k,\gamma}\left[(\bar{q}_{i\alpha}\epsilon_{ijk}\epsilon_{\alpha\beta\gamma}q^C_{j\beta})(\bar{q}^C_{i'\alpha'}\epsilon_{i'j'k}\epsilon_{\alpha'\beta'\gamma}q_{j'\beta'})\right. \\ &+ \left.(\bar{q}_{i\alpha}i\gamma_5\epsilon_{ijk}\epsilon_{\alpha\beta\gamma}q^C_{j\beta})(\bar{q}^C_{i'\alpha'}i\gamma_5\epsilon_{i'j'k}\epsilon_{\alpha'\beta'\gamma}q_{j'\beta'})\right], \quad (1)\end{aligned}$$

where $M^0_{ij} = \mathrm{diag}(m^0_u, m^0_d, m^0_s)$ is the current quark mass matrix in flavor space and $\mu_{ij,\alpha\beta}$ is the chemical potential matrix in color and flavor space. Due to strong and weak interactions, the various chemical potentials are not independent. In the superconducting phases a $U(1)$ gauge symmetry remains unbroken [37], and the associated charge is a linear combination of the electric charge, Q, and two orthogonal generators of the unbroken $SU(2)_c$ symmetry. Hence, there are in total four independent chemical potentials

$$\mu_{ij,\alpha\beta} = (\mu\delta_{ij} + Q\mu_Q)\delta_{\alpha\beta} + (T_3\mu_3 + T_8\mu_8)\delta_{ij}, \quad (2)$$

where $Q = \mathrm{diag}(2/3, -1/3, -1/3)$ is the electric charge in flavor space, and $T_3 = \mathrm{diag}(1, -1, 0)$ and $T_8 = \mathrm{diag}(1/\sqrt{3}, 1/\sqrt{3}, -2/\sqrt{3})$ are the generators in color space. The quark number chemical potential, μ, is related to the baryon chemical potential by $\mu = \mu_B/3$. The quark fields in color, flavor, and Dirac spaces are denoted by $q_{i\alpha}$ and $\bar{q}_{i\alpha} = q^\dagger_{i\alpha}\gamma^0$. τ^a_f are Gell-Mann matrices acting in flavor space. Charge conjugated quark fields are denoted by $q^C = C\bar{q}^T$ and $\bar{q}^C = q^T C$, where $C = i\gamma^2\gamma^0$ is the Dirac charge conjugation matrix. The indices α, β, and γ represent colors ($r = 1$, $g = 2$ and $b = 3$), while i, j, and k represent flavors ($u = 1$, $d = 2$, and $s = 3$). G_S and G_D are dimensionful coupling constants that must be determined by experiments.

Typically, three-flavor NJL models use a 't Hooft determinant interaction that induces a $\mathrm{U}_A(1)$ symmetry breaking in the pseudoscalar isoscalar meson sector, which can be adjusted such that the η-η' mass difference is described. This realization of the $\mathrm{U}_A(1)$ breaking leads to the important consequence that the quark condensates of different flavor sectors get coupled. The dynamically generated strange quark mass contains a contribution from the chiral condensates of the light flavors. There is, however, another possible realization of the $\mathrm{U}_A(1)$ symmetry breaking that does not arise on the mean field level, but only for the mesonic fluctuations in the pseudoscalar isoscalar channel. This is due to the coupling to the nonperturbative gluon sector via the triangle anomaly, see, *e.g.*, [38, 39, 40]. This realization of the η-η' mass difference gives no contribution to the quark thermodynamics at the mean field level, which we will follow in this paper. Up to now it is not known, which of the two $\mathrm{U}_A(1)$ breaking mechanisms that is the dominant one in nature. In the present exploratory study of the mean field thermodynamics of three-flavor quark matter, we will take the point of view that the 't Hooft term might be subdominant and can be disregarded. One possible way to disentangle both mechanisms is due to their different response to chiral symmetry restoration at finite temperatures and densities. While in heavy-ion collisions only the finite temperature aspect can be systematically studied [41], the state of matter in neutron star interiors may be suitable to probe the $\mathrm{U}_A(1)$ symmetry restoration and its possible implications for the quark matter phase diagram at high densities and low temperatures. A comparison of the results presented in this work with the alternative treatment of the phase diagram of three-flavor quark matter including the 't Hooft determinant term, see [42], may therefore be instructive.

The mean-field Lagrangian is

$$\begin{aligned}\mathcal{L}^{MF} &= \bar{q}_{i\alpha}\left[i\partial\!\!\!/\delta_{ij}\delta_{\alpha\beta} - (M^0_{ij} - 4G_S\langle\!\langle\bar{q}_{i\alpha}q_{j\beta}\rangle\!\rangle\delta_{ij})\delta_{\alpha\beta} + \mu_{ij,\alpha\beta}\gamma^0\right]q_{j\beta} \\ &\quad -2G_S\sum_i\langle\!\langle\bar{q}_i q_i\rangle\!\rangle^2 - \sum_{k,\gamma}\frac{|\Delta_{k\gamma}|^2}{4G_D} + \frac{1}{2}\bar{q}_{i\alpha}\widehat{\Delta}_{ij,\alpha\beta}\,q^C_{j\beta} + \frac{1}{2}\bar{q}^C_{i\alpha}\widehat{\Delta}^\dagger_{ij,\alpha\beta}\,q_{j\beta}, \quad (3)\\ \widehat{\Delta}_{ij,\alpha\beta} &= 2G_D i\gamma_5\epsilon_{\alpha\beta\gamma}\epsilon_{ijk}\langle\!\langle\bar{q}_{i'\alpha'}i\gamma_5\epsilon_{\alpha'\beta'\gamma}\epsilon_{i'j'k}q^C_{j'\beta'}\rangle\!\rangle = i\gamma_5\epsilon_{\alpha\beta\gamma}\epsilon_{ijk}\Delta_{k\gamma}. \quad (4)\end{aligned}$$

We define the chiral gaps

$$\phi_i = -4G_S\langle\!\langle\bar{q}_i q_i\rangle\!\rangle, \quad (5)$$

and the diquark gaps

$$\Delta_{k\gamma} = 2G_D\langle\!\langle\bar{q}_{i\alpha}i\gamma_5\epsilon_{\alpha\beta\gamma}\epsilon_{ijk}q^C_{j\beta}\rangle\!\rangle. \quad (6)$$

The chiral condensates contribute to the dynamical masses of the quarks and the constituent quark mass matrix in flavor space is $M = \mathrm{diag}(m_u^0 + \phi_u, m_d^0 + \phi_d, m_s^0 + \phi_s)$, where m_i^0 are the current quark masses. For finite current quark masses the $U(3)_L \times U(3)_R$ symmetry of the Lagrangian is spontaneously broken and only approximately restored at high densities.

The diquark gaps, $\Delta_{k\gamma}$, are antisymmetric in flavor and color, *e.g.*, the condensate corresponding to Δ_{ur} is created by green down and blue strange quarks. Due to this property, the diquark gaps can be denoted with the flavor indices of the interacting quarks

$$\Delta_{ur} = \Delta_{ds}, \quad \Delta_{dg} = \Delta_{us}, \quad \Delta_{sb} = \Delta_{ud}. \tag{7}$$

After reformulating the mean-field lagrangian in 8-component Nambu-Gorkov spinors [43, 44] and performing the functional integrals over Grassman variables [45] we obtain the thermodynamic potential

$$\begin{aligned}\Omega(T,\mu) &= \frac{\phi_u^2+\phi_d^2+\phi_s^2}{8G_S} + \frac{|\Delta_{ud}|^2+|\Delta_{us}|^2+|\Delta_{ds}|^2}{4G_D} \\ &- T\sum_n \int \frac{d^3p}{(2\pi)^3}\frac{1}{2}\mathrm{Tr}\ln\left(\frac{1}{T}S^{-1}(i\omega_n,\vec{p})\right) \\ &+ \Omega_e - \Omega_0. \end{aligned} \tag{8}$$

Here $S^{-1}(p)$ is the inverse propagator of the quark fields at four momentum $p = (i\omega_n, \vec{p})$,

$$S^{-1}(i\omega_n,\vec{p}) = \begin{bmatrix} \not{p} - M + \mu\gamma^0 & \widehat{\Delta} \\ \widehat{\Delta}^\dagger & \not{p} - M - \mu\gamma^0 \end{bmatrix}, \tag{9}$$

and $\omega_n = (2n+1)\pi T$ are the Matsubara frequencies for fermions. The thermodynamic potential of ultrarelativistic electrons,

$$\Omega_e = -\frac{1}{12\pi^2}\mu_Q^4 - \frac{1}{6}\mu_Q^2 T^2 - \frac{7}{180}\pi^2 T^4, \tag{10}$$

has been added to the potential, and the vacuum contribution,

$$\begin{aligned}\Omega_0 = \Omega(0,0) &= \frac{\phi_{0u}^2+\phi_{0d}^2+\phi_{0s}^2}{8G_S} \\ &-2N_c\sum_i \int \frac{d^3p}{(2\pi)^3}\sqrt{M_i^2+p^2}, \end{aligned} \tag{11}$$

has been subtracted in order to get zero pressure in vacuum. Using the identity $\mathrm{Tr}(\ln(D)) = \ln(\det(D))$ and evaluating the determinant (see Appendix A), we obtain

$$\ln\det\left(\frac{1}{T}S^{-1}(i\omega_n,\vec{p})\right) = 2\sum_{a=1}^{18}\ln\left(\frac{\omega_n^2+\lambda_a(\vec{p})^2}{T^2}\right). \tag{12}$$

The quasiparticle dispersion relations, $\lambda_a(\vec{p})$, are the eigenvalues of the Hermitian matrix,

$$\mathcal{M} = \begin{bmatrix} -\gamma^0\vec{\gamma}\cdot\vec{p} - \gamma^0 M + \mu & \gamma^0\widehat{\Delta}C \\ \gamma^0 C\widehat{\Delta}^\dagger & -\gamma^0\vec{\gamma}^T\cdot\vec{p} + \gamma^0 M - \mu \end{bmatrix}, \tag{13}$$

in color, flavor, and Nambu-Gorkov space. This result is in agreement with [31, 42]. Finally, the Matsubara sum can be evaluated on closed form [45],

$$T\sum_n \ln\left(\frac{\omega_n^2+\lambda_a^2}{T^2}\right) = \lambda_a + 2T\ln(1+e^{-\lambda_a/T}), \tag{14}$$

leading to an expression for the thermodynamic potential on the form

$$\begin{aligned}\Omega(T,\mu) &= \frac{\phi_u^2+\phi_d^2+\phi_s^2}{8G_S} + \frac{|\Delta_{ud}|^2+|\Delta_{us}|^2+|\Delta_{ds}|^2}{4G_D} \\ &- \int\frac{d^3p}{(2\pi)^3}\sum_{a=1}^{18}\left(\lambda_a + 2T\ln\left(1+e^{-\lambda_a/T}\right)\right) \\ &+ \Omega_e - \Omega_0. \end{aligned} \tag{15}$$

It should be noted that (14) is an even function of λ_a, so the signs of the quasiparticle dispersion relations are arbitrary. In this paper, we assume that there are no trapped neutrinos. This approximation is valid for quark matter in neutron stars, after the short period of deleptonization is over.

Equations (10), (11), (13), and (15) form a consistent thermodynamic model of superconducting quark matter. The independent variables are μ and T. The gaps, ϕ_i, and Δ_{ij}, are variational order parameters that should be determined by minimization of the grand canonical thermodynamical potential, Ω. Also, quark matter should be locally color and electric charge neutral, so at the physical minima of the thermodynamic potential the corresponding number densities should be zero

$$n_Q = -\frac{\partial\Omega}{\partial\mu_Q} = 0, \tag{16}$$

$$n_8 = -\frac{\partial\Omega}{\partial\mu_3} = 0, \tag{17}$$

$$n_3 = -\frac{\partial\Omega}{\partial\mu_8} = 0. \tag{18}$$

The pressure, P, is related to the thermodynamic potential by $P = -\Omega$ at the global minima of Ω. The quark density, entropy and energy density are then obtained as derivatives of the thermodynamical potential with respect to μ, T and $1/T$, respectively.

III. RESULTS

The numerical solutions to be reported in this Section are obtained with the following set of model parameters, taken from Table 5.2 of Ref. [8] for vanishing 't Hooft interaction,

$$m_{u,d}^0 = 5.5 \text{ MeV}, \tag{19}$$

$$m_s^0 = 112.0 \text{ MeV}, \tag{20}$$

$$G_S\Lambda^2 = 2.319, \tag{21}$$

$$\Lambda = 602.3 \text{ MeV}. \tag{22}$$

With these parameters, the following low-energy QCD observables can be reproduced: $m_\pi = 135$ MeV, $m_K = 497.7$ MeV, $f_\pi = 92.4$ MeV. The value of the diquark coupling strength $G_D = \eta G_S$ is considered as a free parameter of the model. Here we present results for $\eta = 0.75$ (intermediate coupling) and $\eta = 1.0$ (strong coupling).

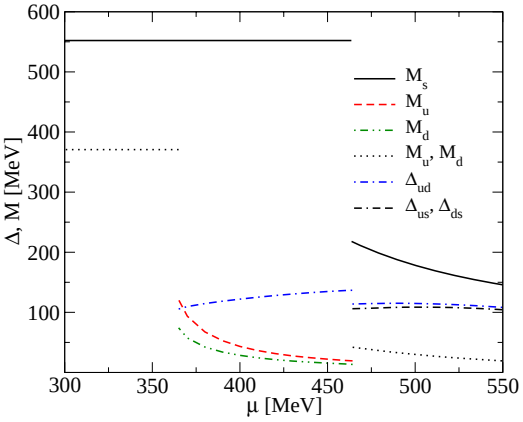

FIG. 1: Gaps and dynamical quark masses as functions of μ at $T = 0$ for intermediate diquark coupling, $\eta = 0.75$.

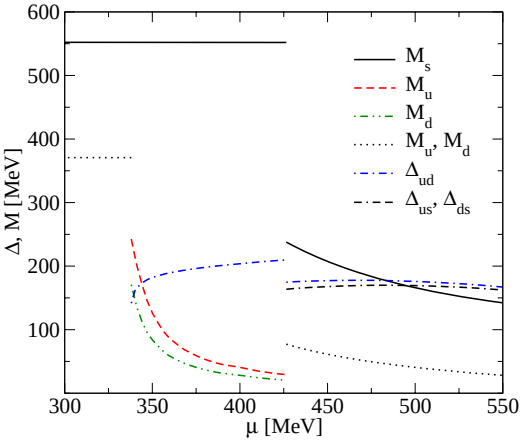

FIG. 2: Gaps and dynamical quark masses as functions of μ at $T = 0$ for strong diquark coupling, $\eta = 1$.

A. Quark masses and pairing gaps at zero temperature

The dynamically generated quark masses and the diquark pairing gaps are determined selfconsistently at the absolute minima of the thermodynamic potential, in the plane of temperature and quark chemical potential. This is done for both the strong and the intermediate diquark coupling strengths. In Figs. 1 and 2 we show the dependence of masses and gaps on the quark chemical potential at $T = 0$ for $\eta = 0.75$ and $\eta = 1.0$, respectively. A characteristic feature of this dynamical quark model

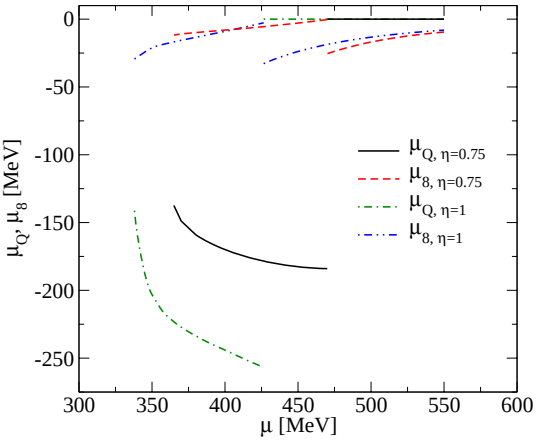

FIG. 3: Chemical potentials μ_Q and μ_8 at $T = 0$ for both values of the diquark coupling, $\eta = 0.75$ and $\eta = 1$. All phases considered in this work have zero n_3 color charge for $\mu_3 = 0$. Hence μ_3 is omitted in the plot.

is that the critical quark chemical potentials where light and strange quark masses jump from their constituent mass values down to almost their current mass values do not coincide. With increasing chemical potential the system undergoes a sequence of two transitions: (1) vacuum → two-flavor quark matter, (2) two-flavor → three-flavor quark matter. The intermediate two-flavor quark matter phase occurs within an interval of chemical potentials typical for compact star interiors. While at intermediate coupling the asymmetry between the up and down quark chemical potentials leads to a mixed NQ-2SC phase below temperatures of $20 - 30$ MeV, at strong coupling the pure 2SC phase extends down to $T = 0$. Simultaneously, the limiting chemical potentials of the two-flavor quark matter region are lowered by about 40 MeV. Three-flavor quark matter is always in the CFL phase where all quarks are paired. The robustness of the 2SC condensate under compact star constraints, with respect to changes of the coupling strength, as well as to a softening of the momentum cutoff by a formfactor, has recently been investigated with a different parametrization [46]. The re-

sults at low temperatures are similar: for $\eta = 0.75$ and the NJL formfactor the 2SC condensate does not occur for moderate chemical potentials, while for $\eta = 1.0$ it occurs simultaneously with chiral symmetry restoration. Fig. 3 shows the corresponding dependences of the chemical potentials conjugate to electric (μ_Q) and color (μ_8) charges. All phases considered in this work have zero n_3 color charge for $\mu_3 = 0$.

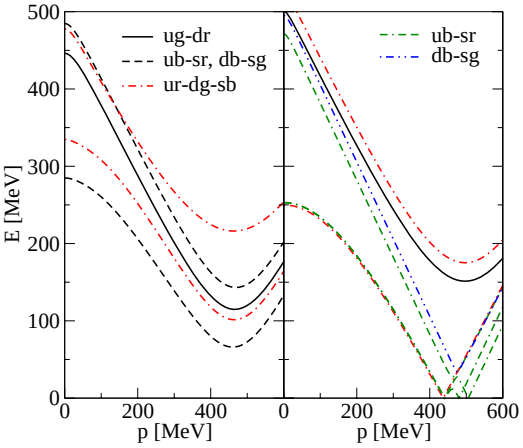

FIG. 4: Quark-quark quasiparticle dispersion relations. For $\eta = 0.75$, $T = 0$, and $\mu = 480$ MeV (left panel) there is a forbidden energy band above the Fermi surface. All dispersion relations are gapped at this point in the $\mu - T$ plane, see Fig. 5. There is no forbidden energy band for the $ub - sr$, $db - sg$, and $ur - dg - sb$ quasiparticles for $\eta = 1$, $T = 84$ MeV, and $\mu = 500$ MeV (right panel). This point in the $\mu - T$ plane constitutes a part of the gapless CFL phase of Fig. 6.

B. Dispersion relations and gapless phases

In Fig. 4 we show the quasiparticle dispersion relations of different excitations at two points in the phase diagram: (I) the CFL phase (left panel), where there is a finite energy gap for all dispersion relations; (II) the gCFL phase (right panel), where the energy spectrum is shifted due to the assymetry in the chemical potentials, such that the CFL gap is zero and (gapless) excitations with zero energy are possible. In the present model, this phenomenon occurs only at rather high temperatures, where the condensates are diminished by thermal fluctuations.

C. Phase diagram

The thermodynamical state of the system is characterized by the values of the order parameters and their dependence on T and μ. Here we illustrate this dependency in a phase diagram. We identify the following phases:

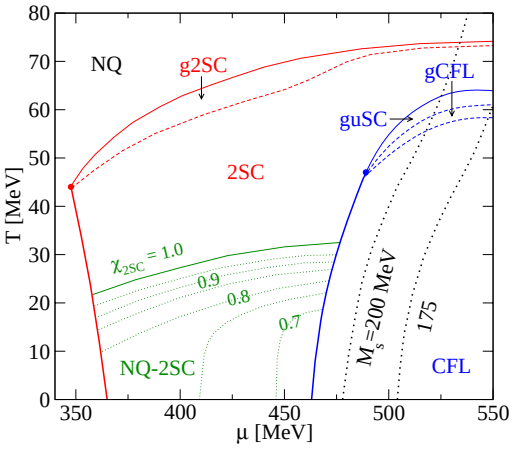

FIG. 5: Phase diagram of neutral three-flavor quark matter for intermediate diquark coupling, $\eta = 0.75$. First-order phase transition boundaries are indicated by bold solid lines, while thin solid lines correspond to second-order phase boundaries. The dashed lines indicate gapless phase boundaries. The volume fraction, χ_{2SC}, of the 2SC component of the mixed NQ-2SC phase is denoted with thin dotted lines, while the constituent strange quark mass is denoted with bold dotted lines.

1. NQ: $\Delta_{ud} = \Delta_{us} = \Delta_{ds} = 0$;
2. NQ-2SC: $\Delta_{ud} \neq 0$, $\Delta_{us} = \Delta_{ds} = 0$, 0¡$\chi_{2SC}$¡1;
3. 2SC: $\Delta_{ud} \neq 0$, $\Delta_{us} = \Delta_{ds} = 0$;
4. uSC: $\Delta_{ud} \neq 0$, $\Delta_{us} \neq 0$, $\Delta_{ds} = 0$;
5. CFL: $\Delta_{ud} \neq 0$, $\Delta_{ds} \neq 0$, $\Delta_{us} \neq 0$;

and their gapless versions. The resulting phase diagrams for intermediate and strong coupling are given in Figs. 5 and 6, respectively and constitute the main result of this work, which is summarized in the following statements:

1. Gapless phases occur only at high temperatures, above 50 MeV (intermediate coupling) or 60 MeV (strong coupling).
2. CFL phases occur only at rather high chemical potential, well above the chiral restoration transition, *i.e.*, above 464 MeV (intermediate coupling) or 426 MeV (strong coupling).
3. Two-flavor quark matter for intermediate coupling is at low temperatures ($T < 20 - 30$ MeV) in a mixed NQ-2SC phase, at high temperatures in the pure 2SC phase.

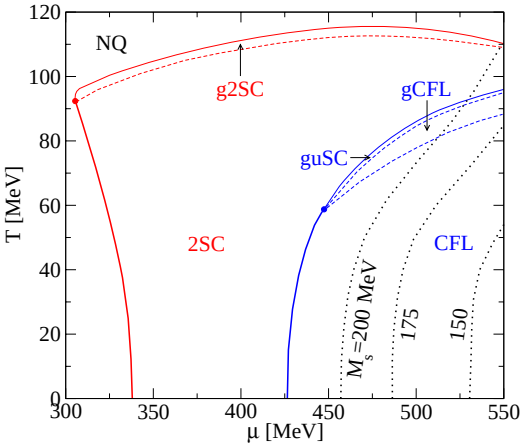

FIG. 6: Phase diagram of neutral three-flavor quark matter for strong diquark coupling, $\eta = 1$. Line styles as in Fig. 5.

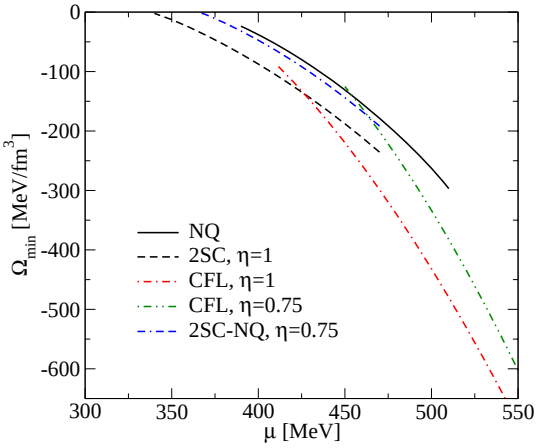

FIG. 7: Minima of the thermodynamical potential for neutral three-flavor quark matter at $T = 0$ as a function of the quark chemical potential. Note that at a given coupling η the state with the lowest $\Omega_{\rm min}$ is attained and the physical pressure is $P = -\Omega_{\rm min}$.

4. Two-flavor quark matter for strong coupling is in the 2SC phase with rather high critical temperatures of ~ 100 MeV.

5. The critical endpoint of first order chiral phase transitions is at (T, μ)=(44 MeV, 347 MeV) for intermediate coupling and at (92 MeV, 305 MeV) for strong coupling.

D. Quark matter equation of state

The various phases of quark matter presented in the previous section have been identified by minimizing the thermodynamic potential, Ω, in the order parameters, Δ_{ij} and ϕ_i. For a homogenous system, the pressure is $P = -\Omega_{\rm min}$, see Fig. 7, where the μ-dependence of $\Omega_{\rm min}$ is shown at $T = 0$ for the different competing phases. The lowest value of $\Omega_{\rm min}$ corresponds to the negative value of the physical pressure. The intersection of two curves corresponds to a first order phase transition. All other thermodynamic quantities can be obtained from the thermodynamic potential by derivatives. At intermediate coupling, we have a first order transition from the NQ-2SC phase to the CFL phase, whereas at strong coupling the first order transition is from the 2SC phase to the CFL phase, with a lower critical energy density. In Fig. 8 the equation of state for cold three-flavor quark matter is given in a form suitable for the investigation of the hydrodynamic stability of gravitating compact objects, so-called quark stars. This is the topic of the next Subsection.

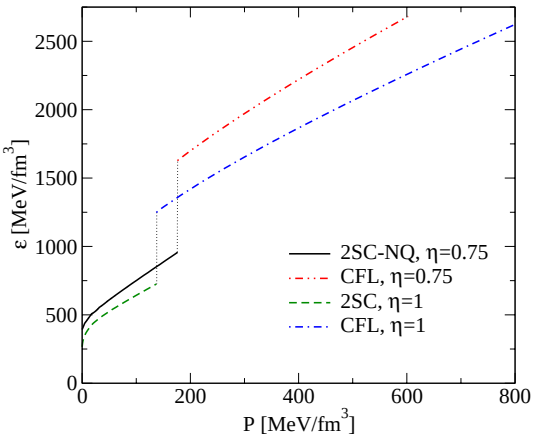

FIG. 8: Equation of state for three-flavor quark matter at $T = 0$ with first order phase transitions. For intermediate diquark coupling ($\eta = 0.75$): from the mixed NQ-2SC phase to the CFL phase. For strong diquark coupling ($\eta = 1$): from the 2SC phase to the CFL phase.

E. Quark star configurations

The properties of spherically symmetric, static configurations of dense matter can be calculated with the well-known Tolman-Oppenheimer-Volkoff equations for hydrostatic equilibrium of self-gravitating matter, see also

[47],

$$\frac{dP(r)}{dr} = -\frac{[\varepsilon(r)+P(r)][m(r)+4\pi r^3 P(r)]}{r[r-2m(r)]} \ . \qquad (23)$$

Here $\varepsilon(r)$ is the energy density and $P(r)$ the pressure at distance r from the center of the star. The mass enclosed in a sphere with radius r is defined by

$$m(r) = 4\pi \int_0^r \varepsilon(r') r'^2 dr' \ . \qquad (24)$$

These equations are solved for given central baryon number densities, $n_B(r=0)$, thereby defining a sequence of quark star configurations. For the generalization to finite temperature configurations, see [48]. Hot quark stars have been discussed, *e.g.*, in [24, 25, 49, 50, 51]. In Fig. 9 we show the stable configurations of quark stars for the three-flavor quark matter equation of state described above. The obtained mass radius relations allow for very compact selfbound objects, with a maximum radius that is less than 10 km. For intermediate diquark coupling, $\eta = 0.75$, stable stars consist of a NQ-2SC mixed phase with a maximum mass of 1.21 $M_\odot$. With incrasing density, a phase transition to the CFL phase renders the sequence unstable. For the strong diquark coupling, $\eta = 1$, quark matter is in the 2SC phase at low densities and the corresponding sequence of quark stars is stable up to a maximum mass of 1.33 $M_\odot$. The phase transition to CFL quark matter entails an instability that leads to a third family of stable stars, with masses in-between 1.30 and 1.33 $M_\odot$. For non-accreting compact stars the baryon number is an invariant during the cooling evolution. By comparing the masses of cold and hot isothermal configurations of quark stars of equal baryon number, the maximum mass defect (energy release due to cooling) can be calculated. The result for the strong diquark coupling, $\eta = 1$, is shown if Fig. 10. For an initial temperature of 40 MeV and a given baryon number of $N = 1.46\ N_\odot$, the initial mass is $M = 1.41\ M_\odot$. By cooling this object down to $T = 0$, a mass defect of $\Delta M = 0.1\ M_\odot$ occurs. For the chosen baryon number, $N = 1.46\ N_\odot$, there are two possible $T = 0$ configurations (twins). A hot star could thus evolve into the more compact mass-equivalent (twin) final state, if a fluctuation triggers the transition to a CFL phase in the core of the star. The structures of these two twin configurations are given in Fig. 11. The energy release of 0.1 $M_\odot$ is of the same order of magnitude as the energy release in supernova explosions and gamma-ray bursts. Disregarding the possible influence of a hadronic shell and the details regarding the heat trans-

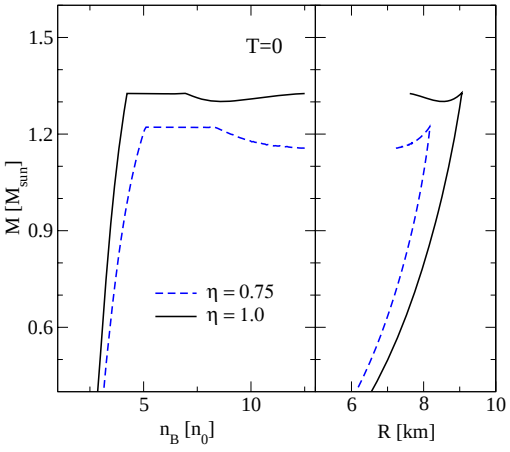

FIG. 9: Sequences of cold quark stars for the three-flavor quark matter equation of state described in the text. The rising branches in the mass-central density relation (left panel) indicate stable compact object configurations. The mass-radius relations (right panel) show that the three-flavor quark matter described in this paper leads to very compact self-bound objects. For intermediate diquark coupling, $\eta = 0.75$, stable stars consist of a mixed phase of NQ-2SC matter with a maximum mass of 1.21 $M_\odot$ (dashed line). At higher densities a phase transition to CFL quark matter occurs, which entails a collapse of the star. For strong coupling, $\eta = 1$, the low density quark matter is in the 2SC phase and corresponding quark stars are stable up to a maximum mass of 1.326 $M_\odot$ (solid line). The phase transition to CFL quark matter entails an instability, which at $T = 0$ leads to a third family of stable stars for central densities above $9n_0$ and a mass twin window of 1.301 - 1.326 $M_\odot$.

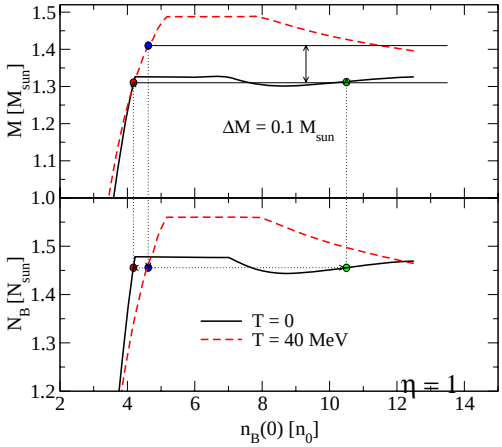

FIG. 10: Cooling an isothermal quark star configuration with initial mass $M = 1.41\ M_\odot$ at temperature $T = 40$ MeV under conservation of the given baryon number $N = 1.46\ N_\odot$ down to $T = 0$ leads to a mass defect $\Delta M = 0.1\ M_\odot$ for the strong coupling case ($\eta = 1.0$). Due to the twin structure at $T = 0$, two alternatives for the final state can be attained, a homogeneous 2SC quark star or a dense 2SC-CFL quark hybrid star.

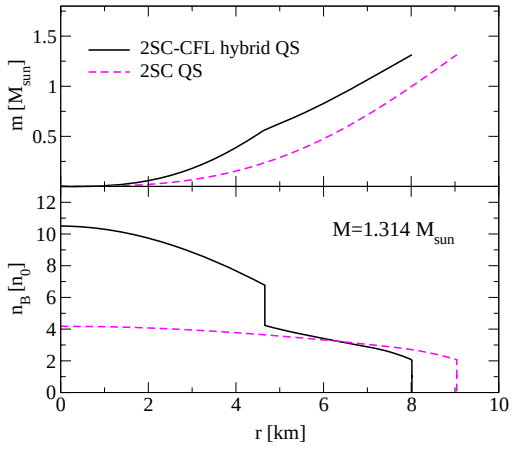

FIG. 11: Structure of two quark star (QS) configurations with $M = 1.314\ M_\odot$ (mass twins) for the three-flavor quark matter equation of state described in the text in the case of strong coupling ($\eta = 1$). The low-density twin has a radius of 9 km and is a homogeneous 2SC quark star, the high-density twin is more compact with a radius of 8 km and consists of a CFL quark matter core with 4.65 km radius and a 2SC quark matter shell.

port, the cooling induced first order phase transition to the CFL phase could serve as a candidate process for the puzzling engine of these energetic phenomena [24, 25, 51].

IV. CONCLUSIONS

We have investigated the phase diagram of three-flavor quark matter within an NJL model under compact star constraints. Local color and electric charge neutrality is imposed for $\beta-$equilibrated superconducting quark matter. The constituent quark masses are selfconsistently determined. The model refrains from adopting the 't Hooft determinant interaction in the mean field Lagrangian as a realization of the $U_A(1)$ symmetry breaking. Instead, it is assumed that the $\eta - \eta'$ mass difference originates from an anomalous coupling of the pseudoscalar isosinglet fluctuation to the nonperturbative gluon sector, which gives no contribution to the quark thermodynamics at the mean field level. The resulting parametrization of this $SU_f(3)$ NJL model results in a stronger coupling than NJL models with a 't Hooft term and thus in different phase diagrams, cf. Ref. [42]. The diquark condensates are determined selfconsistently by minimization of the grand canonical thermodynamic potential. The various condensates are order parameters that characterize the different phases in the plane of temperature and quark chemical potential. These phases are in particular the NQ-2SC mixed phase, the 2SC, uSC, and CFL phases, as well as the corresponding gapless phases. We have investigated strong and intermediate diquark coupling strengths. It is shown that in both cases gapless superconducting phases do not occur at temperatures relevant for compact star evolution, *i.e.*, below ~ 50 MeV. Three-flavor quark matter phases, *e.g.*, the CFL phase, occur only at rather large chemical potential, so the existence of such phases in stable compact stars is questionable. The stability and stucture of isothermal quark star configurations are evaluated. For the strong diquark coupling, 2SC stars are stable up to a maximum mass of $1.33\ M_\odot$. A second family of more compact stars (twins) with a CFL quark matter core and masses in-between 1.30 and $1.33\ M_\odot$ are found to be stable. For intermediate coupling, the quark stars are composed of a mixed NQ-2SC phase up to a maximum mass of $1.21\ M_\odot$, where a phase transition to the CFL phase occurs and the configurations become unstable. When isothermal star configurations with an initial temperature of 40 MeV cools under conservation of baryon number, the mass defect is $0.1\ M_\odot$ for the strong diquark coupling. It is important to investigate the robustness of these statements, in particular by including nonlocal formfactors [29, 52, 53] and by going beyond the mean-field level by including the effects of a hadronic medium on the quark condensates. Finally, any statement concerning the occurence and stability of quark matter in compact stars shall include an investigation of the influence of a hadronic shell [54, 55, 56] on the solutions of the equations of compact star structure.

V. ACKNOWLEDGMENTS

F.S. acknowledges support from the Swedish National Graduate School of Space Technology. A research visit of H.G. has been supported by Luleå University of Technology. S.F. visited Rostock thanks to EU support within the Erasmus program. A.M.Ö. received support from Hacettepe University Research Fund, grant No. 02 02 602 001. D.B. thanks for partial support of the Department of Energy during the program INT-04-1 on *QCD and Dense Matter: From Lattices to Stars* at the University of Washington, where this project has been started. This work has been supported in part by the Virtual Institute of the Helmholtz Association under grant No. VH-VI-041. We are grateful to our colleagues in Darmstadt and Frankfurt who made the results of their study in Ref. [42] available to us prior to submission.

APPENDIX A: DISPERSION RELATIONS

The dispersion relations of the quasiparticles that appear in the expression for the thermodynamic potential (15) are the eigenvalues of the Nambu-Gorkov matrix (13). For each color and flavor combination of the eight component Nambu-Gorkov spinors, there is a corre-

sponding 8x8 entry in this matrix. For three flavors and three colors (13) is a 72x72 matrix. The explicit form of this matrix can be represented by a table, where the rows and columns denote the flavor and color degrees of freedom

	q_{ur}	q_{ug}	q_{ub}	q_{dr}	q_{dg}	q_{db}	q_{sr}	q_{sg}	q_{sb}	$q^\dagger_{ur}$	$q^\dagger_{ug}$	$q^\dagger_{ub}$	$q^\dagger_{dr}$	$q^\dagger_{dg}$	$q^\dagger_{db}$	$q^\dagger_{sr}$	$q^\dagger_{sg}$	$q^\dagger_{sb}$
$q^\dagger_{ur}$	A_{ur}	0	0	0	0	0	0	0	0	0	0	0	0	D_{ud}	0	0	0	D_{us}
$q^\dagger_{ug}$	0	A_{ug}	0	0	0	0	0	0	0	0	0	0	$-D_{ud}$	0	0	0	0	0
$q^\dagger_{ub}$	0	0	A_{ub}	0	0	0	0	0	0	0	0	0	0	0	0	$-D_{us}$	0	0
$q^\dagger_{dr}$	0	0	0	A_{dr}	0	0	0	0	0	0	$-D_{ud}$	0	0	0	0	0	0	0
$q^\dagger_{dg}$	0	0	0	0	A_{dg}	0	0	0	0	D_{ud}	0	0	0	0	0	0	0	D_{ds}
$q^\dagger_{db}$	0	0	0	0	0	A_{db}	0	0	0	0	0	0	0	0	0	0	$-D_{ds}$	0
$q^\dagger_{sr}$	0	0	0	0	0	0	A_{sr}	0	0	0	0	$-D_{us}$	0	0	0	0	0	0
$q^\dagger_{sg}$	0	0	0	0	0	0	0	A_{sg}	0	0	0	0	0	0	$-D_{ds}$	0	0	0
$q^\dagger_{sb}$	0	0	0	0	0	0	0	0	A_{sb}	D_{us}	0	0	0	D_{ds}	0	0	0	0
q_{ur}	0	0	0	0	$D^\dagger_{ud}$	0	0	0	$D^\dagger_{us}$	B_{ur}	0	0	0	0	0	0	0	0
q_{ug}	0	0	0	$-D^\dagger_{ud}$	0	0	0	0	0	0	B_{ug}	0	0	0	0	0	0	0
q_{ub}	0	0	0	0	0	0	$-D^\dagger_{us}$	0	0	0	0	B_{ub}	0	0	0	0	0	0
q_{dr}	0	$-D^\dagger_{ud}$	0	0	0	0	0	0	0	0	0	0	B_{dr}	0	0	0	0	0
q_{dg}	$D^\dagger_{ud}$	0	0	0	0	0	0	0	$D^\dagger_{ds}$	0	0	0	0	B_{dg}	0	0	0	0
q_{db}	0	0	0	0	0	0	0	$-D^\dagger_{ds}$	0	0	0	0	0	0	B_{db}	0	0	0
q_{sr}	0	0	$-D^\dagger_{us}$	0	0	0	0	0	0	0	0	0	0	0	0	B_{sr}	0	0
q_{sg}	0	0	0	0	0	$-D^\dagger_{ds}$	0	0	0	0	0	0	0	0	0	0	B_{sg}	0
q_{sb}	$D^\dagger_{us}$	0	0	0	$D^\dagger_{ds}$	0	0	0	0	0	0	0	0	0	0	0	0	B_{sb}

(A1)

Each entry is a 4x4 Hermitian matrix in Dirac space. The diagonal submatrices are

$$A_{i\alpha} = \begin{bmatrix} p+\mu_{i\alpha} & 0 & -M_i & 0 \\ 0 & -p+\mu_{i\alpha} & 0 & -M_i \\ -M_i & 0 & -p+\mu_{i\alpha} & 0 \\ 0 & -M_i & 0 & p+\mu_{i\alpha} \end{bmatrix}, \qquad \text{(A2)}$$

$$B_{j\beta} = \begin{bmatrix} -p-\mu_{j\beta} & 0 & M_j & 0 \\ 0 & p-\mu_{j\beta} & 0 & M_j \\ M_j & 0 & p-\mu_{j\beta} & 0 \\ 0 & M_j & 0 & -p-\mu_{j\beta} \end{bmatrix}, \qquad \text{(A3)}$$

whereas the off-diagonal blocks are given by

$$D_{ij} = \begin{bmatrix} 0 & 0 & 0 & i\Delta_{ij} \\ 0 & 0 & -i\Delta_{ij} & 0 \\ 0 & i\Delta_{ij} & 0 & 0 \\ -i\Delta_{ij} & 0 & 0 & 0 \end{bmatrix}. \qquad \text{(A4)}$$

The eigenvalues of (A1) are the quasiparticle energies, λ_a, that enter the thermodynamic potential (15), *i.e.*, the 72 dispersion relations of the various quark-quark and antiquark-antiquark excitations. These eigenvalues can be calculated using a standard numerical library. However, in order to reduce the computational cost, the matrix can be decomposed into a block-diagonal matrix by elementary row and column operations.

	q_{ur}	q_{dg}	q_{sb}	$q^\dagger_{ur}$	$q^\dagger_{dg}$	$q^\dagger_{sb}$	q_{ug}	$q^\dagger_{dr}$	q_{dr}	$q^\dagger_{ug}$	q_{ub}	$q^\dagger_{sr}$	q_{sr}	$q^\dagger_{ub}$	q_{db}	$q^\dagger_{sg}$	q_{sg}	$q^\dagger_{db}$
$q^\dagger_{ur}$	A_{ur}	0	0	0	D_{ud}	D_{us}	0	0	0	0	0	0	0	0	0	0	0	0
$q^\dagger_{dg}$	0	A_{dg}	0	D_{ud}	0	D_{ds}	0	0	0	0	0	0	0	0	0	0	0	0
$q^\dagger_{sb}$	0	0	A_{sb}	D_{us}	D_{ds}	0	0	0	0	0	0	0	0	0	0	0	0	0
q_{ur}	0	$D^\dagger_{ud}$	$D^\dagger_{us}$	B_{ur}	0	0	0	0	0	0	0	0	0	0	0	0	0	0
q_{dg}	$D^\dagger_{ud}$	0	$D^\dagger_{ds}$	0	B_{dg}	0	0	0	0	0	0	0	0	0	0	0	0	0
q_{sb}	$D^\dagger_{us}$	$D^\dagger_{ds}$	0	0	0	B_{sb}	0	0	0	0	0	0	0	0	0	0	0	0
$q^\dagger_{ug}$	0	0	0	0	0	0	A_{ug}	$-D_{ud}$	0	0	0	0	0	0	0	0	0	0
q_{dr}	0	0	0	0	0	0	$-D^\dagger_{ud}$	B_{dr}	0	0	0	0	0	0	0	0	0	0
$q^\dagger_{dr}$	0	0	0	0	0	0	0	0	A_{dr}	$-D_{ud}$	0	0	0	0	0	0	0	0
q_{ug}	0	0	0	0	0	0	0	0	$-D^\dagger_{ud}$	B_{ug}	0	0	0	0	0	0	0	0
$q^\dagger_{ub}$	0	0	0	0	0	0	0	0	0	0	A_{ub}	$-D_{us}$	0	0	0	0	0	0
q_{sr}	0	0	0	0	0	0	0	0	0	0	$-D^\dagger_{us}$	B_{sr}	0	0	0	0	0	0
$q^\dagger_{sr}$	0	0	0	0	0	0	0	0	0	0	0	0	A_{sr}	$-D_{us}$	0	0	0	0
q_{ub}	0	0	0	0	0	0	0	0	0	0	0	0	$-D^\dagger_{us}$	B_{ub}	0	0	0	0
$q^\dagger_{db}$	0	0	0	0	0	0	0	0	0	0	0	0	0	0	A_{db}	$-D_{ds}$	0	0
q_{sg}	0	0	0	0	0	0	0	0	0	0	0	0	0	0	$-D^\dagger_{ds}$	B_{sg}	0	0
$q^\dagger_{sg}$	0	0	0	0	0	0	0	0	0	0	0	0	0	0	0	0	A_{sg}	$-D_{ds}$
q_{db}	0	0	0	0	0	0	0	0	0	0	0	0	0	0	0	0	$-D^\dagger_{ds}$	B_{db}

(A5)

This matrix has one 24x24 and six 8x8 independent submatrices. Expressing these submatrices explicitely, using (A2-A4), the 24x24 matrix can be decomposed into two independent 12x12 submatrices by elementary row and column operations. Similarly, the six 8x8 matrices can be transformed into twelve independent 4x4 submatrices. There is a two-fold degeneracy due to the Nambu-Gorkov basis, each matrix appears both as $\mathcal{M}$ and $\mathcal{M}^\dagger$, so there are only one independent 12x12 matrix and six 4x4 matrices. The 12x12 matrix is

$$\mathcal{M}_{12} = \begin{bmatrix}
p+\mu_{ur} & 0 & 0 & -M_u & 0 & 0 & 0 & i\Delta_{ud} & i\Delta_{us} & 0 & 0 & 0 \\
0 & p+\mu_{dg} & 0 & 0 & -M_d & 0 & i\Delta_{ud} & 0 & i\Delta_{ds} & 0 & 0 & 0 \\
0 & 0 & p+\mu_{sb} & 0 & 0 & -M_s & i\Delta_{us} & i\Delta_{ds} & 0 & 0 & 0 & 0 \\
-M_u & 0 & 0 & -p+\mu_{ur} & 0 & 0 & 0 & 0 & 0 & i\Delta_{ud} & i\Delta_{us} & \\
0 & -M_d & 0 & 0 & -p+\mu_{dg} & 0 & 0 & 0 & 0 & i\Delta_{ud} & 0 & i\Delta_{ds} \\
0 & 0 & -M_s & 0 & 0 & -p+\mu_{sb} & 0 & 0 & 0 & i\Delta_{us} & i\Delta_{ds} & 0 \\
0 & -i\Delta_{ud} & -i\Delta_{us} & 0 & 0 & 0 & -p-\mu_{ur} & 0 & 0 & M_u & 0 & 0 \\
-i\Delta_{ud} & 0 & -i\Delta_{ds} & 0 & 0 & 0 & 0 & -p-\mu_{dg} & 0 & 0 & M_d & 0 \\
-i\Delta_{us} & -i\Delta_{ds} & 0 & 0 & 0 & 0 & 0 & 0 & -p-\mu_{sb} & 0 & 0 & M_s \\
0 & 0 & 0 & 0 & -i\Delta_{ud} & -i\Delta_{us} & M_u & 0 & 0 & p-\mu_{ur} & 0 & 0 \\
0 & 0 & 0 & -i\Delta_{ud} & 0 & -i\Delta_{ds} & 0 & M_d & 0 & 0 & p-\mu_{dg} & 0 \\
0 & 0 & 0 & -i\Delta_{us} & -i\Delta_{ds} & 0 & 0 & 0 & M_s & 0 & 0 & p-\mu_{sb}
\end{bmatrix}, \quad \text{(A6)}$$

and the 4x4 matrices are

$$\mathcal{M}_4 = \begin{bmatrix}
p+\mu_{i\alpha} & -i\Delta_{ij} & -M_i & 0 \\
i\Delta_{ij} & -p-\mu_{j\beta} & 0 & M_j \\
-M_i & 0 & -p+\mu_{i\alpha} & -i\Delta_{ij} \\
0 & M_j & i\Delta_{ij} & p-\mu_{j\beta}
\end{bmatrix}, \quad \text{(A7)}$$

for spinor products $ug-dr$, $ub-sr$, $db-sg$, $dr-ug$, $sr-ub$, and $sg-db$, respectively.

Since these matrices are Hermitian, the eigenvalues appear in $\pm$ pairs. Thus, in general, there are nine independent dispersion relations for quark-quark excitations and

nine for antiquark-antiquark excitations. The eigenvalues of (A6) must be calculated numerically. The eigenvalues of (A7) can be obtained analytically by solving for the roots of the quartic characteristic polynomial,

$$\lambda^4 + a_3\lambda^3 + a_2\lambda^2 + a_1\lambda + a_0 = 0, \qquad \text{(A8)}$$

where

$$\begin{aligned}
a_0 &= P^4 + \left(M_i^2 + M_j^2 + 2\Delta_{ij}^2 - \mu_{i\alpha}^2 - \mu_{j\beta}^2\right) P^2 \\
&+ \left(\mu_{i\alpha}\mu_{j\beta} + M_i M_j + \Delta_{ij}^2 + \mu_{i\alpha} M_j + \mu_{j\beta} M_i\right) \\
&\left(\mu_{i\alpha}\mu_{j\beta} + M_i M_j + \Delta_{ij}^2 - \mu_{i\alpha} M_j - \mu_{j\beta} M_i\right), \\
a_1 &= 2\left(\mu_{i\alpha} - \mu_{j\beta}\right) P^2 + 2\Delta_{ij}^2\left(\mu_{i\alpha} - \mu_{j\beta}\right) \\
&+ 2\left(\mu_{i\alpha} M_j^2 - \mu_{j\beta} M_i^2 + \mu_{i\alpha}^2\mu_{j\beta} - \mu_{j\beta}^2\mu_{i\alpha}\right), \\
a_2 &= \mu_{i\alpha}^2 + \mu_{j\beta}^2 - 2P^2 - M_i^2 - M_j^2 - 2\Delta_{ij}^2 - 4\mu_{i\alpha}\mu_{j\beta}, \\
a_3 &= -2\left(\mu_{i\alpha} - \mu_{j\beta}\right).
\end{aligned}$$

In the limit when $M_i = M_j = M$, which is approximately valid for the $ug - dr$ and $dr - ug$ quasiparticles, the four solutions are

$$\lambda = \frac{\mu_{i\alpha} - \mu_{j\beta}}{2} \pm \sqrt{\left(\frac{\mu_{i\alpha} + \mu_{j\beta}}{2} \pm E\right)^2 + \Delta_{ij}^2}, \qquad \text{(A9)}$$

where $E = \sqrt{p^2 + M^2}$. This result is in agreement with [42]. More generally, the solutions of the quartic equation can be found in textbooks, see, *e.g.*, [57]. In this work the eigenvalues of the 4x4 matrices were calculated with the exact solutions of the quartic equation and the eigenvalues of the 12x12 matrix were calculated with LAPACK. The momentum integral in (15) was calculated with a Gaussian quadrature. The minimization of the thermodynamic potential was performed with conjugate gradient methods, choosing the initial values of the variational parameters carefully, and then comparing the free energies of the various minima. The color and electric charges were neutralized with a globally convergent Newton-Raphson method in multidimensions.

Gapless quasiparticle excitations are characterized by a non-zero gap, Δ_{ij}, and a corresponding dispersion relation that is zero for at least one value of the quasiparticle momentum, *i.e.*, the dispersion relation reaches the Fermi surface and there is no forbidden energy band.

[1] R. Rapp, T. Schäfer, E. V. Shuryak and M. Velkovsky, Phys. Rev. Lett. **81**, 53 (1998).
[2] M. G. Alford, K. Rajagopal and F. Wilczek, Phys. Lett. B **422**, 247 (1998).
[3] D. Blaschke and C. D. Roberts, Nucl. Phys. A **642**, 197 (1998).
[4] B.C. Barrois, Nucl. Phys. **B129**, 390 (1977).
[5] D. Bailin and A. Love, Phys. Rep. **107**, 325 (1984).
[6] K. Rajagopal and F. Wilczek, arXiv:hep-ph/0011333.
[7] M. G. Alford, Ann. Rev. Nucl. Part. Sci. **51**, 131 (2001).
[8] M. Buballa, Phys. Rep. **407**, 205 (2005).
[9] A. Schmitt, Phys. Rev. D **71**, 054016 (2005).
[10] D. Blaschke, N.K. Glendenning, A. Sedrakian (Eds.), *Physics of Neutron Star Interiors* (Springer, Heidelberg, 2001).
[11] D.K. Hong et al. (Eds.), *Compact Stars: The quest for new states of matter* (World Scientific, Singapore, 2004).
[12] D. Blaschke, D. Sedrakian (Eds.), *Superdense QCD Matter in Compact Stars* (Springer, Heidelberg, 2005).
[13] J. E. Horvath, O. G. Benvenuto and H. Vucetich, Phys. Rev. D **44**, 3797 (1991).
[14] D. Blaschke, T. Klähn and D. N. Voskresensky, Astrophys. J. **533**, 406 (2000).
[15] D. Page, M. Prakash, J. M. Lattimer and A. Steiner, Phys. Rev. Lett. **85**, 2048 (2000).
[16] D. Blaschke, H. Grigorian and D. N. Voskresensky, Astron. Astrophys. **368**, 561 (2001).
[17] H. Grigorian, D. Blaschke and D. Voskresensky, Phys. Rev. **C** (2005) in press; [arXiv:astro-ph/0411619].
[18] D. Blaschke, D. M. Sedrakian and K. M. Shahabasian, Astron. Astrophys. **350**, L47 (1999).
[19] M. G. Alford, J. Berges and K. Rajagopal, Nucl. Phys. B **571**, 269 (2000).
[20] K. Iida and G. Baym, Phys. Rev. D **66**, 014015 (2002).
[21] D. M. Sedrakian, D. Blaschke, K. M. Shahabasian and D. N. Voskresensky, Phys. Part. Nucl. **33**, S100 (2002).
[22] D. K. Hong, S. D. H. Hsu and F. Sannino, Phys. Lett. B **516**, 362 (2001).
[23] R. Ouyed and F. Sannino, Astron. Astrophys. **387**, 725 (2002).
[24] D. N. Aguilera, D. Blaschke and H. Grigorian, Astron. Astrophys. **416**, 991 (2004).
[25] D. N. Aguilera, D. Blaschke and H. Grigorian, arXiv:astro-ph/0402073.
[26] R. Ouyed, R. Rapp and C. Vogt, arXiv:astro-ph/0503357.
[27] F. Neumann, M. Buballa and M. Oertel, Nucl. Phys. A **714**, 481 (2003).
[28] M. Oertel and M. Buballa, arXiv:hep-ph/0202098.
[29] C. Gocke, D. Blaschke, A. Khalatyan and H. Grigorian, arXiv:hep-ph/0104183.
[30] M. Alford and K. Rajagopal, JHEP **0206**, 031 (2002).
[31] A. W. Steiner, S. Reddy and M. Prakash, Phys. Rev. D **66**, 094007 (2002).
[32] M. G. Alford, C. Kouvaris and K. Rajagopal, Phys. Rev. Lett. **92**, 222001 (2004).
[33] M. Alford, C. Kouvaris and K. Rajagopal, Phys. Rev. D **71**, 054009 (2005).
[34] S. B. Rüster, I. A. Shovkovy and D. H. Rischke, Nucl. Phys. A **743**, 127 (2004).
[35] I. Shovkovy and M. Huang, Phys. Lett. B **564**, 205 (2003).
[36] M. Huang and I. Shovkovy, Nucl. Phys. **A729**, 835 (2003).
[37] M. G. Alford, K. Rajagopal and F. Wilczek, Nucl. Phys. **B537**, 443 (1999).

[38] D. Blaschke, H. P. Pavel, V. N. Pervushin, G. Ropke and M. K. Volkov, Phys. Lett. B **397**, 129 (1997).
[39] L. von Smekal, A. Mecke and R. Alkofer, arXiv:hep-ph/9707210.
[40] H. B. Nielsen, M. Rho, A. Wirzba and I. Zahed, Phys. Lett. B **281**, 345 (1992).
[41] R. Alkofer, P. A. Amundsen and H. Reinhardt, Phys. Lett. B **218**, 75 (1989).
[42] S. B. Rüster, V. Werth, M. Buballa, I. A. Shovkovy and D. H. Rischke, arXiv:hep-ph/0503184.
[43] L. P. Gor'kov, Zh. Eksp. Teor. Fiz. **36**, 1918 (1959).
[44] Y. Nambu, Phys. Rev. **117**, 648 (1960).
[45] J. I. Kapusta, *Finite-temperature field theory* (University Press, Cambridge, 1989).
[46] D. N. Aguilera, D. Blaschke and H. Grigorian, Nucl. Phys. **A**, in press (2005); arXiv:hep-ph/0412266.
[47] N. K. Glendenning, *Compact Stars* (Springer, New York, 2000).
[48] S. L. Shapiro and S. A. Teukolsky, *Black Holes, White Dwarfs, and Neutron Stars* (Wiley, New York, 1983).
[49] C. Kettner, F. Weber, M. K. Weigel and N. K. Glendenning, Phys. Rev. D **51**, 1440 (1995).
[50] D. Blaschke, H. Grigorian, G. S. Poghosyan, C. D. Roberts and S. M. Schmidt, Phys. Lett. B **450**, 207 (1999).
[51] D. Blaschke, S. Fredriksson, H. Grigorian and A. M. Oztas, Nucl. Phys. A **736**, 203 (2004).
[52] D. Blaschke, H. Grigorian, A. Khalatyan and D. N. Voskresensky, Nucl. Phys. Proc. Suppl. **141**, 137 (2005).
[53] R. S. Duhau, A. G. Grunfeld and N. N. Scoccola, Phys. Rev. D **70**, 074026 (2004).
[54] M. Baldo, M. Buballa, F. Burgio, F. Neumann, M. Oertel and H. J. Schulze, Phys. Lett. B **562**, 153 (2003).
[55] I. Shovkovy, M. Hanauske and M. Huang, Phys. Rev. D **67**, 103004 (2003).
[56] H. Grigorian, D. Blaschke and D. N. Aguilera, Phys. Rev. C **69**, 065802 (2004).
[57] M. Abramowitz and I. A. Stegun, *Handbook of Mathematical Functions with Formulas, Graphs, and Mathematical Tables* (Dover, New York, 1972), pp. 17-18.

Paper II

Preon stars: a new class of cosmic compact objects

J. Hansson* and F. Sandin†
Department of Physics, Luleå University of Technology, SE-971 87 Luleå, Sweden

In the context of the standard model of particle physics, there is a definite upper limit to the density of stable compact stars. However, if a more fundamental level of elementary particles exists, in the form of preons, stability may be re-established beyond this limiting density. We show that a degenerate gas of interacting fermionic preons does allow for stable compact stars, with densities far beyond that in neutron stars and quark stars. In keeping with tradition, we call these objects "preon stars", even though they are small and light compared to white dwarfs and neutron stars. We briefly note the potential importance of preon stars in astrophysics, *e.g.*, as a candidate for cold dark matter and sources of ultra-high energy cosmic rays, and a means for observing them.

PACS numbers: 12.60.Rc - 04.40.Dg - 97.60.-s - 95.35.+d

I. INTRODUCTION

The three different types of compact objects traditionally considered in astrophysics are white dwarfs, neutron stars (including quark and hybrid stars), and black holes. The first two classes are supported by Fermi pressure from their constituent particles. For white dwarfs, electrons provide the pressure counterbalancing gravity. In neutron stars, the neutrons play this role. For black holes, the degeneracy pressure is overcome by gravity and the object collapses indefinitely, or at least to the Planck density.

The distinct classes of degenerate compact stars originate directly from the properties of gravity, as was made clear by a theorem of Wheeler and collaborators in the mid 1960s [1]. The theorem states that for the solutions to the stellar structure equations, whether Newtonian or relativistic, there is a change in stability of one radial mode of normal vibration whenever the mass reaches a local maximum or minimum as a function of central density. The theorem assures that distinct classes of stars, such as white dwarfs and neutron stars, are separated in central density by a region in which there are no stable configurations.

In the standard model of particle physics (SM), the theory of the strong interaction between quarks and gluons predicts that with increasing energy and density, the coupling between quarks asymptotically fades away [2, 3]. As a consequence of this "asymptotic freedom", matter is expected to behave as a gas of free fermions at sufficiently high densities. This puts a definite upper limit to the density of stable compact stars, since the solutions to the stellar equations end up in a never-ending sequence of unstable configurations, with increasing central density. Thus, in the light of the standard model, the densest stars likely to exist are neutron stars, quark stars or the potentially more dense hybrid stars [4, 5, 6]. However, if there is a deeper layer of constituents, below that of quarks and leptons, asymptotic freedom will break down at sufficiently high densities, as the quark matter phase dissolves into the preon sub-constituent phase.

There is a general consensus among the particle physics community, that something new should appear at an energy-scale of around one TeV. The possibilities are, *e.g.*, supersymmetric particles, new dimensions and compositeness. In this letter we consider "preon models" [7, 8], *i.e.*, models in which quarks and leptons, and sometimes some of the gauge bosons, are composite particles built out of more elementary preons. If fermionic preons exist, it seems reasonable that a new type of

*Electronic address: c.johan.hansson@ltu.se
†Electronic address: fredrik.sandin@ltu.se

astrophysical compact object, a *preon star*, could exist. The density in preon stars should far exceed that inside neutron stars, since the density of preon matter must be much higher than the density of nuclear and deconfined quark matter. The sequence of compact objects, in order of increasing compactness, would thus be: white dwarfs, neutron stars, preon stars and black holes.

II. MASS-RADIUS RELATIONS

Assuming that a compact star is composed of non-interacting fermions with mass m_f, the non-general relativistic (Chandrasekhar) expression for the maximum mass is [9, 10]:

$$M \simeq \frac{1}{m_f^2}\left(\frac{\hbar c}{G}\right)^{3/2}. \tag{1}$$

This expression gives a correct order of magnitude estimate for the mass of a white dwarf and a neutron star. For quark stars, this estimate cannot be used literally, since the mass of quarks cannot be defined in a similar way as for electrons and neutrons. However, making the simplifying assumption that quarks are massless and subject to a 'bag constant', a maximum mass relation can be derived [11]. The bag constant is a phenomenological parameter. It represents the strong interactions that, in addition to the quark momenta, contribute mass-energy to deconfined quark matter, *i.e.*, in the same way as the bag constant for ordinary hadrons [12]. The result in [11] is somewhat similar to the Chandrasekhar expression, but the role of the fermion mass is replaced by the bag constant B:

$$M = \frac{16\pi B R^3}{3c^2}, \tag{2}$$

$$R = \frac{3c^2}{16\sqrt{\pi G B}}. \tag{3}$$

For preon stars, one can naively insert a preon mass of $m_f \simeq 1$ TeV/c^2 in eq. (1) to obtain a preon star mass of approximately one Earth mass ($M_\oplus \simeq 6\times 10^{24}$ kg). However, the energy scale of one TeV should rather be interpreted as a length scale, since it originates from the fact that in particle physics experiments, no substructure has been found down to a scale of a few hundred GeV ($\hbar c/\mathrm{GeV} \simeq 10^{-18}$ m). Since preons must be able to give light particles, *e.g.*, neutrinos and electrons, the "bare" preon mass presumably is fairly small and a large fraction of the mass-energy should be due to interactions. This is the case for deconfined quark matter, where the bag constant contributes more than 10% of the energy density. Guided by this observation, and lacking a quantitative theory for preon interactions, we assume that the mass-energy contribution from preon interactions can be accounted for by a bag constant. We estimate the order of magnitude for the preon bag constant by fitting it to the minimum density of a composite electron, with mass $m_e = 511$ keV/c^2 and "radius" $R_e \lesssim \hbar c/\mathrm{TeV} \simeq 10^{-19}$ m. The bag-energy is roughly $4B\langle V\rangle$ [12], where $\langle V\rangle$ is the time-averaged volume of the bag (electron), so the bag constant is:

$$B \simeq \frac{E}{4\langle V\rangle} \gtrsim \frac{3\times 511\,\mathrm{keV}}{16\pi(10^{-19}\mathrm{m})^3} \simeq 10^4\,\mathrm{TeV/fm^3} \Longrightarrow B^{1/4} \gtrsim 10\,\mathrm{GeV}. \tag{4}$$

Inserting this value of B in eqs. (2), (3), we obtain an estimate for the maximum mass, $M_{max} \simeq 10^2\ \mathrm{M}_\oplus$, and radius, $R_{max} \simeq 1$ m, of a preon star.

Since $B^{1/4} \simeq 10$ GeV only is an order of magnitude estimate for the minimum value of B, in the following, we consider the bag constant as a free parameter of the model, with a lower limit of $B^{1/4} = 10$ GeV and an upper limit chosen as $B^{1/4} = 1$ TeV. The latter value corresponds to an electron "radius" of $\hbar c/10^3\,\mathrm{TeV} \simeq 10^{-22}$ m. In figs. 1 and 2 the (Chandrasekhar) maximum mass and radius of a preon star are plotted as a function of the bag constant.

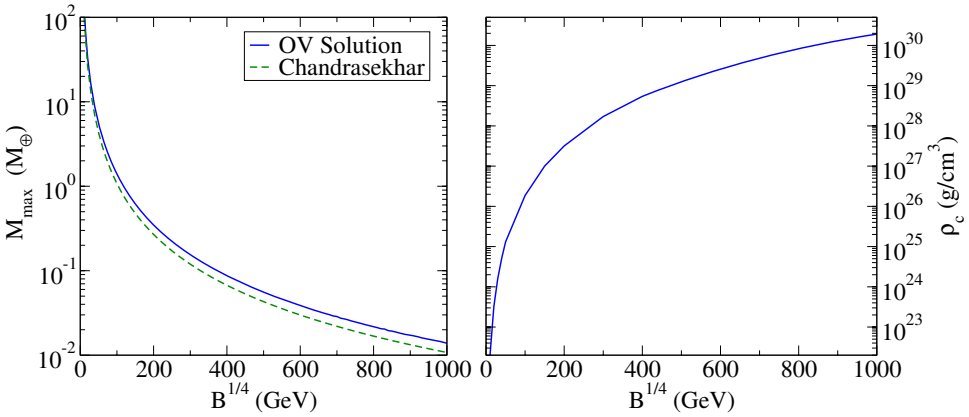

FIG. 1: The maximum mass and corresponding central density ρ_c of a preon star vs. the bag constant B. The solid lines represent the general relativistic OV solutions, while the dashed line represents the Newtonian (Chandrasekhar) estimate. Despite the high central density, the mass of these objects is below the Schwarzschild limit, as is always the case for static solutions to the stellar equations. $M_\oplus \simeq 6\times 10^{24}$ kg is the Earth mass.

Due to the extreme density of preon stars, a general relativistic treatment is necessary. This is especially important for the analysis of stability when a preon star is subject to small radial vibrations. In this introductory article we will neglect the effects of rotation on the composition. Thus, we can use the Oppenheimer-Volkoff (OV) equations [13] for hydrostatic, spherically symmetric equilibrium:

$$\frac{dp}{dr} = -\frac{G\left(p+\rho c^2\right)\left(mc^2+4\pi r^3 p\right)}{r\left(rc^4-2Gmc^2\right)}, \tag{5}$$

$$\frac{dm}{dr} = 4\pi r^2 \rho. \tag{6}$$

Here p is the pressure, ρ the total density and $m = m(r)$ the mass within the radial coordinate r. The total mass of a preon star is $M = m(R)$, where R is the coordinate radius of the star. Combined with an equation of state (EoS), $p = p(\rho)$, obtained from some microscopic theory, the OV solutions give the possible equilibrium states of preon stars.

Since no theory for the interaction between preons yet exists, we make a simple assumption for the EoS. The EoS for a gas of massless fermions is $\rho c^2 = 3p$ (see, *e.g.*, [14]), independently of the degeneracy factor of the fermions. By adding a bag constant B, one obtains $\rho c^2 = 3p + 4B$. This is the EoS that we have used when solving the OV equations. The obtained (OV) maximum mass and radius configurations are also plotted in figs. 1 and 2.

III. STABILITY ANALYSIS

A necessary, but not sufficient, condition for stability of a compact star is that the total mass is an increasing function of the central density $dM/d\rho_c > 0$ [14]. This condition implies that a slight compression or expansion of a star will result in a less favourable state, with higher total energy. Obviously, this is a necessary condition for a stable equilibrium configuration. Equally important, a star must be stable when subject to radial oscillations. Otherwise, any small perturbation would bring about a collapse of the star.

The equations for the analysis of such radial modes of oscillation are due to Chandrasekhar [15]. An overview of the theory, and some applications, can be found in [16]. For clarity, we reproduce

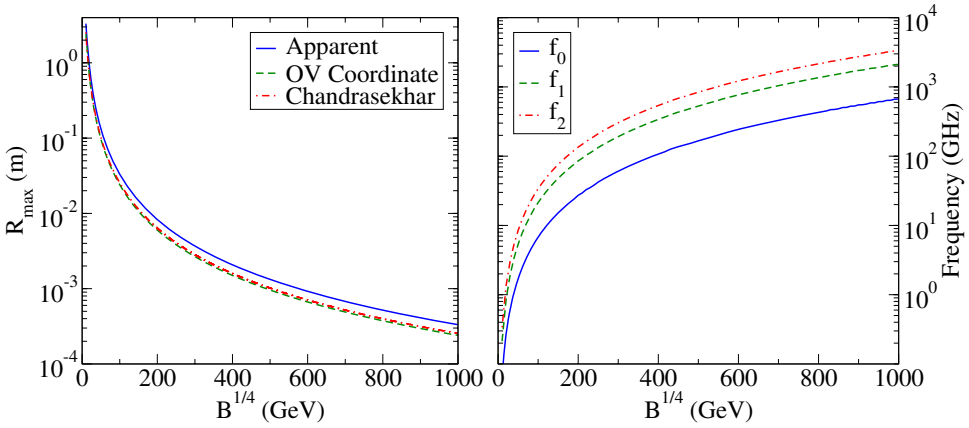

FIG. 2: The maximum radius and the corresponding first three eigenmode oscillation frequencies (f_0, f_1, f_2) vs. the bag constant. The solid line in the left-hand picture is the "apparent" radius, $R^{\infty} = R/\sqrt{1-2GM/Rc^2}$, as seen by a distant observer. The dashed line represents the general relativistic coordinate radius obtained from the OV solution, while the dotted line represents the Newtonian (Chandrasekhar) estimate. Since the fundamental mode f_0 is real ($\omega_0^2 > 0$), preon stars with mass below the maximum are stable, for each value of B.

some of the important points. Starting with the metric of a spherically symmetric equilibrium stellar model,

$$ds^2 = -e^{2\nu(r)}dt^2 + e^{2\lambda(r)}dr^2 + r^2\left(d\theta^2 + \sin^2(\theta)d\phi^2\right), \tag{7}$$

and the energy-momentum tensor of a perfect fluid, $T_{\mu\nu} = (\rho + p)u_\mu u_\nu + p g_{\mu\nu}$, the equation governing radial adiabatic oscillations can be derived from Einstein's equation. By making an ansatz for the time dependence of the radial displacement of fluid elements of the form:

$$\delta r(r,t) = r^{-2}e^{\nu(r)}\zeta(r)e^{i\omega t}, \tag{8}$$

the equation simplifies to a Sturm-Liouville eigenvalue equation for the eigenmodes [15, 16]:

$$\frac{d}{dr}\left(P\frac{d\zeta}{dr}\right) + (Q + \omega^2 W)\zeta = 0. \tag{9}$$

The coefficients P, Q and W are [16] (in geometric units where $G = c = 1$):

$$P = \Gamma r^{-2} p e^{\lambda(r)+3\nu(r)}, \tag{10}$$

$$Q = e^{\lambda(r)+3\nu(r)}\left[(p+\rho)^{-1}r^{-2}\left(\frac{dp}{dr}\right)^2 - 4r^{-3}\frac{dp}{dr} - 8\pi r^{-2}p(p+\rho)e^{2\lambda(r)}\right], \tag{11}$$

$$W = (p+\rho)r^{-2}e^{3\lambda(r)+\nu(r)}, \tag{12}$$

where the adiabatic index Γ is:

$$\Gamma = \frac{p+\rho}{p}\left(\frac{\partial p}{\partial \rho}\right)_S. \tag{13}$$

The boundary conditions for $\zeta(r)$ are that $\zeta(r)/r^3$ is finite or zero as $r \to 0$, and that the Lagrangian variation of the pressure,

$$\Delta p = -\frac{\Gamma p e^{\nu}}{r^2}\frac{d\zeta}{dr}, \tag{14}$$

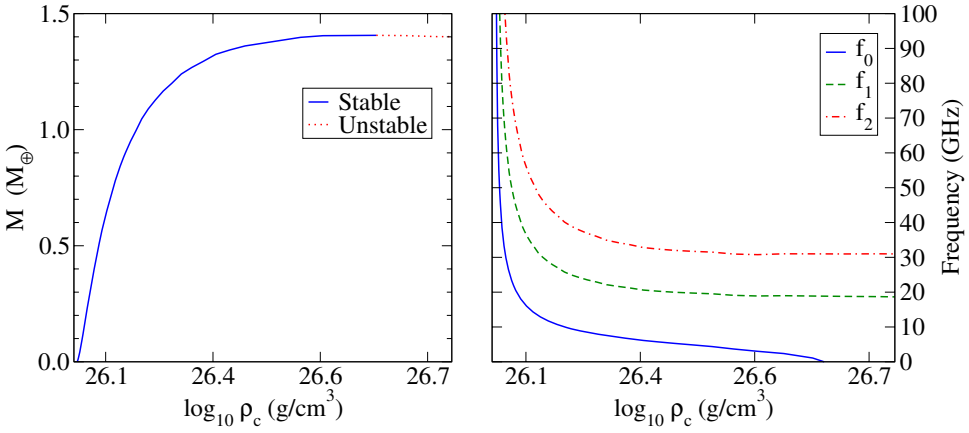

FIG. 3: The mass and the first three eigenmode oscillation frequencies (f_0, f_1, f_2) vs. the central density ρ_c of preon stars. Here, a fixed value of $B^{1/4} = 100$ GeV has been used. For the maximum mass configuration, the fundamental mode f_0 has zero frequency, indicating the onset of instability. Preon stars with mass and density below the maximum mass configuration of this sequence are stable.

vanishes at the surface of the star.

A catalogue of various numerical methods for the solution of eq. (9) can be found in [17]. In principle, we first solve the OV equations, thereby obtaining the metric functions $\lambda(r)$ and $\nu(r)$, as well as $p(r)$, $\rho(r)$ and $m(r)$. Then, the metric functions $\lambda(r)$ and $\nu(r)$ must be corrected for, so that they match the Schwarzschild metric at the surface of the star (see, *e.g.*, [14]). Once these quantities are known, eq. (9) can be solved for $\zeta(r)$ and ω^2 by a method commonly known as the "shooting" method. One starts with an initial guess on ω^2, and integrates eq. (9) from $r = 0$ to the surface of the star. At this point $\zeta(r)$ is known, and Δp can be calculated. The number of nodes of $\zeta(r)$ is a non-decreasing function of ω^2 (due to Sturm's oscillation theorem). Thus, one can continue making educated guesses for ω^2, until the correct boundary condition ($\Delta p = 0$) and number of nodes are obtained. This method is simple to use when only a few eigenmodes are needed.

Due to the time dependence in eq. (8), a necessary (and sufficient) condition for stability is that all ω_i^2 are positive. Since ω_i^2 are eigenvalues of a Sturm-Liouville equation, and governed by Sturm's oscillation theorem, it is sufficient to prove that the fundamental mode, ω_0^2, is greater than zero for a star to be stable. In fig. 3 the first three oscillation frequencies, $f_i = \omega_i/2\pi$, for various stellar configurations with $B^{1/4} = 100$ GeV are plotted. In agreement with the turning point theorem of Wheeler *et al.* [1], the onset of instability is the point of maximum mass, as ω_0^2 becomes negative for higher central densities. Thus, for this value of the bag constant, preon stars are stable up to the maximum mass configuration. In order to see if the same is true for other values of B, we plot the first three oscillation frequencies as a function of B, choosing the maximum radius configuration for each B. The result can be found in fig. 2. Indeed, the previous result is confirmed; all configurations up to the maximum mass are stable.

The eigenmode frequencies for radial oscillations of preon stars are about six orders of magnitude higher than for neutron stars. This result can also be obtained by making a simple estimate for the frequency of the fundamental mode. The radius of a preon star is a factor of $\sim 10^5$ smaller than neutron stars. Hence, if the speed of sound is similar in preon stars and neutron stars, the frequency would increase by a factor of $\sim 10^5$, giving GHz frequencies. If the speed of sound is higher in preon stars, say approaching the speed of light, the maximum frequency is $\sim 10^8$ m s^{-1}/0.1 m $\simeq 1$ GHz. Thus, in either case, GHz oscillation frequencies are expected for preon stars.

IV. POTENTIAL ASTROPHYSICAL CONSEQUENCES AND DETECTION

If preon stars do exist, and are as small as $10^{-1} - 10^{-4}$ m, it is plausible that primordial preon stars (or "nuggets") formed from density fluctuations in the early universe. As this material did not take part in the ensuing nucleosynthesis, the abundance of preon nuggets is not constrained by the hot big bang model bounds on baryonic matter. Also, preon nuggets are immune to Hawking radiation [18] that rapidly evaporates small primordial black holes, making it possible for preon nuggets to survive to our epoch. They can therefore serve as the mysterious dark matter needed in many dynamical contexts in astrophysics and cosmology [19, 20].

Preon stars born out of the collapse of massive ordinary stars [21] cannot contribute much to cosmological dark matter, as that material originally is baryonic and thus constrained by big bang nucleosynthesis. However, they could contribute to the dark matter in galaxies. Roughly 4% of the total mass of the universe is in baryonic form [22], but only 0.5% is observed as visible baryons [23]. Assuming, for simplicity, that all dark matter $\rho_{DM} = 10^{-25}$ g/cm^3 in spiral galaxies, *e.g.*, our own Milky Way, is in the form of preon stars with mass 10^{24} kg, the number density of preon stars is of the order of 10^4 per cubic parsec (1 parsec$\simeq 3.1 \times 10^{16}$ m). This translates into one preon star per 10^6 solar system volumes. However, even though it is not ruled out a priori, the possibility to form a very small and light preon star in the collapse of a large massive star remains to be more carefully investigated. In any case, preon nuggets formed in the primordial density fluctuations could account for the dark matter in galaxies. The existence of such objects can in principle be tested by gravitational microlensing experiments.

Today there is no known mechanism for the acceleration of cosmic rays with energies above $\sim 10^{17}$ eV. These so-called ultra-high energy cosmic rays [24] (UHE CR) are rare, but have been observed with energies approaching 10^{21} eV. The sources of UHE CR must, cosmologically speaking, be nearby ($\lesssim 50$ Mpc $\simeq 150$ million light years) due to the GZK-cutoff energy $\sim 10^{19}$ eV [25, 26], since the cosmic microwave background is no longer transparent to cosmic rays at such high energies. This requirement is very puzzling, as there are no known sources capable of accelerating UHE CR within this distance. Preon stars open up a new possibility. It is known that neutron stars, in the form of pulsars, can be a dominant source of galactic cosmic rays [27], but cannot explain UHE CR. If for preon stars we assume, as in models of neutron stars, that the magnetic flux of the parent star is (more or less) frozen-in during collapse, induced electric fields more than sufficient for the acceleration of UHE CR become possible. As an example, assume that the collapse of a massive star is slightly too powerful for the core to stabilize as a 10 ms pulsar with radius 10 km, mass $1.4M_\odot$ ($M_\odot \simeq 2 \times 10^{30}$ kg is the mass of our sun) and magnetic field 10^8 T, and instead collapses to a preon star state with radius 1 m and mass $10^2 M_\oplus$. An upper limit estimate of the induced electric field of the remaining "preon star pulsar" yields $\sim 10^{34}$ V/m, which is more than enough for the acceleration of UHE CR. Also, such strong electric fields are beyond the limit where the quantum electrodynamic vacuum is expected to break down, $|\mathbf{E}| > 10^{18}$ V/m, and spontaneously start pair-producing particles [28]. This could provide an intrinsic source of charged particles that are accelerated by the electric field, giving UHE CR. With cosmic ray detectors, like the new Pierre Auger Observatory [29], this could provide means for locating and observing preon stars.

V. CONCLUSIONS

In this letter we suggest that if there is a deeper layer of fermionic constituents, so-called preons, below that of quarks and leptons, a new class of stable compact stars could exist. Since no detailed theory yet exists for the interaction between preons, we assume that the mass-energy contribution from preon interactions can be accounted for by a 'bag constant'. By fitting the bag constant to the energy density of a composite electron, the maximum mass for preon stars can be estimated to $\sim 10^2$ M$_\oplus$ ($M_\oplus \simeq 6 \times 10^{24}$ kg being the Earth mass), and their maximum radius to ~ 1 m. The

central density is at least of the order of 10^{23} g/cm^3. Preon stars could have formed by primordial density fluctuations in the early universe, and in the collapse of massive stars. We have briefly noted their potential importance for dark matter and ultra-high energy cosmic rays, connections that also could be used to observe them. This might provide alternative means for constraining and testing different preon models, in addition to direct tests [8] performed at particle accelerators.

VI. ACKNOWLEDGEMENTS

F. Sandin acknowledges support from the Swedish National Graduate School of Space Technology. We thank S. Fredriksson for several useful discussions and for reading the manuscript.

---

[1] Harrison B.K., Thorne K.S., Wakano M. & Wheeler J.A., *Gravitation Theory and Gravitational Collapse* (University of Chicago Press, Chicago, 1965).
[2] Gross D.J. & Wilczek F., Phys. Rev. Lett. **30**, 1323 (1973).
[3] Politzer H.D., Phys. Rev. Lett. **30**, 1346 (1973).
[4] Gerlach U.H., Phys. Rev. **172**, 1325 (1968),
Gerlach U.H., *A third family of stable equilibria*, Ph.D. thesis, Princeton University, 1968.
[5] Glendenning N.K. & Kettner C., Astron. Astrophys. **353**, L9 (2000).
[6] Schertler K. *et al.*, Nucl. Phys. **A 677**, 463 (2000).
[7] D'Souza I.A. & Kalman C.S., *Preons* (World Scientific, Singapore, 1992).
[8] Dugne J.-J., Fredriksson S. & Hansson J., Europhys. Lett. **57**, 188 (2002).
[9] Chandrasekhar S., *An Introduction to the Study of Stellar Structure* (Dover Publications, New York, 1958).
[10] Landau L.D., Phys. Z. Sowjetunion **1**, 285 (1932).
[11] Banerjee S., Ghosh S.K. & Raha S., J. Phys. **G 26**, L1 (2000).
[12] Chodos A. *et al.*, Phys. Rev. **D 9**, 3471 (1974).
[13] Oppenheimer J.R. & Volkoff G., Phys. Rev. **55**, 374 (1939).
[14] Glendenning N.K., *Compact Stars* (Springer-Verlag, New York, 1997).
[15] Chandrasekhar S., Phys. Rev. Lett. **12**, 114 (1964).
[16] Misner C.W., Thorne K.S. & Wheeler J.A., *Gravitation* (Freeman and Co., San Francisco, 1973).
[17] Bardeen J.M., Thorne K.S. & Meltzer D.W., Astrophys. J. **145**, 505 (1966).
[18] Hawking S.W., Commun. Math. Phys. **43**, 199 (1975).
[19] Turner M.S., Phys. Rep. **333**, 619 (2000).
[20] Bergström L., Rep. Progr. Phys. **63**, 793 (2000).
[21] Paczyński B., Astrophys. J. **494**, L45 (1998).
[22] Spergel D.N. *et al.*, Astrophys. J. Suppl. **148**, 175 (2003).
[23] Hagiwara K. *et al.*, Phys. Rev. **D 66**, 010001 (2002).
[24] Nagano M. & Watson A.A., Rev. Mod. Phys. **72**, 689 (2000).
[25] Greisen K., Phys. Rev. Lett. **16**, 748 (1966).
[26] Zatsepin G.T. & Kuzmin V.A., JETP Lett. **41**, 78 (1966).
[27] Gold T., Nature **221**, 25 (1969).
[28] Schwinger J., Phys. Rev. **82**, 664 (1951).
[29] Dova M.T. *et al.*, Nucl. Phys. Proc. Suppl. **122**, 170 (2003).

Paper III

Eur Phys J C (2005)
Digital Object Identifier (DOI) 10.1140/epjcd/s2005-03-003-y

EPJ C direct
electronic only

Young Scientist

Compact stars in the standard model – and beyond

F. Sandin

Department of Physics, Luleå University of Technology, 97187 Luleå, Sweden, e-mail: fredrik.sandin@ltu.se

Received: 24 January 2005 / Accepted: 10 February 2005 /
Published online: 23 February 2005 –

Abstract. In the context of the standard model of particle physics, there is a definite upper limit to the density of stable compact stars. However, if there is a deeper layer of constituents, below that of quarks and leptons, stability may be re-established far beyond this limiting density and a new class of compact stars could exist. These objects would cause gravitational lensing of gamma-ray bursts and white dwarfs, which might be observable as line features in the spectrum. Such observations could provide means for obtaining new clues about the fundamental particles and the nature of cold dark matter.

PACS. 12.60.Rc, 04.40.Dg, 95.35.+d

1 Introduction

The different types of compact objects traditionally considered in astrophysics are white dwarfs, neutron stars (including quark and hybrid stars), and black holes. The first two classes are supported by Fermi degeneracy pressure from their constituent particles. For white dwarfs, electrons provide the pressure counterbalancing gravity. In neutron stars, the neutrons play this role. For black holes, the degeneracy pressure is overcome by gravity and the object collapses to a singularity, or at least to the Planck scale ($\rho \sim 10^{93}$ g/cm^3). For a recent review of neutron stars, hybrid stars, and quark stars, see, e.g., [1] and references therein.

The distinct classes of degenerate compact stars originate directly from the properties of gravity, as was made clear by a theorem of Wheeler and collaborators in the mid 1960s [2]. This theorem states that for the solutions to the stellar structure equations, whether Newtonian or relativistic, there is a change in stability of one radial mode of vibration whenever the mass reaches a local maximum or minimum as a function of the central density. The theorem assures that distinct classes of stars, such as white dwarfs and neutron stars, are separated in central density by a region in which there are no stable configurations.

In the standard model of quarks and leptons (SM), the theory of the strong interaction between quarks and gluons predicts that with increasing energy and density, the coupling between quarks asymptotically fades away [3, 4]. As a consequence of this so-called asymptotic freedom, matter is expected to behave as a gas of free fermions at sufficiently high densities. This puts a definite upper limit to the density of stable compact stars, since the solutions to the stellar equations end up in a never-ending sequence of unstable configurations, with increasing central density. Thus, in the light of the standard model, the densest stars likely to exist are neutron stars, quark stars, or the slightly more dense hybrid stars [5–7]. However, if there is a deeper layer of constituents, below that of quarks and leptons, the possibility of a new class of compact stars opens up [8].

Though being a quantitatively successful theory, the SM consists of a large number of exogenous *ad hoc* rules and parameters, which were introduced solely to fit the experimental data. The SM provides no explanation for the deeper meaning of these rules. At a closer look, however, the SM seems to be full of hints to its deeper background. By considering these rules from a historical point of view, a "simple" and appealing explanation is *compositeness* [9], i.e., that the quarks, leptons, and gauge bosons are composite particles, built out of more elementary *preons* [10]. Preons provide natural explanations for the particle families of the SM and phenomena such as neutrino oscillations, mixing of the weak gauge bosons, and quarks of different flavour.

Over the last decades, many papers have been written about preons, but so far there are no direct evidence for (or against!) their existence. In the late 1970s, a number of consistency conditions were formulated by 't Hooft [11]. In the same work, a vector-like non-Abelian $SU(3)$ gauge group was considered, but no solution to the consistency conditions was found. Later, it was shown that with another choice for the gauge group and the flavour structure of preons, e.g., three different preon flavours, the consistency conditions are satisfied [12]. For a more detailed discussion of preon models, see [9, 10, 13] and references therein.

Not all clues favour preon models, but the existence of preons is still an open question and, as a consequence, so is the question whether a new class of compact stars exists or not. This paper is based on the ideas and results presented in [8]. Assuming that quarks and leptons are composite particles, built out of more elementary preons, I will:

I. Give an estimate for the mass and radius of stars composed of preons.
II. Show that for some particular equations of state, stable solutions to the general relativistic stellar equations do exist, with densities far beyond the maximum density in stars composed of quarks and leptons.
III. Briefly discuss some potential astrophysical consequences and how these objects could be observed. Herein lies the potential importance of this qualitative speculation, since these objects are candidates for cold dark matter and could be found as, e.g., gravitational "femtolenses".

2 The maximum density prophecy

In order to explain why there is a maximum density for stars composed of quarks and leptons, or any other composite particle composed of these two species, e.g., nucleons and ^{56}Fe, some basic knowledge about the theory of compact stars is needed. In the following, I give a short introduction and a summary of the main points.

Due to the high density and large mass of compact stars, a general relativistic treatment of the equilibrium configurations is necessary. This is especially important for the analysis of stability when a star is subject to radial oscillations. Such oscillations are inevitably excited to some extent, and for a star to be stable the amplitude of the oscillations must not grow spontaneously with time. The starting point for a general relativistic consideration of compact stars is the Oppenheimer-Volkoff (OV) equations [14] for hydrostatic, spherically symmetric equilibrium:

$$\frac{dp}{dr} = -\frac{G\left(p+\rho c^2\right)\left(mc^2+4\pi r^3 p\right)}{r\left(rc^4-2Gmc^2\right)}, \tag{1}$$

$$\frac{dm}{dr} = 4\pi r^2 \rho. \tag{2}$$

Here p is the pressure, ρ the density and $m = m(r)$ the mass within the radial coordinate r. The total mass of the star is:

$$M = 4\pi \int_0^R r^2 \rho \, dr, \tag{3}$$

where R is the coordinate radius of the star. Combined with an equation of state (EOS), $p = p(\rho)$, obtained from some microscopic (quantum field) theory, the OV solutions give the possible equilibrium states of spherically symmetric stars.

As an example, I show two sequences of compact star configurations. One is composed of nuclear matter (neutron stars) and the other of a deconfined quark matter core with a nuclear matter crust (hybrid stars), see Fig. 1. These configurations were obtained by solving the OV equations (1)–(2) numerically. The low-density part of the nuclear matter EOS was extracted from [15] and the high-density part comes from [16]. For the deconfined quark matter phase an unpaired massless quark approximation, $\rho c^2 = 3p + 4B$, was used. The "bag pressure", B, was fitted such that the transition from quark matter to nuclear matter occurs at 1% of the nuclear saturation density, $n_0 \sim 0.16$ fm^{-3}. The density where cold nuclear matter decompose into quark matter is unknown, so the transition density used here serves as an example only.

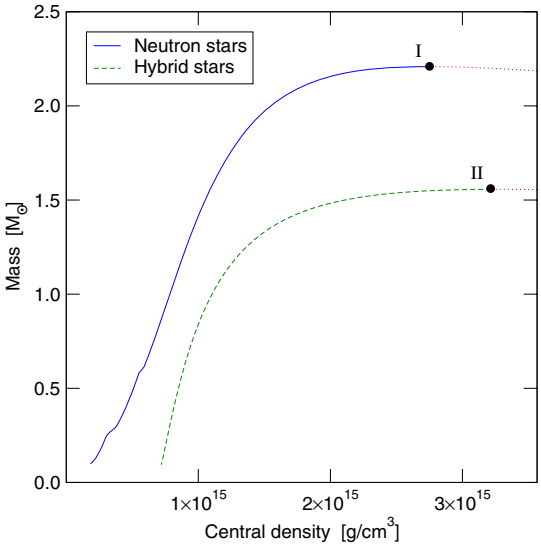

Fig. 1. Two sequences of compact stars obtained by solving the OV equations. The hybrid stars have a core of unpaired quarks and the nuclear matter crust extends down to 1% of the nuclear saturation density. The neutron star sequence is stable up to the maximum mass configuration (I). For this particular equation of state, this configuration has the highest possible (central) density, as stars more massive and dense than this are unstable and collapse into black holes. The stable hybrid star sequence terminates at II. $M_\odot \simeq 2 \times 10^{30}$ kg is the solar mass

The composition of matter at neutron star densities is an open question and many different models for the EOS exist, e.g., EOSs for nuclear matter, matter with hyperons, and superconducting quark matter. Regardless of the specific model, the maximum mass and corresponding radius are roughly a few solar masses, $M_\odot \simeq 2 \times 10^{30}$ kg, and 10 km. No substantially more dense configurations composed of quarks and leptons are possible. The motivation goes roughly like this: At white dwarf densities, the nucleons occupy nuclei that contribute little to the pressure, and electrons provide the pressure counterbalancing gravity. With increasing density, the pressure rises and the electrons become more energetic. Eventually, the elec-

trons are captured by protons and the pressure drops. As a consequence, the white dwarf sequence becomes unstable and terminates. At roughly six to seven orders of magnitude higher density than in the maximum-mass white dwarf, nuclei dissolve and the Fermi pressure of nucleons (in nuclear matter) and quarks (in quark matter) stabilize the next sequence of stable stars. The maximum mass of this sequence is a few solar masses, for all compositions (nuclear matter, quark matter, hyperons etc.). The reason why this is the limiting mass of stable compact stars, composed of quarks and leptons, is simply that there is no particle that may stabilize another sequence of stars. Each quark flavour is accompanied by an extra Fermi sea that relieves the growth of pressure and quark Fermi pressure is only won at the expense of pressure from other species. Also, the chemical potential is lower than the charm mass, so quarks heavier than the strange quark do not appear in stable stars [17, 18].

Hence, beyond the very rich and beautiful landscape of structures composed of quarks and leptons, at 10^{16} g/cm^3, there is again a desert of instability, just like there are no stable stellar configurations in-between white dwarfs and neutron stars. The question is now if the desert ends before the Planck scale.

3 Compact stars beyond the desert

A definite upper limit to the density of any spherically symmetric star can be obtained from the Schwarzschild radius,

$$R = 2GM/c^2, \tag{4}$$

since any object more dense than this would collapse into a black hole. By using the expression for the Schwarzschild radius and the relations:

$$M \sim mA, \tag{5}$$

$$R \sim d_0 A^{1/3}, \tag{6}$$

where A is the number of constituent particles, m their mass, and d_0 the distance between adjacent particles, an order of magnitude estimate for the maximum mass and radius of the corresponding class of compact stars can be calculated. For a neutron star composed of nucleons of mass $m_n \simeq 939$ MeV/c^2 and size $d_n \simeq 0.5 \times 10^{-15}$ m, (4)–(6) give $A \sim 3 \times 10^{57}$ baryons, $R \sim 7$ km, and $M \sim 5 \times 10^{30}$ kg~ 2.5 M$_\odot$. In reality, a somewhat larger radius and smaller mass are expected, since the density is non-uniform in the star, say $R \sim 10$ km and $M \sim 2$ M$_\odot$. In any case, the correct order of magnitude for the maximum mass and corresponding radius of a neutron star is obtained. The average density is $\bar{\rho} \simeq 10^{15}$ g/cm^3.

Since the Schwarzschild limit is almost reached already for the most massive neutron stars, it is reasonable to assume that this should be the case also for a more dense class of compact stars. Then, in order to provide similar estimates for the mass and radius of a star composed of preons, something must be known about the mass and "size" of preons. Before trying to achieve this, it should be emphasized that we know nothing about preons, not even if they exist. So whatever method used, the result is a speculative order of magnitude estimate. But as I will show, it is still possible to reach some qualitative results.

Guided by the observation that the density of nuclear matter is roughly of the same order of magnitude as for deconfined quark matter, I assume that the density of preon matter is roughly of the same order of magnitude as for a closely spaced lattice of some "fundamental" particle of the SM. In this case the problem is simplified to finding a fundamental SM particle, with known mass and maximum spatial extension. The simplest and least ambiguous choice seems to be the electron, since the mass of an electron is well known, and from scattering experiments it is known that electrons do not have any visible substructure down to a scale of $\sim \hbar c/\text{TeV} \sim 10^{-19}$ m. Using the electron mass, $m_e \simeq 511$ keV/c^2, and an upper estimate for its radius, $r_e \sim 10^{-19}$ m, the maximum mass and radius of a star composed of preons is found to be of the order $M \sim 10^2$ M$_\oplus$ and $R \sim 1$ m. Here M$_\oplus \simeq 6 \times 10^{24}$ kg is the mass of the Earth. The average density is of the order $\sim 10^{23}$ g/cm^3.

This crude estimate gives metre-sized objects that are a hundred times more massive than the Earth. Now, I will try to be a bit more specific. Especially, it would be interesting to see whether such objects could be stable or not. In order to do this, I extrapolate an effective model for hadrons, the so-called MIT bag model [19]. In its simplest form the MIT bag is a gas of massless fermions (partons), enclosed in a region of space (the bag) subject to an external pressure B (the bag constant). The EOS for a gas of massless fermions is $\rho c^2 = 3p$ and by including B one obtains:

$$\rho c^2 = 3p + 4B. \tag{7}$$

This result does not depend on the degeneracy factor, i.e., the number of fermion species, spin, etc. For a single hadron the pressure is practically zero, so that $\rho c^2 = 4B$ and the total energy, E, of a hadron is [19]:

$$E = 4B\langle V \rangle, \tag{8}$$

where $\langle V \rangle$ is the time-averaged volume of the bag. Hence, the bag pressure, B, must be of the order of 1 GeV/fm^3 for hadrons. This is in agreement with experiments and other independent methods of calculating light-quark hadronic masses; most of the mass-energy is not due to the "bare mass" of the constituents, but the confining interactions.

The MIT bag model is frequently used for the description of deconfined quark matter and applications to compact stars. Its usefulness in this regime originates in asymptotic freedom, simplicity and the possibility to include pertubative corrections. The bag pressure, B, is introduced in order to confine partons, it is a phenomenological parametrization of the strong interactions that confine quarks into hadrons. These interactions are present also in deconfined quark matter, so the "bag model" should be applicable also in this regime. However, the value of the bag pressure is different, since the density is higher and the interactions weaker. Thus, the so-called bag constant, B,

is not really a constant, but a density dependent parameter. For strange quark matter, the bag constant is roughly $B^{1/4} \sim 150$ MeV$/(\hbar c)^{3/4}$ [20] and the corresponding contribution to the energy density is $4B \sim 260$ MeV/fm^3. This means that a considerable fraction of the density in quark matter, roughly 10^{15} g/cm^3, is due to the bag constant, i.e., interactions.

Now, the fundamental assumption here is that preons exist and are fermions. Since preons constitute light particles, such as neutrinos and electrons, the "bare" preon mass should be fairly small. Then a massless fermion approximation, $\rho c^2 = 3p$, can be used. This EOS does not allow for stable super-dense stars, however, so something more is needed. And that 'something' is dynamics, the preon interactions that give mass-energy to the particles of the SM. The question is how, since there is so far no quantitative model for preon interactions. Indeed, a fundamental problem in preon models is to find a suitable dynamics, capable of binding preons into fermions with masses essentially negligible with respect to their inverse radius. With this in mind, the principle of parsimony ("Occam's razor") seems to be the only guidance.

A simple solution is to include the dynamics in terms of a bag constant [8], which roughly reproduces the minimum energy density of an electron,

$$B = \frac{E}{4\langle V\rangle} \sim \frac{3\times 511\,\mathrm{keV}}{16\pi(10^{-19}\,\mathrm{m})^3} \sim 10^4\,\mathrm{TeV/fm^3}$$
$$\Longrightarrow B^{1/4} \sim 10\,\mathrm{GeV}/(\hbar c)^{3/4}. \quad (9)$$

The very high density contribution from the bag constant, $4B/c^2 \sim 10^5$ TeV $c^{-2} fm^{-3} \sim 10^{23}$ g/cm^3, might seem a bit peculiar. But then it should be kept in mind that the density contribution from the bag constant in deconfined quark matter is $\sim 10^{15}$ g/cm^3, which is a large fraction of the maximum density in any type of star composed of quark matter. So the high density is not that peculiar. On the contrary, if something is to be expected, it should be that B is much higher for preon matter than for quark matter, since a "preon bag" is smaller and more dense than a hadron. In the following, for simplicity, I put $\hbar c = 1$ for the bag constant and express $B^{1/4}$ in eV.

The density introduced by the bag constant is of the same order of magnitude as the density used in the mass-radius estimate above. The improvement here is the transition to a proper EOS for fermions; the possibility to apply the EOS in a general relativistic framework, for the analysis of mass-radius relations and stability. In addition to the general relativistic analysis, the mass and radius can be estimated from first principles as a function of the bag constant [21]. The result is somewhat similar to the original Chandrasekhar limit, but the role of the fermion mass is replaced by the bag constant, B,

$$M = \frac{16\pi}{3c^2} B R^3, \quad (10)$$

$$R = \frac{3c^2}{16\sqrt{\pi G B}}. \quad (11)$$

Inserting $B^{1/4} \sim 10$ GeV in (10)–(11) an estimate for the (maximum) mass $M \simeq 10^2$ M$_\oplus$ and radius $R \sim 1$ m of a preon star is obtained. This is consistent with the somewhat simpler mass-radius estimate given above.

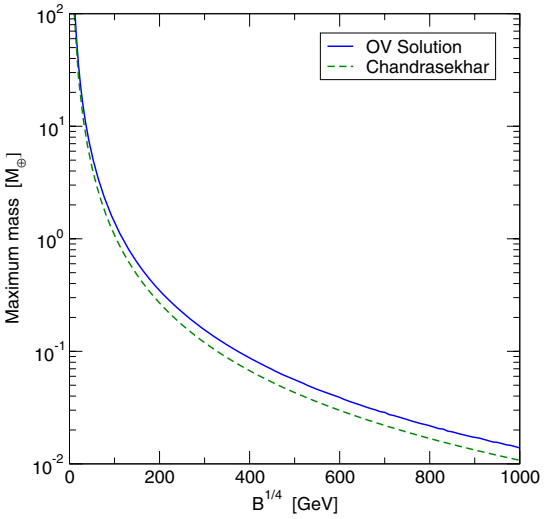

Fig. 2. The maximum mass of preon stars vs. the bag constant B. The solid line represents the general relativistic OV solutions, while the dashed line represents the Newtonian (Chandrasekhar) estimate. Despite the high central density, the mass of these objects is below the Schwarzschild limit, as is always the case for static solutions to the stellar equations. M$_\oplus \simeq 6\times 10^{24}$ kg is the Earth mass

Since $B^{1/4} \sim 10$ GeV is only an order of magnitude estimate for the lower limit, the bag constant is considered as a free parameter of the model, constrained by a lower limit of $B^{1/4} = 10$ GeV and an upper limit chosen as $B^{1/4} = 1$ TeV. The latter value corresponds to a spatial extension of the electron of the order $\sim \hbar c/10^3$ TeV $\sim 10^{-22}$ m. In Figs. 2 and 3 the maximum mass and radius of a preon star are plotted as a function of the bag constant.

A necessary (but not sufficient) condition for stability of a compact star is that the total mass is an increasing function of the central density, $dM/d\rho_c > 0$. This condition is a consequence of a generic microscopic relation known as Le Chatelier's principle. Roughly, this condition implies that a slight compression or expansion of a star will result in a less favourable state, with higher total energy. Obviously, this is a necessary condition for a stable equilibrium configuration. Equally important, a star must be stable when subject to (small) radial oscillations, in the sense that the amplitude of the oscillations must not grow spontaneously with time. Otherwise a small perturbation would bring about a collapse of the star.

The equation for the analysis of such radial modes of oscillation is due to Chandrasekhar [22]. An overview of the theory, and some applications, can be found in [23]. A catalogue of various numerical methods for solving the original set of equations can be found in [24]. However, a far more practical form of the oscillation equations has

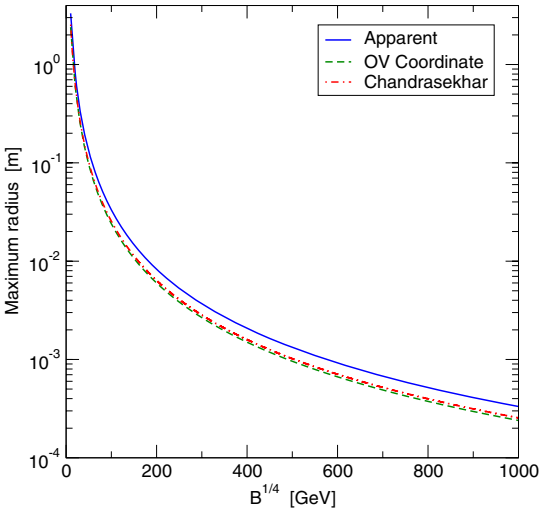

Fig. 3. The maximum radius of preon stars vs. the bag constant. The solid line is the "apparent" radius, $R^{\infty} = R/\sqrt{1-2GM/Rc^2}$, as seen by a distant observer. The dashed line represents the general relativistic coordinate radius obtained from the OV solution. The dotted line represents the Newtonian (Chandrasekhar) estimate

been derived by Gondek et al. [25]. The details of the stability analysis can be found in [8]. Here I summarise only the main points.

Assuming a time dependence of the radial displacement of fluid elements of the form $e^{i\omega t}$, the equation governing the radial oscillations is a Sturm-Liouville eigenvalue equation for ω^2. A necessary and sufficient condition for stability is that all ω_i^2 are positive, since imaginary frequencies give exponentially increasing amplitudes. Furthermore, since ω_i^2 are eigenvalues of a Sturm-Liouville equation, it turns out that it is sufficient to prove that the fundamental (nodeless) mode, ω_0^2, is positive for a star to be stable. In Fig. 4, the first three oscillation frequencies, $f_i = \omega_i/2\pi$, for various stellar configurations with $B^{1/4} = 100$ GeV are plotted. In agreement with the theorem of Wheeler et al. [2] the onset of instability is the point of maximum mass, as ω_0^2 becomes negative for higher central densities. Thus, for $B^{1/4} = 100$ GeV, preon stars are stable up to the maximum mass configuration. The same is true for other values of B [8].

Despite the large uncertainty regarding preon interactions, here manifested as a large uncertainty in the bag constant, preon stars should have central densities beyond $\sim 10^{23}$ g/cm^3. This makes preon stars fundamentally different from the traditional types of compact stars, since such high densities implies that the stars must be very small and light in order to be stable, see Fig. 5.

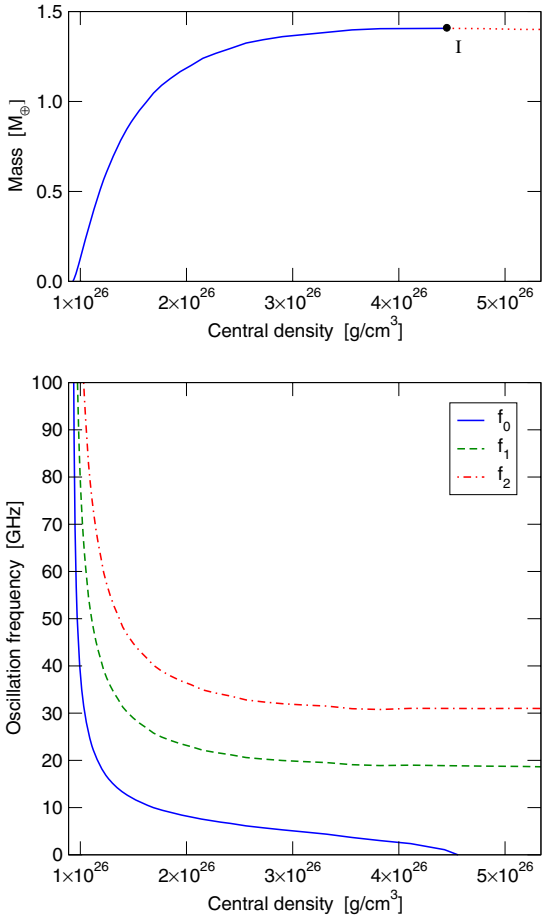

Fig. 4. The mass and the first three eigenmode oscillation frequencies (f_0, f_1, f_2) vs. the central density of preon stars. Here, a fixed value of $B^{1/4} = 100$ GeV has been used. For the maximum mass configuration (I) the fundamental (nodeless) mode, f_0, has zero frequency, indicating the onset of instability. Preon stars with densities below the density of the maximum mass configuration are stable

4 Formation and detection

The list of possible connections between the properties of the fundamental particles and the large scale structures in the universe is long. However, beyond a density of $\sim 10^{23}$ g/cm^3, not much has been proposed, since there are strong arguments against the existence of stable objects beyond $\rho \sim 10^{16}$ g/cm^3. That is, if quarks and leptons are fundamental entities.

If preons exist and objects composed of preon matter as small and light as suggested here are stable, density fluctuations in the early universe might have produced primordial preon stars (or "nuggets"). As this ma-

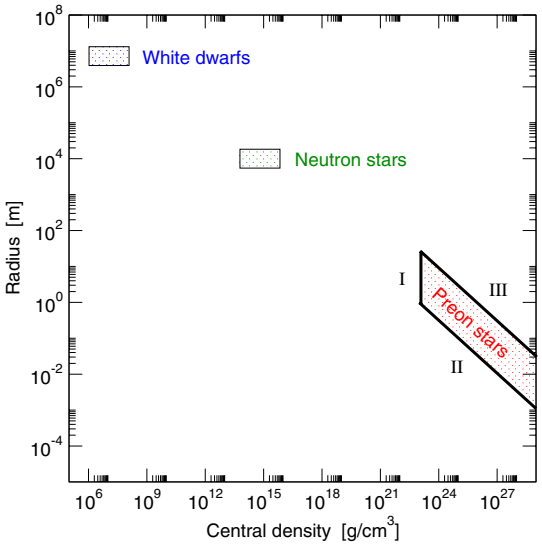

Fig. 5. The different types of compact stars traditionally considered in astrophysics are white dwarfs and neutron stars (including quark and hybrid stars). In white dwarfs, electrons provide the Fermi pressure counterbalancing gravity. In neutron stars, the neutrons (quarks, hyperons etc.) play this role. If quarks and leptons are composite particles, a new class of compact stars (preon stars) could exist. The minimum density (I) of preon stars is roughly given by the minimum density of leptons and quarks. The minimum size (II) for a given central density is due to the Schwarzschild radius (actually 4/3 of it) and a maximum size (III) exists due to instability

terial did not take part in the ensuing nucleosynthesis, the abundance of preon nuggets is not constrained by the hot big bang model bounds on baryonic matter. Also, preon nuggets are immune to Hawking radiation [26] that rapidly evaporates small primordial black holes, making it possible for them to survive to our epoch. They can therefore serve as the mysterious dark matter needed in many dynamical contexts in astrophysics and cosmology [27, 28]. The idea that preons could be connected to dark matter is already recognized in the literature [29, 30], but the picture presented here is rather different.

The Friedmann equation for the early universe is:

$$H^2(t) = \frac{8\pi G\rho}{3}, \tag{12}$$

where $\rho c^2 \sim T^4$ in the radiation-dominated era (Boltzmann's law). When including the number of internal degrees of freedom, $g_{\rm eff}$, an expression for the Hubble parameter, H, in units where $\hbar = c = k_B = 1$, is [31]:

$$H \simeq 1.66\sqrt{g_{\rm eff}}\frac{T^2}{m_{pl}}. \tag{13}$$

Here T is the temperature in eV, $g_{\rm eff}$ the effective number of degrees of freedom and $m_{pl} \simeq 1.2 \times 10^{19}$ GeV the Planck mass. For the SM, the fermions, and the gauge and Higgs bosons give $g_{\rm eff}(T = 1\,{\rm TeV}) = 106.75$. In the preon phase, this number should be smaller, say $g_{\rm eff} \sim 10$ for simplicity. Then the Hubble radius at a temperature of 1 TeV is $H^{-1} \sim 1$ mm and the mass within the Horizon (a causally connected region) is $\rho H^{-3} \sim 10^{-1}$ M$_\oplus$. This is the maximum mass of any structure that could have been formed in this early epoch. Hence, the maximum mass within causally connected regions, at the minimum temperature when deconfined preon matter might have formed preon nuggets (and the particles of the SM), is of the correct order of magnitude for stable configurations.

A potential problem is that the Jeans length, which defines the minimum length scale of regions that can contract gravitationally, was roughly of the same order of magnitude as the Hubble radius at that temperature. The Jeans length, λ_J, is [31]:

$$\lambda_J = v_s\sqrt{\frac{\pi}{G\rho_0}}, \tag{14}$$

where v_s is the speed of sound and ρ_0 the average background density. For a relativistic fluid with EOS $\rho c^2 = 3p + 4B$ the speed of sound is $v_s = c/\sqrt{3}$ and $\lambda_J \sim 1$ mm $\sim H^{-1}$. However, considering the high level of approximation used here, this is not yet a serious problem. It merely shows that the numbers are in the correct intervals.

But, perhaps it will be the other way around. After all, Popper's idea that we make progress by falsifying theories is not always true. By utilizing gamma-ray bursts (GRB) or white dwarfs in the large magellanic cloud as light sources, gravitational lenses with very small masses might be observable as diffraction line features in the spectrum [32–35]. For a lens of mass 10^{-16} M$_\odot \leq M \leq 10^{-11}$ M$_\odot$ the angular separation of images would be in the femto-arcsec range ("femtolensing"). For more massive lenses, $M \leq 10^{-7}$ M$_\odot$, the angular separation is in the pico-arcsec range ("picolensing"). The mass within the Hubble radius at $T = 1$ TeV is $\sim 10^{-1}$ M$_\oplus \sim 10^{-7}$ M$_\odot$. This roughly defines the maximum mass of preon nuggets that could be abundant enough to be observed as gravitational lenses. Hence, preon nuggets fall in the correct mass range for picolensing and femtolensing.

In Fig. 6, the magnification of a distant point light source due to gravitational lensing by an intermediate preon nugget is plotted as a function of the dimensionless frequency:

$$\nu = \frac{\tilde{\nu}(1+z_L)2GM}{c^3}, \tag{15}$$

where M (z_L) is the mass (redshift) of the lens and $\tilde{\nu}$ the frequency of light. This result was calculated with a physical-optics model, as described in [34]. In principle, the time dependent amplitude due to a single light pulse from the source was calculated and then the power spectrum was obtained by a Fourier transform of the amplitude. The magnification is normalized to a unit flux in the absence of a lens, i.e., the flux entering the detector is obtained by multiplying the magnification with the flux

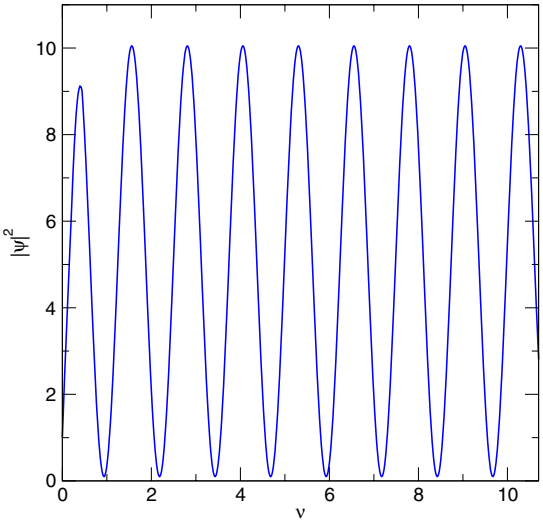

Fig. 6. $|\psi|^2$, the magnification of a distant point light source vs. the dimensionless frequency, $\nu = \tilde{\nu}(1 + z_L)2GM/c^3$, due to gravitational lensing by an intermediate preon star (or "nugget"). The flux entering the detector is obtained by multiplying the magnification, $|\psi|^2$, with the flux in the absence of a lens. For a 10^{-6} $M_\oplus$ preon star located in the halo of our galaxy, $\nu = 1$ corresponds to a photon energy of 0.14 keV. See the text for further details

in the absence of a lens. The shape of the magnification function depends on the relative position of the source and the lens. Here the source is slightly off-axis, corresponding to $\theta = 0.2$ in [34].

As mentioned in [8], preon stars might also form in the collapse of ordinary massive stars, if the collapse is slightly too powerful for the core to stabilize as a neutron star, but not sufficiently violent for the formation of a black hole. Due to the potentially very large magnetic field and rapid rotation of preon stars formed in this way, the astrophysical consequences could be important, e.g., for acceleration of ultra-high energy (UHE) cosmic rays. However, the possibility to expel such a large fraction of the mass of the progenitor star needs to be better understood. What should be noted here is merely a potential connection to UHE cosmic rays, which might provide a second means for locating and observing preon stars.

5 Conclusions

If there is a deeper layer of fermionic constituents (preons), below that of quarks and leptons, a new class of stable compact stars could exist. By fitting a simple equation of state for fermions to the minimum energy density of an electron, the maximum mass for stars composed of preons can be estimated to $\sim 10^2$ Earth masses and the maximum radius to ~ 1 m. The minimum central density is of the order of $\sim 10^{23}$ g/cm^3. Preon stars (or "nuggets") with a maximum mass of $\sim 10^{-1}$ Earth masses and radius $\sim 10^{-3}$ m could have been formed by the primordial density fluctuations in the early universe. By utilizing gamma-ray bursts, or white dwarfs in the large magellanic cloud as light sources, an intermediate preon star would produce diffraction lines in the spectrum, which might be observable. Due to the need for observational clues in the cold dark matter sector, this could prove compositeness plausible without much dedicated effort. This approach might complement direct tests of preon models at particle accelerators, especially at high energies, since preon stars might be observable even if the energy scale of preon interactions is far beyond reach of any existing or near future particle accelerator.

Acknowledgements. I acknowledge support from the Swedish National Graduate School of Space Technology. S. Fredriksson and J. Hansson deserve my gratitude for several useful discussions and for reading an early version of the manuscript. I thank M. Alford for providing me with the data tables of the high density nuclear matter equations of state, J. Goodman for useful discussions regarding the femtolensing signature, and J. Bourjaily, D. Casadei, A. Geiser, A. Giazotto, and J. Kamenik for interesting discussions about the astrophysical consequences of preon stars. Finally, I thank G. 't Hooft and A. Zichichi for organizing an excellent 42nd course of the international school of subnuclear physics, and for the award that was designated this work.

References

1. F. Weber, Prog. Part. Nucl. Phys. **54**, 193 (2005)
2. B.K. Harrison, K.S. Thorne, M. Wakano, J.A. Wheeler, *Gravitation Theory and Gravitational Collapse* (University of Chicago Press, Chicago, 1965)
3. D.J. Gross, F. Wilczek, Phys. Rev. Lett. **30**, 1323 (1973)
4. H.D. Politzer, Phys. Rev. Lett. **30**, 1346 (1973)
5. U.H. Gerlach, Phys. Rev. **172**, 1325 (1968); U.H. Gerlach, Ph.D. thesis, Princeton University, 1968
6. N.K. Glendenning, C. Kettner, Astron. Astrophys. **353**, L9 (2000)
7. K. Schertler et al., Nucl. Phys. A **677**, 463 (2000)
8. J. Hansson, F. Sandin, Preon stars: a new class of cosmic compact objects. astro-ph/0410417
9. S. Fredriksson, in: Proc. of the Fourth Tegernsee Int. Conf. on Particle Physics Beyond the Standard Model, 2004, ed. by H.-V. Klapdor-Kleingrothaus (Springer-Verlag, Heidelberg, 2004), p. 211, hep-ph/0309213
10. I.A. D'Souza, C.S. Kalman, Preons (World Scientific, Singapore, 1992)
11. G. 't Hooft, Cargèse Lecture Notes, 1979
12. R. Barbieri, L. Maiani, R. Petronzio, Phys. Lett. B **96**, 63 (1980)
13. J.-J. Dugne, S. Fredriksson, J. Hansson, Europhys. Lett. **57**, 188 (2002)
14. J.R. Oppenheimer, G. Volkoff, Phys. Rev. **55**, 374 (1939)
15. J.W. Negele, D. Vautherin, Nucl. Phys. A **207**, 298 (1973)
16. A. Akmal, V.R. Pandharipande, D.G. Ravenhall, Phys. Rev. C **58**, 1804 (1998)
17. C. Kettner et al., Phys. Rev. D **51**, 1440 (1995)

18. M. Prisznyak, B. Lukacs, P. Levai, Are There Top Quarks in Superdense Hybrid Stars? astro-ph/9412052
19. A. Chodos et al., Phys. Rev. D **9**, 3471 (1974)
20. N.K. Glendenning, Compact Stars (Springer-Verlag, New York, 1997)
21. S. Banerjee, S.K. Ghosh, S. Raha, J. Phys. G **26**, L1 (2000)
22. S. Chandrasekhar, Phys. Rev. Lett. **12**, 114 (1964)
23. C.W. Misner, K.S. Thorne, J.A. Wheeler, Gravitation (Freeman and Co., San Francisco, 1973)
24. J.M. Bardeen, K.S. Thorne, D.W. Meltzer, Astrophys. J. **145**, 505 (1966)
25. D. Gondek, P. Haensel, J.L. Zdunik, Astron. Astrophys. **325**, 217 (1997)
26. S.W. Hawking, Commun. Math. Phys. **43**, 199 (1975)
27. M.S. Turner, Phys. Rep. **333**, 619 (2000)
28. L. Bergström, Rep. Progr. Phys. **63**, 793 (2000)
29. V. Burdyuzha et al., in: Proc. of the Second Int. Workshop on Particle Physics and the Early Universe, 1999, ed. by D.O. Caldwell (Springer-Verlag, 1999), p. 392, astro-ph/9912555
30. O. Lalakulich, G. Vereshkov, in: Proc. of the Second Int. Conf. on Dark Matter in Astro and Particle Physics, 1999, ed. by H.-V. Klapdor-Kleingrothaus and L. Baudis (IOP Publishing, Great Yarmouth, 1999), p. 668
31. L. Bergström, A. Goobar, Cosmology and Particle Astrophysics, 2nd ed. (Springer-Verlag, Germany, 2004)
32. A. Gould, ApJ **386**, L5 (1992)
33. K.Z. Stanek, B. Paczyński, J. Goodman, ApJ **413**, L7 (1993)
34. A. Ulmer, J. Goodman, ApJ **442**, 67 (1995)
35. R.J. Nemiroff, A. Gould, Probing for MACHOs of Mass $10^{-15}M_{\odot}$–$10^{-7}M_{\odot}$ with Gamma-Ray Burst Parallax Spacecraft. astro-ph/9505019

Paper IV

Looking in the right direction for fundamental constituents?

J. Hansson[1,*] and F. Sandin[1,†]

[1]*Department of Physics, Luleå University of Technology, SE-97187 Luleå, Sweden*

The maximum density of cosmic compact objects composed of quarks and leptons is $\sim 10^{16}$ g/cm^3. At higher densities, an instability gives a collapse into a black hole. Hence, if objects more dense than this do exist, it is compelling evidence for a new state of matter that must be composed of yet unobserved particles. The abundance of such objects is not limited by big bang nucleosynthesis and they could therefore constitute the bulk of the dark matter content of the universe. Here we suggest that the line-features observed in some high-energy gamma-ray burst spectra could be due to gravitational diffraction by such objects. A refined observational search for line features in high-energy spectra could therefore complement particle physics experiments in the search for new fundamental constituents, at an energy scale that is beyond reach of other methods.

PACS numbers: 12.60.Rc, 04.40.Dg, 95.35.+d, 98.70.Rz

I. INTRODUCTION

The matter content of the universe is apparently dominated by so-called dark matter (DM), an obscure non-luminous and effectively transparent form of matter [1, 2]. Big bang nucleosynthesis limits the amount of baryonic matter to 20%, out of which only 10% is luminous "ordinary" matter and 90% seems to be in the form of intergalactic gas [3]. DM thus constitutes the bulk ($\gtrsim$ 80%) of the matter content in the universe. This modern view is supported by several independent and consistent astrophysical observations [4]. The nature of DM is, however, controversial. There seems to be no hope of explaining the abundance of DM without introducing new fundamental particles. The current standard model of particle physics (SM) – presently our most fundamental description of matter – is hence incomplete.

Some interesting DM candidates are in reach of the next generation of particle accelerators and dedicated dark matter detectors. Hopefully, a better understanding of matter will therefore emerge during the next five to ten years, as these instruments become operational. However, since the energy range of future accelerators is severely constrained both by technical and economical demands, astrophysical observations constitute an increasingly important complementary source of information. Especially, the properties of matter at extremely high densities and low temperatures can so far only be studied by observations of compact stars. At higher temperatures, remnants from the early universe, *e.g.*, the cosmic microwave background, also provide valuable information.

In this letter, we suggest that new fundamental constituents could be revealed by a yet unobserved class of compact objects, which is in reach of already existing and near future astronomical instruments. While being less systematic and precise than particle physics experiments, the method suggested here can address much higher energies. If such objects were to be observed, it would provide information about the constituent particles and the nature of cold DM.

II. THE MAXIMUM DENSITY PROPHECY

The structure of compact stars, *e.g.*, white dwarfs and neutron stars, is governed by the hydrostatic equations and the properties of the constituent particles, mainly the equation of state (EOS). In the mid 1960s, it was shown that for the solutions to the stellar structure equations, whether Newtonian or relativistic, there is a change in stability whenever the mass reaches a local maximum or minimum as a function of central density [5]. The instability in-between white dwarfs and neutron stars, which spans several orders of magnitude of central densities, is one example of this property. Also, it is well known that the density of compact objects cannot exceed $\sim 10^{16}$ g/cm^3. Beyond this, inevitable radial pulsations cause a collapse of the star into a black hole. It has been shown that even if exotic phases of (standard model) matter form in compact stars, *e.g.*, hyperons and quark-gluon plasma, the instability remains and prevents significantly higher densities [6, 7, 8, 9, 10].

Beyond the maximum density of neutron stars, there is hence a desert of instability where all objects are assumed to end up in black holes. This picture is, however, valid only in the context of the SM, where quarks and leptons are considered as fundamental particles. If there is a deeper layer of constituents, "below" the particles of the SM, denser classes of stable compact objects could exist. Observations of objects that are far denser than 10^{16} g/cm^3 would therefore be compelling evidence for a new state of matter not composed of quarks and leptons. Since the mass and radius of compact objects are connected to the properties of the EOS, observations of such objects could provide valuable information about the properties of the exotic constituent particles.

We have recently shown that such extremely compact objects could be stable [11]. Unknown to us, the idea that

*Electronic address: c.Johan.Hansson@ltu.se
†Electronic address: Fredrik.Sandin@ltu.se

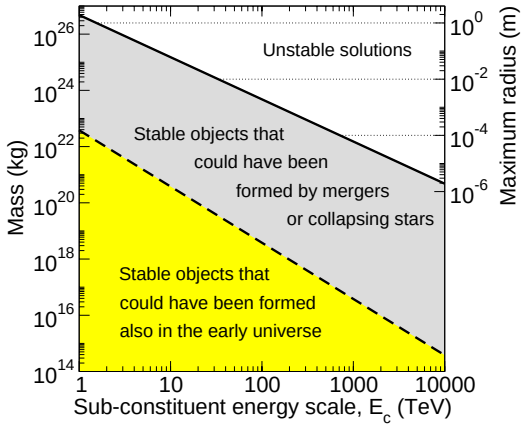

FIG. 1: Estimated mass, M, and maximum radius of stable objects vs. the sub-constituent energy scale, E_c. The density of the primordial plasma and the size of causally connected regions at $k_B T \sim E_c$ puts an upper limit on the mass of objects that could have been formed in the early universe (dashed line). The astrophysically observable range is $10^{14} \lesssim M \lesssim 10^{24}$ kg, see Section IV. The next generation of particle accelerators will probe $E_c \lesssim 10$ TeV.

macroscopic "sub-quark" objects could exist had independently been suggested in [12]. If these objects formed by the primordial density fluctuations in the early universe, they could constitute all, or a considerable fraction of DM and might be observable as gravitational pico- or femtolenses [13], see Section IV.

III. CONSTRAINING MASSES AND RADII

A number of different models have been used to estimate the mass, size, and region of stability of these objects. Independently of the method used, the maximal radius is roughly a few meters and the corresponding maximum mass is one hundred earth masses [11, 13], see Fig. 1. An order of magnitude estimate for the mass and radius can be obtained from the Schwarzschild radius, $R = 2GM/c^2$. For a spherically symmetric object of uniform density, ρ, this expression yields

$$R \sim \sqrt{\frac{3\,c^2}{8\pi G\rho}}, \tag{1}$$

$$M \sim \sqrt{\frac{3\,c^3}{32\pi G^3\rho}}. \tag{2}$$

As an example, the density of a neutron star is roughly $\rho \sim 10^{15}$ g/cm^3. The corresponding estimates for its radius (1) and mass (2) are $R \sim 13$ km and $M \sim 4$ M$_\odot$, which is of the correct order of magnitude for neutron stars. Assuming that there is a deeper layer of particles, below that of quarks and leptons, the maximum mass and radius of objects composed of these particles can be estimated in a similar way. A lower limit estimate for the density can be obtained from, *e.g.*, electron–positron scattering experiments,

$$\rho \gtrsim \frac{511\,\mathrm{keV}/c^2}{(\ c/\mathrm{TeV})^3} \simeq 10^{23}\,\mathrm{g/cm^3}, \tag{3}$$

see also [14]. Here, c/TeV is an estimate of the maximum length scale where sub-structure can appear and 511 keV/c^2 is the mass-energy enclosed in the corresponding volume. The hereby obtained upper limit estimates for the radius (1) and mass (2) of sub-quark stars are $R \sim 1.3$ m and $M \sim 140$ M$_\oplus$. The corresponding minimum density is $\sim 10^{23}$ g/cm^3. Actually, static solutions to the general relativistic stellar equations always fulfil $2GM/Rc^2 < 8/9$ [15], where the limit corresponds to an object of uniform density, *i.e.*, incompressible matter. If the properties of matter is such that the pressure is lower than the energy density, the condition is even more restrictive, $2GM/Rc^2 < 3/4$. The latter is believed to be valid, since for low pressure the energy density is dominated by the rest mass of the baryons and causality prevents the pressure from growing faster than the energy density. In any case, the same order of magnitude for the mass and radius is obtained.

The small sizes of these objects, see Fig. 1, can explain why we have not yet observed them. Even if they constitute all dark matter in galaxies, on average we would have to search hundreds or thousands of solar system volumes to find a single one of them. Surprisingly, there still might be methods to detect them.

IV. OBSERVATIONAL SIGNATURE

Line features have been observed in the 10-1000 keV spectra of some gamma-ray bursts (GRB) with instruments on three different satellites (*Konus*, *HEAO 1*, and *Ginga*), see [16, 17, 18, 19, 20, 21, 22]. The line spectra were originally interpreted as evidence for cyclotron absorption and, as a consequence, a galactic origin of some GRBs [23]. However, if GRBs originate at cosmological distances, as suggested by recent observations (GRB afterglows, supernova-GRB connection) the lines can instead be due to gravitational lensing by compact objects. Due to diffraction, a dense intervening object of mass 10^{14} to 10^{17} kg would produce lines in the hard x- and γ-ray spectra, see [24, 25]. To obtain a reasonable lensing rate, the abundance of such objects must be large enough to constitute a substantial part of DM. By utilizing instruments on different satellites, lenses of mass 10^{14} to 10^{24} kg can be resolved. There is to date no result that rules out, nor confirms, an abundance of dark compact objects with masses in this range [26].

If quarks and leptons are composite particles, macroscopic lumps composed of their sub-constituents could have been formed by the density fluctuations in the early universe [11, 13]. If such lumps are stable and constitute

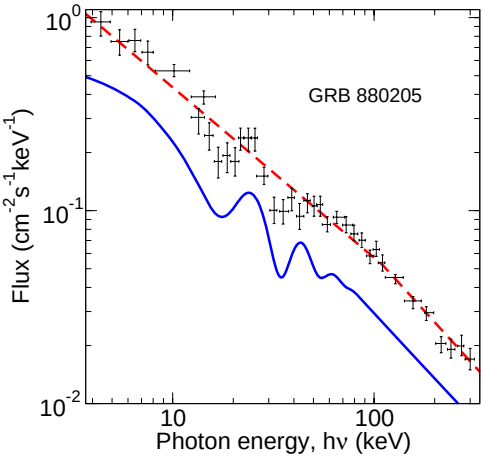

FIG. 2: Ginga spectral data of GRB 880205 for a power law model of the incoming spectrum (dashed line), which is ruled out at more than 99.99% confidence level [21]. The observed spectrum has line features at $h\nu \simeq 20$ and 40 keV, which can be due to gravitational diffraction of a Gaussian source by a $\sim 10^{16}$ kg point-like object at redshift $z \sim 1$ (solid line). Due to the nature of the detector response functions, the spectral data depend on the model and should not be directly compared to the diffraction spectrum, which therefore has been shifted downwards. The main concern here is the location and relative sizes of the absorption features. Similar line features have been found in spectra of other GRBs, *e.g.*, GRB 870303 [22]. For more information about GRB spectral analysis and the detector response functions, see [27].

a large fraction of DM, they could cause the observed lines in high-energy spectra, see Fig. 2. Even if the subconstituent particles appear at the 10^{15} eV scale, far beyond reach of terrestrial experiments in the foreseeable future, stable solutions in the astrophysically observable range exist, see Fig. 1. The main observational difficulty is to constrain the size of the lenses, to distinguish these objects from "lumps" of other dark matter line candidates, *e.g.*, axions and neutralinos. Nevertheless, since x- and γ-ray instruments are already deployed for other purposes, this is an inexpensive and complementary way to search for physics beyond the SM, which hopefully will inspire a continued and refined observational search.

V. CONCLUSIONS

In this letter, we suggest that the line features that have been observed in spectra of some gamma-ray bursts (GRB) could be due to gravitational diffraction by a new class of cosmic compact objects. Previously, we have shown [11, 13] that if quarks and leptons are *composite* particles, stability can be restored way beyond the traditional density limit of compact stars. If the observed lines are due to an abundance of such objects, which were created, *e.g.*, in the early universe, a refined observational search could provide information about the subconstituent particles and the nature of cold DM. Even though the suggested approach is less systematic and precise than controlled particle physics experiments, it addresses an energy scale that is beyond reach of terrestrial experiments.

[1] M. S. Turner, Phys. Rep. **333**, 619 (2000).
[2] L. Bergström, Rep. Progr. Phys. **63**, 793 (2000).
[3] F. Nicastro *et al.*, Nature **433**, 495 (2005).
[4] N. A. Bahcall *et al.*, Science **284**, 1481 (1999).
[5] B. K. Harrison, K. S. Thorne, M. Wakano & J. A. Wheeler, *Gravitation Theory and Gravitational Collapse* (University of Chicago Press, Chicago, 1965).
[6] U. H. Gerlach, Phys. Rev. **172**, 1325 (1968).
[7] U. H. Gerlach, Ph.D. thesis, Princeton University, 1968.
[8] C. Kettner *et al.*, Phys. Rev. D **51**, 1440 (1995).
[9] N. K. Glendenning & C. Kettner, Astron. Astrophys. **353**, L9 (2000).
[10] K. Schertler *et al.*, Nucl. Phys. A **677**, 463 (2000).
[11] J. Hansson & F. Sandin, Phys. Lett. B, in press (2005); arXiv:astro-ph/0410417.
[12] G. H. A. Cole & J. Dunning-Davies, Gravitation **4**, 79 (1999) (in Russian).
[13] F. Sandin, Euro. Phys. J. C, doi:10.1140/epjcd/s2005-03-003-y; arXiv:astro-ph/0410407.
[14] J. C. Pati, Phys. Rev. D **30**, 1144 (1984).
[15] S. Weinberg, *Gravitation and Cosmology* (John Wiley & Sons, New York, 1972).
[16] E. P. Mazets *et al.*, Nature **290**, 378 (1981).
[17] E. P. Mazets *et al.*, Ap&SS **84**, 173 (1982).
[18] G. J. Hueter, in the *Proc. of High Energy Transients in Astrophysics, 1984*, ed. by S. Woosely (New York: AIP), p. 373.
[19] G. J. Hueter, Ph.D. thesis, University of California, San Diego, 1987.
[20] T. Murakami *et al.*, Nature **335**, 234 (1988).
[21] E. E. Fenimore *et al.*, ApJ **335**, L71 (1988).
[22] P. E. Freeman *et al.*, ApJ **524**, 753 (1999).
[23] J. C. L. Wang *et al.*, PRL **63**, 1550 (1989).
[24] A. Gould, ApJ **386**, L5 (1992).
[25] K. Z. Stanek, B. Paczyński & J. Goodman, ApJ **413**, L7 (1993).
[26] G. F. Marani *et al.*, ApJ **512**, L13 (1999).
[27] T. J. Loredo & R. I. Epstein, ApJ **336**, 896 (1989).

Selected
Posters and Awards

Comments

The poster "Compact stars in the standard model – and beyond" was presented at the International School of Subnuclear Physics, Erice, 2004. The title of the course was "How and Where to Go Beyond the Standard Model". The directors of the school were Professor Gerardus 't Hooft and Professor Antonino Zichichi.

The award for "An original work in theoretical physics" was designated to the preceding poster and the talk that I gave on the same topic. The jury consisted of the directors of the school and a number of other professors from the high-energy physics and astrophysics communities. The poster and the talk were based on the original work on preon stars presented in Paper II. The essence of the talk is presented in Paper III.

Compact Stars in
THE STANDARD MODEL - AND BEYOND

by Fredrik Sandin

Division of Physics, Luleå University of Technology, 971 87 Luleå, Sweden
E-mail: fredrik.sandin@ltu.se

White Dwarfs

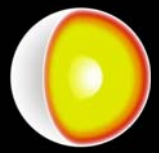

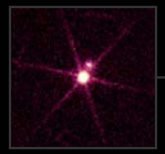

A Chandra X-ray image of the Sirius star system, located 8.6 light years from Earth. The bright source is Sirius B, a white dwarf star with a surface temperature of about 25 000 ºC, which produces low-energy X-rays. The dim source is Sirius A, the brightest star in the northern sky.

In white dwarfs, the degeneracy pressure of electrons provides the force counterbalancing gravity. The maximum mass of white dwarfs is ~ 1.4 M_{Sun}, the so-called Chandrasekhar limit. The radius of these objects is ~ 6×10^3 km, and the maximum density is ~ 10^8 g/cm^3.

Neutron Stars, Quark Stars and Hybrid Stars

A Chandra X-ray image of the Crab Nebula, located in the constellation Taurus, about 6000 light years from Earth. This is the remnant of a giant explosion, a supernova, which was seen in 1054 AD. At the centre of the bright nebula is a rapidly spinning neutron star, a so-called pulsar.

At roughly seven orders of magnitude higher density than in the limiting-mass white dwarf, nuclei dissolve, and the degeneracy pressure of nucleons (in nuclear matter) and quarks (in quark matter) stabilize the next class of compact stars, the "neutron stars". The maximum mass of this sequence is model dependent and unknown, but not larger than a few solar masses. The characteristic radius is ~ 10 km, and the density is < 10^{16} g/cm^3.

Black Holes

A Spitzer false-colour infrared image of NGC 7331, located at 50 million light-years from Earth, in the constellation Pegasus. NGC 7331 is a spiral galaxy that resembles our own Milky Way. Data indicates the presence of a black hole within the galaxy's central region.

When matter is compressed such that the Schwarzschild radius R = 2GM/c^2 is reached, the degeneracy pressure is overcome by gravity and the object collapses to a singularity, or at least to the Planck scale ρ ~ 10^{93} g/cm^3. For stable compact stars the relation is somewhat more restrictive 2GM/Rc^2 < 3/4.

10^7 g/cm^3

White Dwarfs

Desert of Instability

10^{15} g/cm^3

Neutron Stars

Desert of Instability

10^{23} g/cm^3

Preon Stars?

Central density

LULEÅ UNIVERSITY OF TECHNOLOGY

The Maximum Density Prophecy

The distinct classes of degenerate compact stars originate directly from the properties of gravity. In-between white dwarfs and neutron stars there is a large interval of central densities where no stable configurations exist.

Also, beyond the density of the limiting-mass neutron star, no stable configurations exist. That is, if quarks and leptons are fundamental entities in our world!

Compact Stars Beyond the Desert

Under the assumption that quarks and leptons are composite particles, built out of more elementary fermions, so-called *preons*, a new class of degenerate compact stars could exist. A simple estimate of the maximum mass of such objects gives ~ 10^2 M_{Earth} ~ 6×10^{26} kg, and a radius of ~ 1 m.

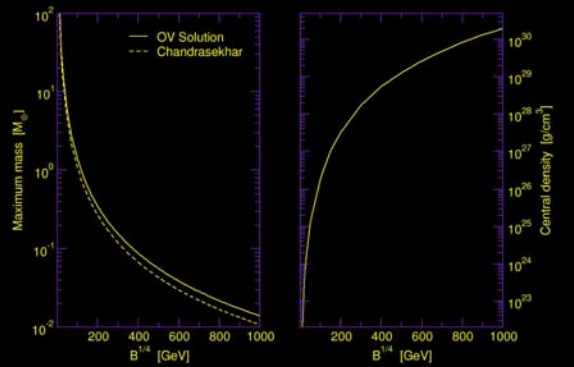

The maximum mass and central density of preon stars vs. the exogenous parameter of the model, the "bag pressure" B. The mass is given in units of the Earth mass ($M_\oplus$).

Formation and Detection

If fermionic preons exist, and configurations of preon matter as small and light as suggested here are stable, preon stars (or "nuggets") might have formed in the early universe.

If preon stars are abundant enough, *e.g.*, a large fraction of the cold dark matter in galaxies, these objects would cause gravitational lensing of gamma-ray bursts (so-called picolensing or femtolensing), which might be observable.

WORLD FEDERATION OF SCIENTISTS

«ETTORE MAJORANA» FOUNDATION AND CENTRE FOR SCIENTIFIC CULTURE

INTERNATIONAL SCHOOL OF SUBNUCLEAR PHYSICS

42nd Course:

How and Where to go beyond the Standard Model

Erice, 29 August - 7 September 2004

"New Talents" Award

for an

ORIGINAL WORK IN THEORETICAL PHYSICS

Jan Fredrik SANDIN

Gerardus 't Hooft and Antonino Zichichi

Directors

Erice, 6 - IX - 2004